Signal Formation in Particle Detectors

Werner Riegler, CERN, werner.riegler@cern.ch

II Seminario Nazionale Rivelatori Innovativi

18-22 October 2010, Trieste

Lecture1/3

History of Instrumentation
↔
History of Particle Physics

History of Particle Physics

1895: X-rays, W.C. Röntgen
1896: Radioactivity, H. Becquerel
1899: Electron, J.J. Thomson
1911: Atomic Nucleus, E. Rutherford
1919: Atomic Transmutation, E. Rutherford
1920: Isotopes, E.W. Aston
1920-1930: Quantum Mechanics, Heisenberg, Schrödinger, Dirac
1932: Neutron, J. Chadwick
1932: Positron, C.D. Anderson
1937: Mesons, C.D. Anderson
1947: Muon, Pion, C. Powell
1947: Kaon, Rochester
1950: QED, Feynman, Schwinger, Tomonaga
1955: Antiproton, E. Segre
1956: Neutrino, Rheines
etc. etc. etc.

History of Instrumentation

1906: **Geiger Counter, H. Geiger, E. Rutherford**

1910: **Cloud Chamber, C.T.R. Wilson**

1912: **Tip Counter, H. Geiger**

1928: **Geiger-Müller Counter, W. Müller**

1929: **Coincidence Method, W. Bothe**

1930: **Emulsion, M. Blau**

1940-1950: **Scintillator, Photomultiplier**

1952: **Bubble Chamber, D. Glaser**

1962: **Spark Chamber**

1968: **Multi Wire Proportional Chamber, C. Charpak**

Etc. etc. etc.

On Tools and Instrumentation

"New directions in science are launched by new tools much more often than by new concepts.

The effect of a concept-driven revolution is to explain old things in new ways.

The effect of a tool-driven revolution is to discover new things that have to be explained"

Freeman Dyson

→ New tools and technologies will be extremely important to go beyond LHC

Physics Nobel Prices for Instrumentation

1927: C.T.R. Wilson, Cloud Chamber

1939: E. O. Lawrence, Cyclotron & Discoveries

1948: P.M.S. Blacket, Cloud Chamber & Discoveries

1950: C. Powell, Photographic Method & Discoveries

1954: Walter Bothe, Coincidence method & Discoveries

1960: Donald Glaser, Bubble Chamber

1968: L. Alvarez, Hydrogen Bubble Chamber & Discoveries

1992: Georges Charpak, Multi Wire Proportional Chamber

History of Instrumentation

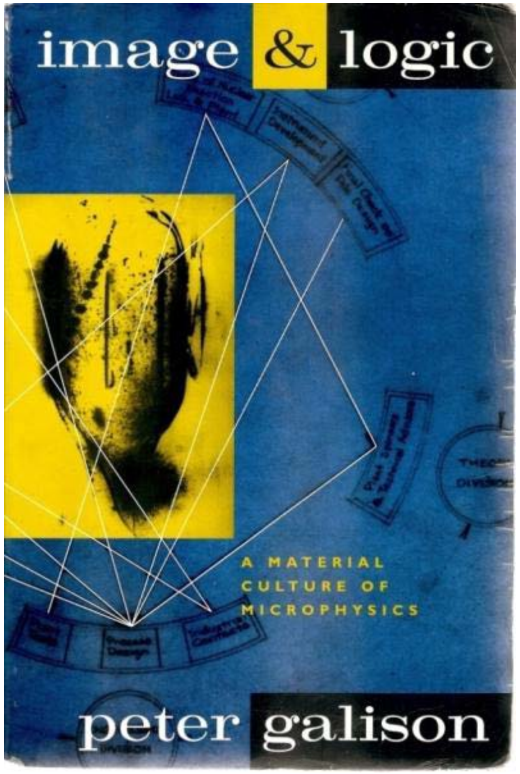

Peter Galison, Image and Logic
A Material Culture of Microphysics

History of 'Particle Detection'

Image Tradition: Cloud Chamber
Emulsion
Bubble Chamber

Logic Tradition: Scintillator
Geiger Counter
Tip Counter
Spark Counter

Electronics Image: Wire Chambers
Silicon Detectors
…

IMAGES

Cloud Chamber

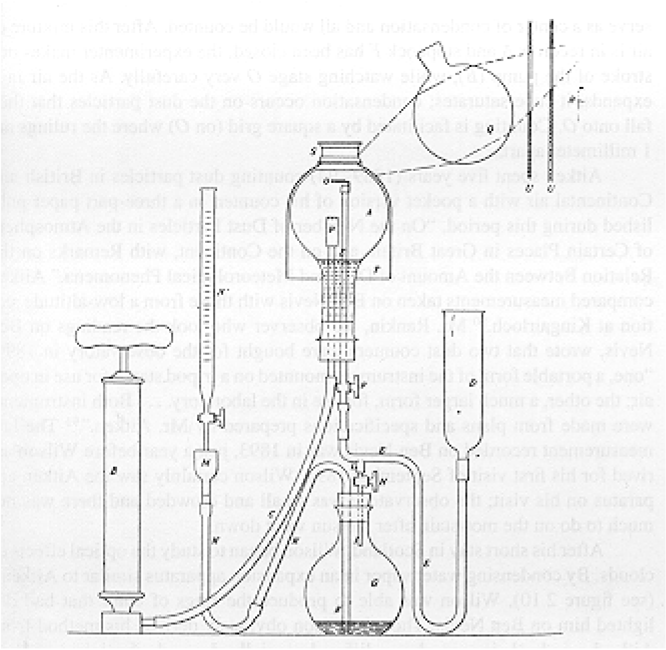

Dust Chamber, Aitken 1888

John Aitken, *1839, Scotland:

Aitken was working on the meteorological question of cloud formation. It became evident that cloud droplets only form around condensation nuclei.

Aitken built the 'Dust Chamber' to do controlled experiments on this topic. Saturated water vapor is mixed with dust. Expansion of the volume leads to super-saturation and condensation around the dust particles, producing clouds.

From steam nozzles it was known and speculated that also electricity has a connection to cloud formation.

Cloud Chamber

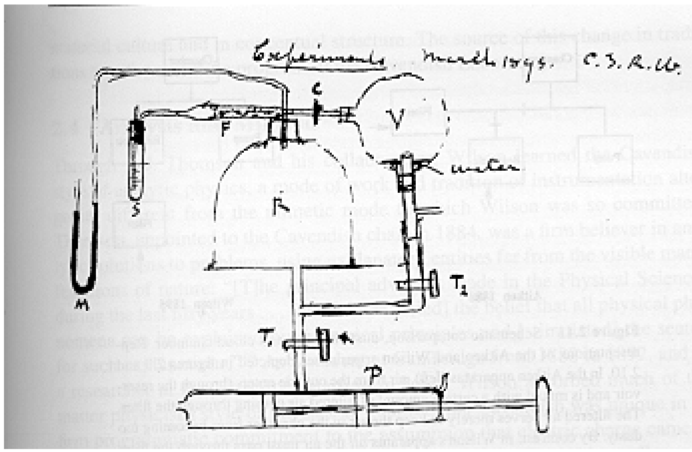

Cloud Chamber, Wilson 1895

Charles Thomson Rees Wilson, * 1869, Scotland:

Wilson was a meteorologist who was, among other things, interested in cloud formation initiated by electricity.

In 1895 he arrived at the Cavendish Laboratory where J.J. Thompson, one of the chief proponents of the corpuscular nature of electricity, had studied the discharge of electricity through gases since 1886.

Wilson used a 'dust free' chamber filled with saturated water vapor to study the cloud formation caused by ions present in the chamber.

Cloud Chamber

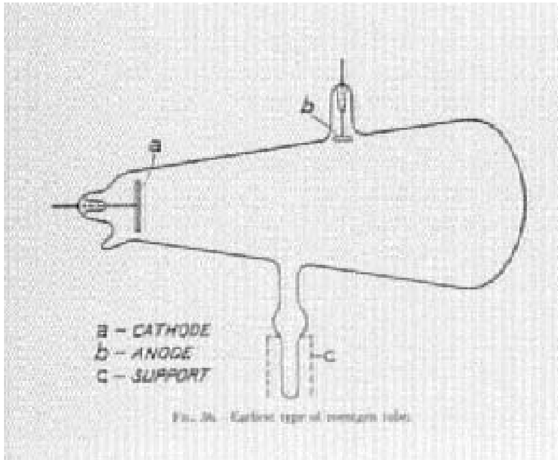

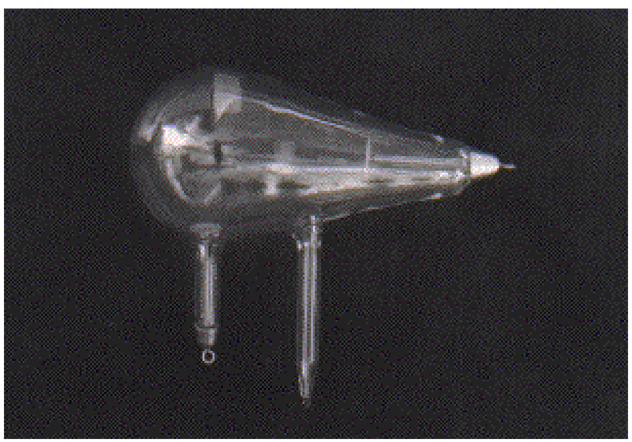

Conrad Röntgen discovered X-Rays in 1895.

At the Cavendish Lab Thompson and Rutherford found that irradiating a gas with X-rays increased it's conductivity suggesting that X-rays produced ions in the gas.

Wilson used an X-Ray tube to irradiate his Chamber and found 'a very great increase in the number of the drops', confirming the hypothesis that ions are cloud formation nuclei.

Radioactivity ('Uranium Rays') discovered by Becquerel in 1896. It produced the same effect in the cloud chamber.

1899 J.J. Thompson claimed that cathode rays are fundamental particles → electron.

Soon afterwards it was found that rays from radioactivity consist of alpha, beta and gamma rays (Rutherford).

Cloud Chamber

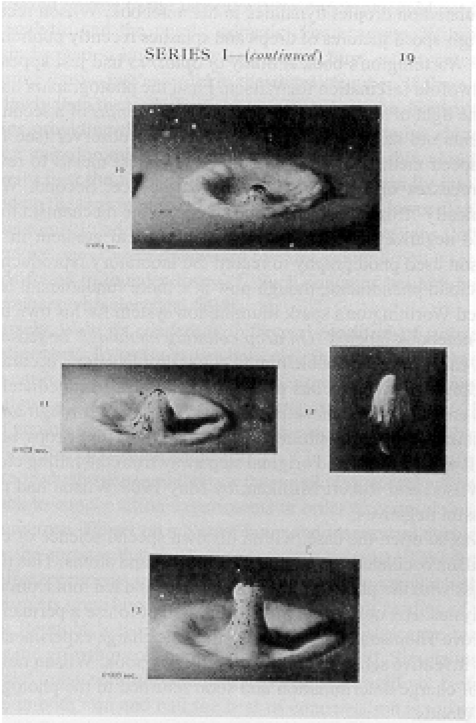

Worthington 1908

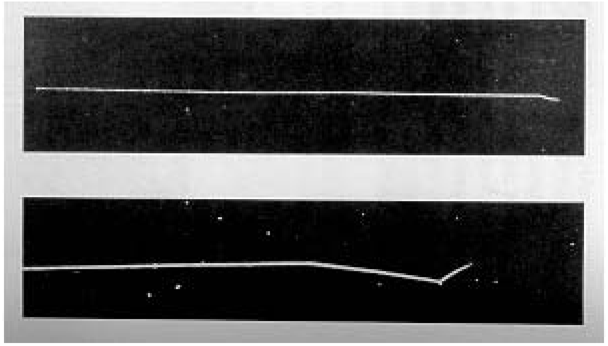

Early Alpha-Ray picture, Wilson 1912

Using the cloud chamber Wilson also did rain experiments i.e. he studied the question on how the small droplets forming around the condensation nuclei are coalescing into rain drops.

In 1908 Worthington published a book on ‘A Study of Splashes’ where he shows high speed photographs that exploited the light of sparks enduring only a few microseconds.

This high-speed method offered Wilson the technical means to reveal the elementary processes of condensation and coalescence.

He found particle tracks on the photographs !
With a bright lamp he started to see tracks even by eye !

By Spring 1911 Wilson had track photographs from from alpha rays, X-Rays and gamma rays.

Cloud Chamber

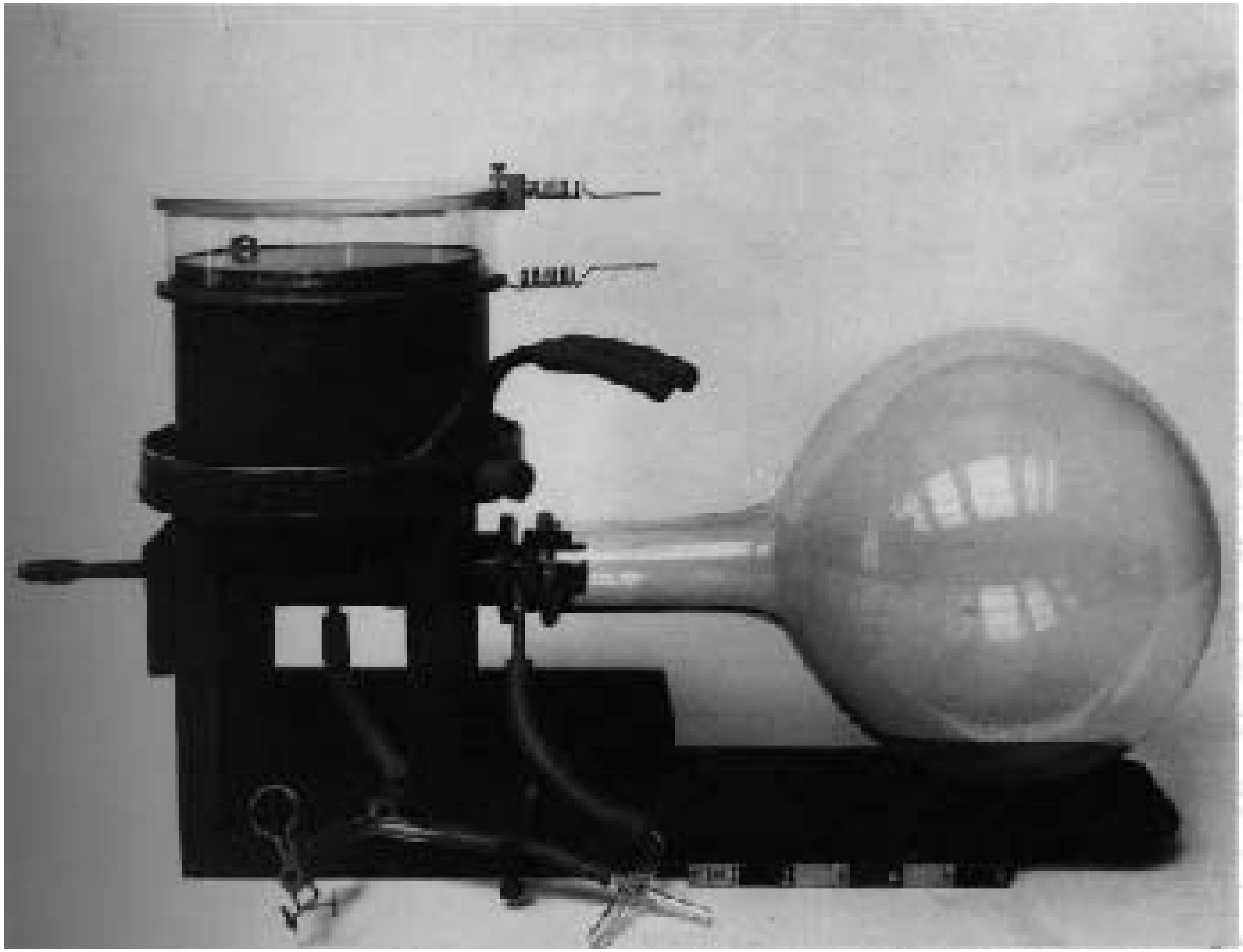

Wilson Cloud Chamber 1911

Cloud Chamber

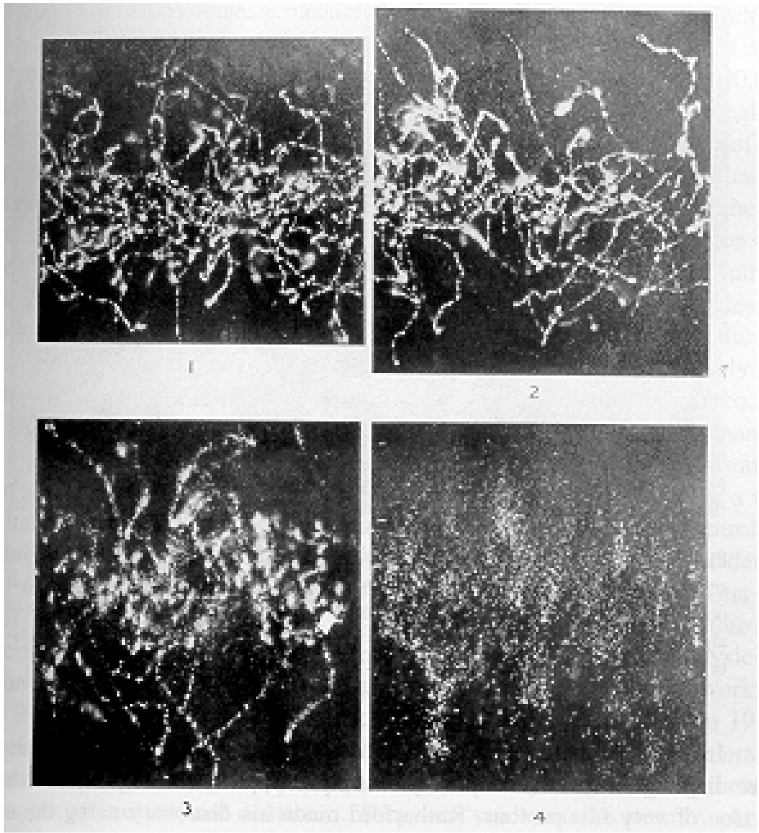

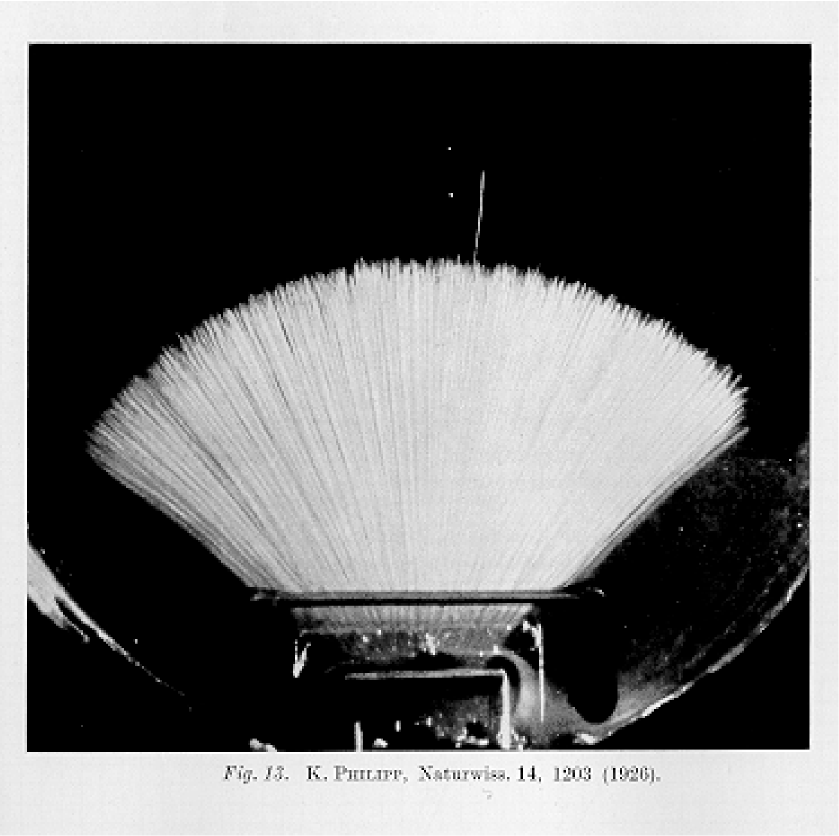

X-rays, Wilson 1912

Alphas, Philipp 1926

Cloud Chamber

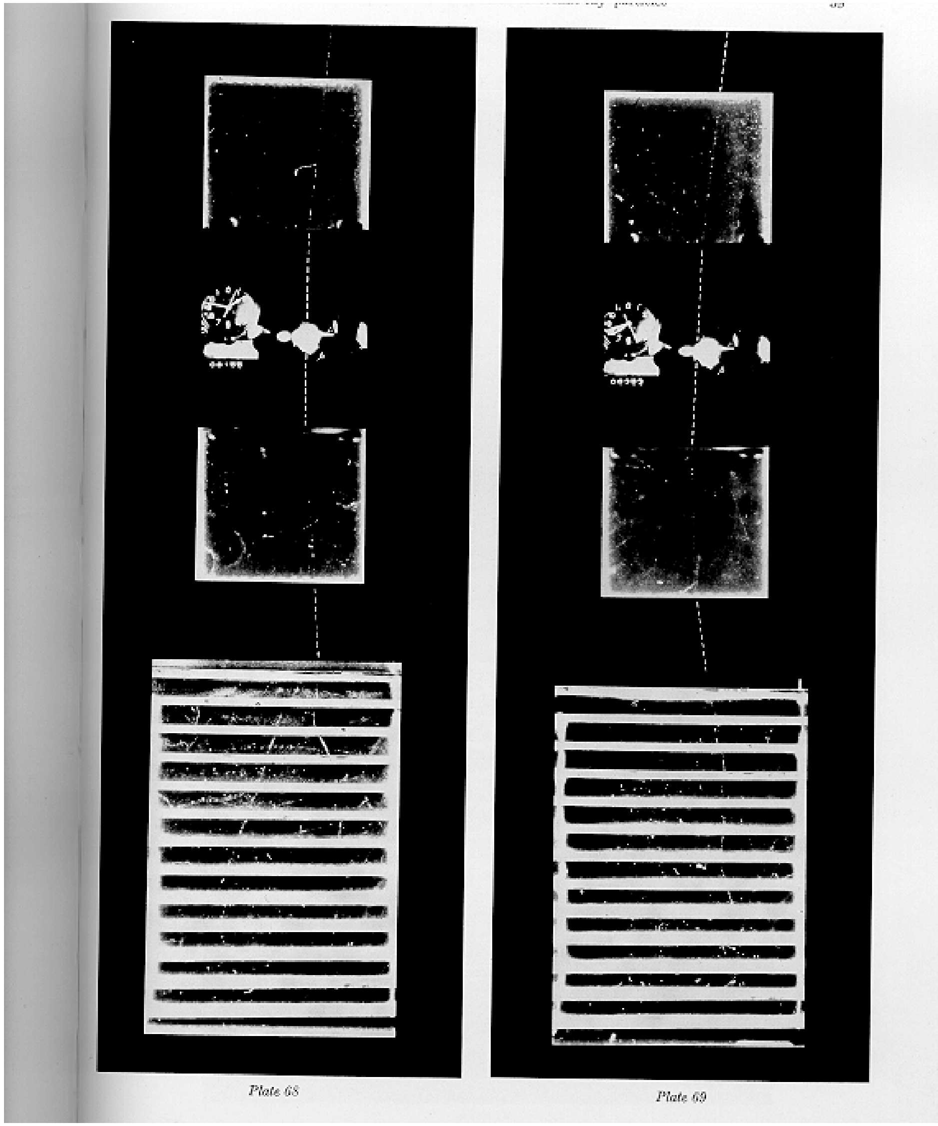

1931 Blackett and Occhialini began work on a counter controlled cloud chamber for cosmic ray physics to observe selected rare events.

The coincidence of two Geiger Müller tubes above and below the Cloud Chamber triggers the expansion of the volume and the subsequent Illumination for photography.

Cloud Chamber

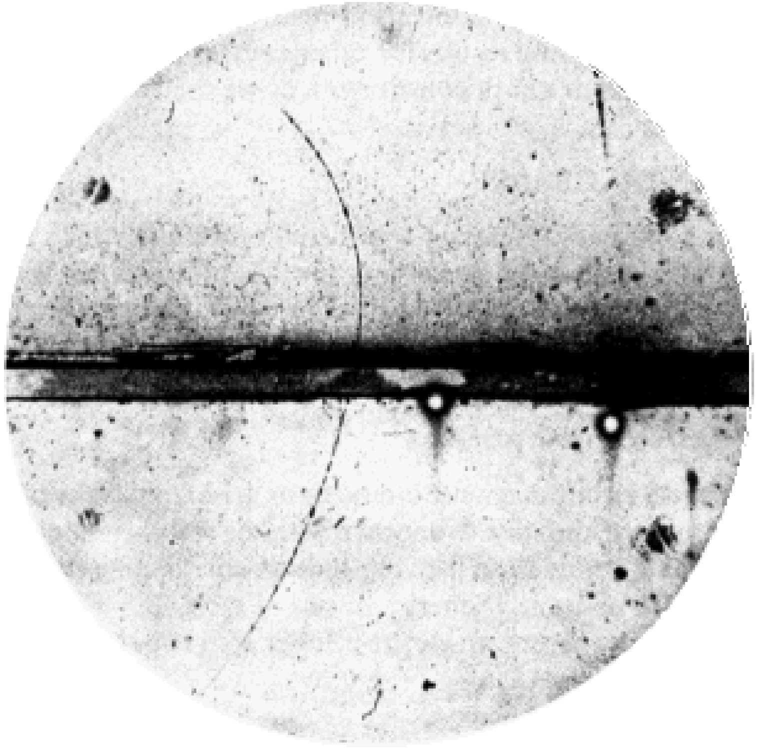

Magnetic field 15000 Gauss,
chamber diameter 15cm. A 63 MeV
positron passes through a 6mm lead plate,
leaving the plate with energy 23MeV.

The ionization of the particle, and its
behaviour in passing through the foil are
the same as those of an electron.

Positron discovery,
Carl Andersen 1933

Cloud Chamber

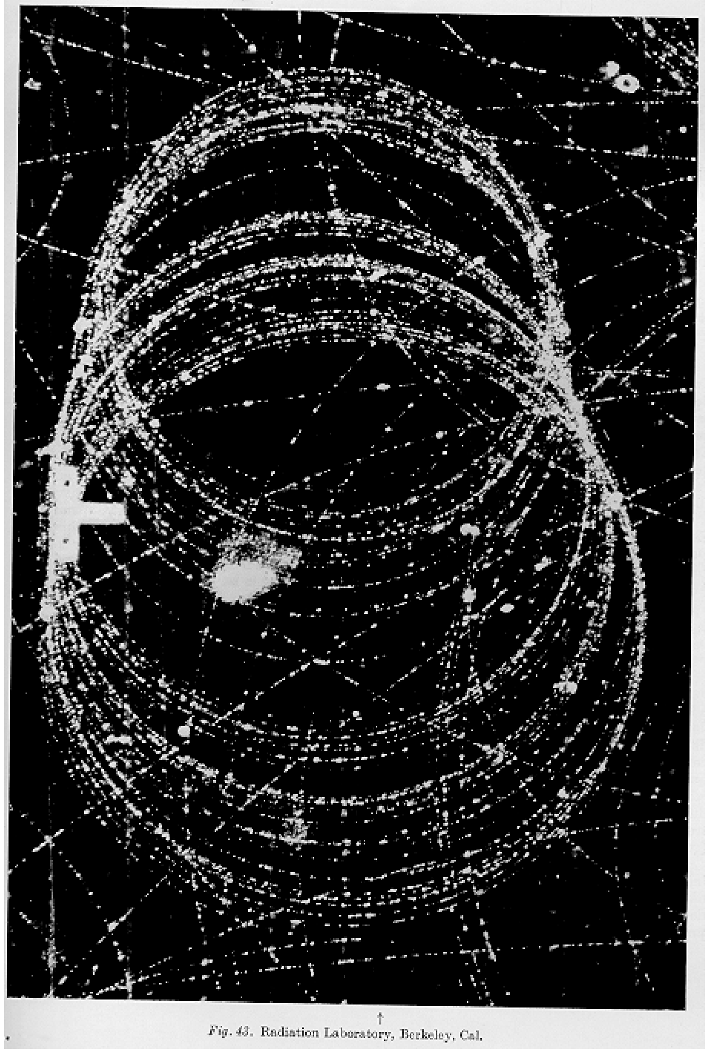

The picture shows and electron with 16.9 MeV initial energy. It spirals about 36 times in the magnetic field.

At the end of the visible track the energy has decreased to 12.4 MeV. from the visible path length (1030cm) the energy loss by ionization is calculated to be 2.8MeV.

The observed energy loss (4.5MeV) must therefore be cause in part by

Bremsstrahlung. The curvature indeed shows sudden changes as can

Most clearly be seen at about the seventeenth circle.

Fast electron in a magnetic field at the Bevatron, 1940

Cloud Chamber

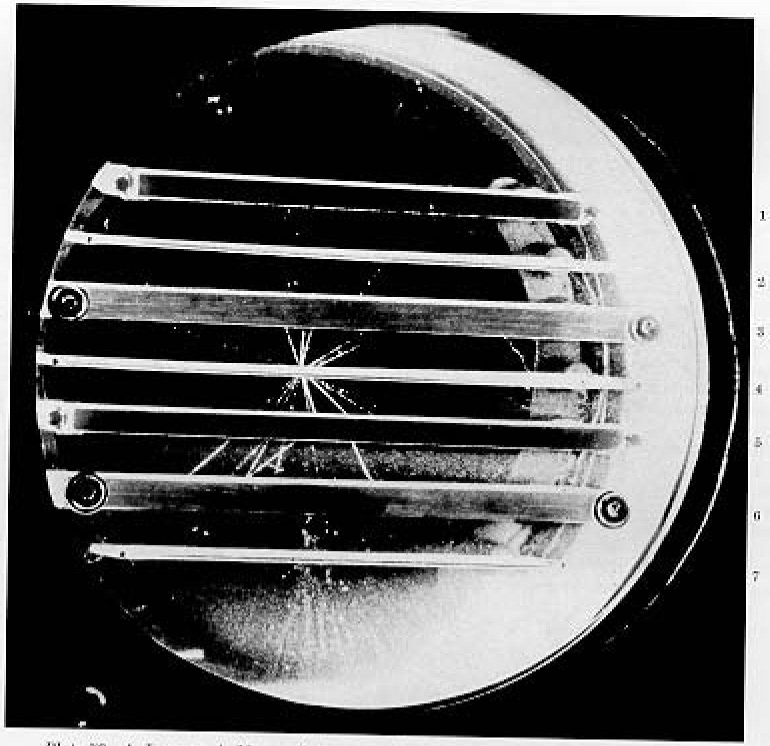

Plate 79. A. Lovati, A. Mura, G. Salvini, G. Tagliaferri, Milan. (Unpublished.)

Taken at 3500m altitude in counter controlled cosmic ray Interactions.

Nuclear disintegration, 1950

Cloud Chamber

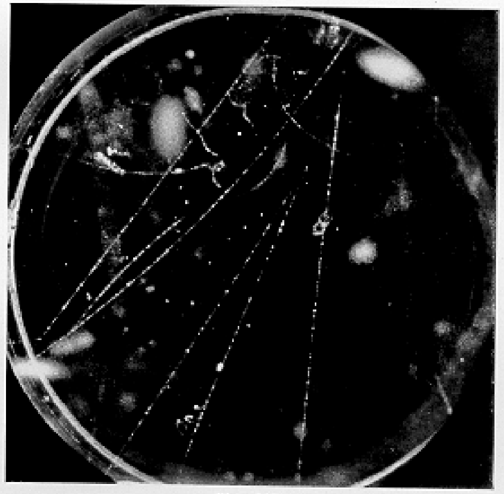

Plate 115

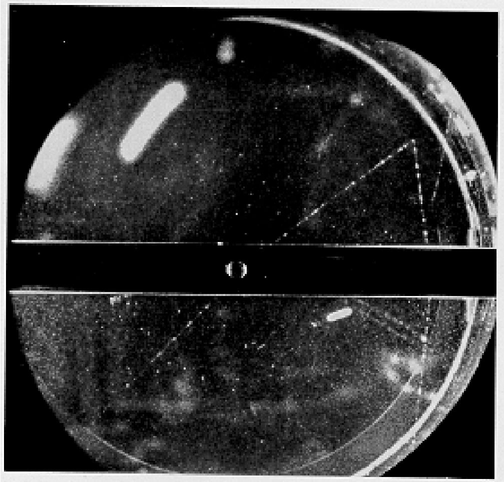

Plate 116

Rochester and Wilson

Particle momenta are measured by the bending in the magnetic field.

' … The V0 particle originates in a nuclear Interaction outside the chamber and decays after traversing about one third of the chamber. The momenta of the secondary particles are 1.6+-0.3 BeV/c and the angle between them is 12 degrees … '

By looking at the specific ionization one can try to identify the particles and by assuming a two body decay on can find the mass of the V0.

'… if the negative particle is a negative proton, the mass of the V0 particle is 2200 m, if it is a Pi or Mu Meson the V0 particle mass becomes about 1000m …'

Nuclear Emulsion

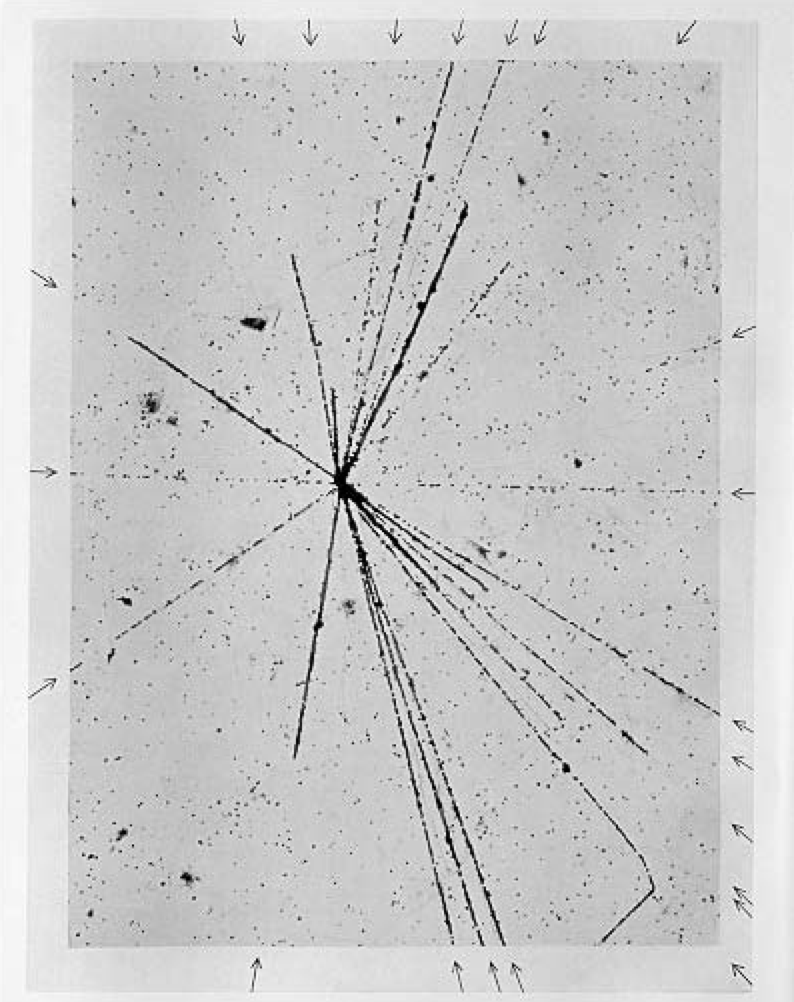

'EXPLOSIVE' DISINTEGRATION OF A NUCLEUS

Film played an important role in the discovery of radioactivity but was first seen as a means of studying radioactivity rather than photographing individual particles.

Between 1923 and 1938 Marietta Blau pioneered the nuclear emulsion technique.

E.g.
Emulsions were exposed to cosmic rays at high altitude for a long time (months) and then analyzed under the microscope.
In 1937, nuclear disintegrations from cosmic rays were observed in emulsions.

The high density of film compared to the cloud chamber 'gas' made it easier to see energy loss and disintegrations.

Nuclear Emulsion

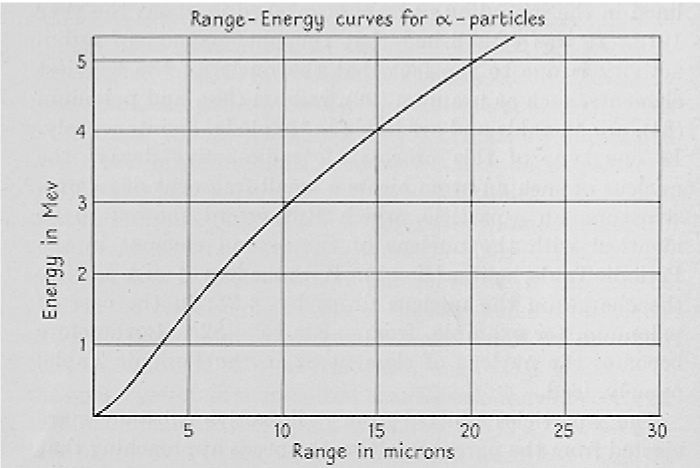

FIG. 2*a*. Range–energy curve for α-particles in the Ilford 'Nuclear Research' emulsions.

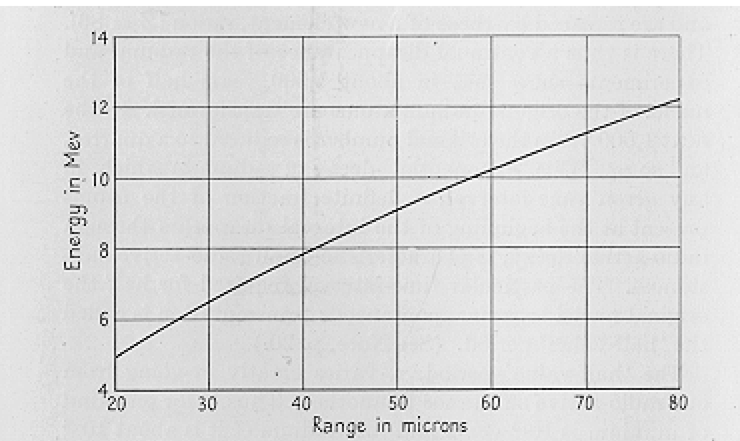

FIG. 2*b*. Range–energy curve for α-particles in the Ilford 'Nuclear Research' emulsions.

In 1939 Cecil Powell called the emulsion 'equivalent to a continuously sensitive high-pressure expansion chamber'.

A result analog to the cloud chamber can be obtained with a picture 1000x smaller (emulsion density is about 1000x larger than gas at 1 atm).

Due to the larger 'stopping power' of the emulsion, particle decays could be observed easier.

Stacks of emulsion were called 'emulsion chamber'.

Nuclear Emulsion

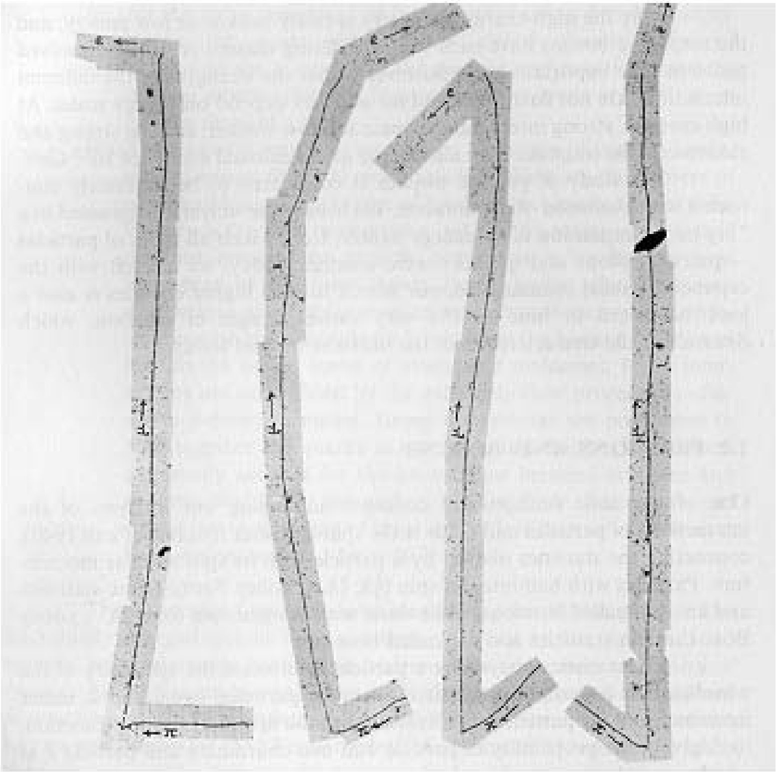

Discovery of muon and pion

Discovery of the Pion:

The muon was discovered in the 1930ies and was first believed to be Yukawa's meson that mediates the strong force.

The long range of the muon was however causing contradictions with this hypothesis.

In 1947, Powell et. al. discovered the Pion in Nuclear emulsions exposed to cosmic rays, and they showed that it decays to a muon and an unseen partner.

The constant range of the decay muon indicated a two body decay of the pion.

Nuclear Emulsion

Energy Loss is proportional to Z^2 of the particle

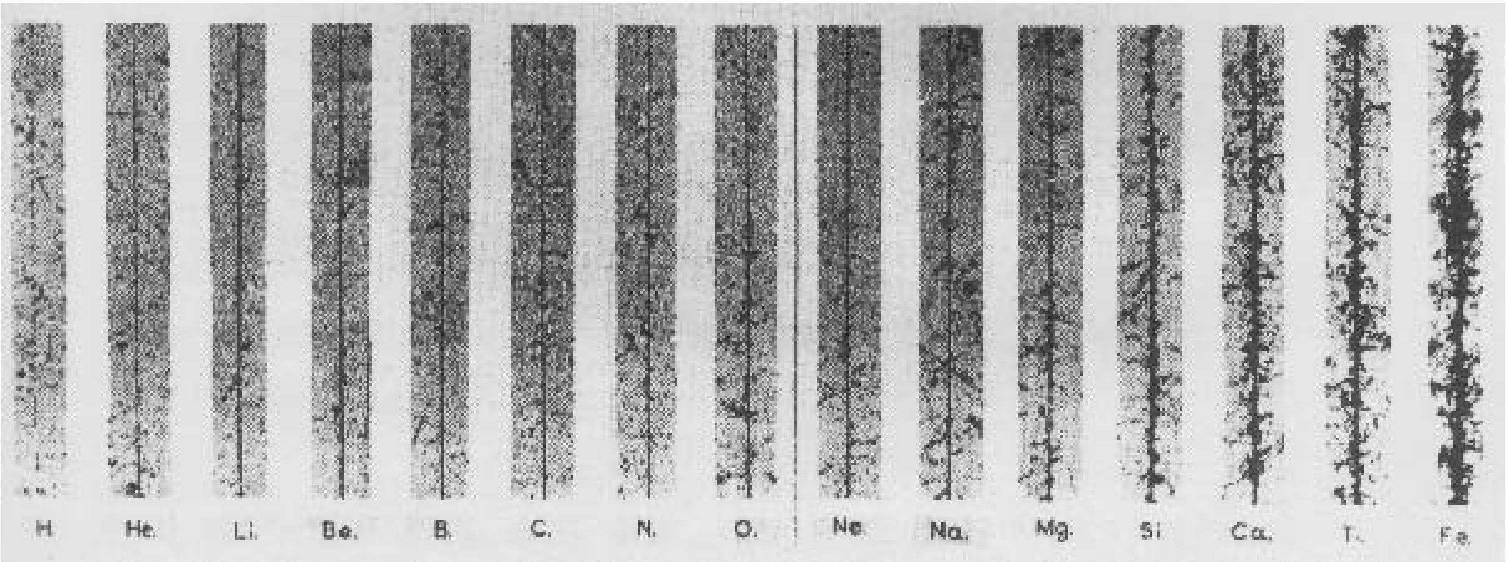

The cosmic ray composition was studied by putting detectors on balloons flying at high altitude.

Nuclear Emulsion

First evidence of the decay of the Kaon into 3 Pions was found in 1949.

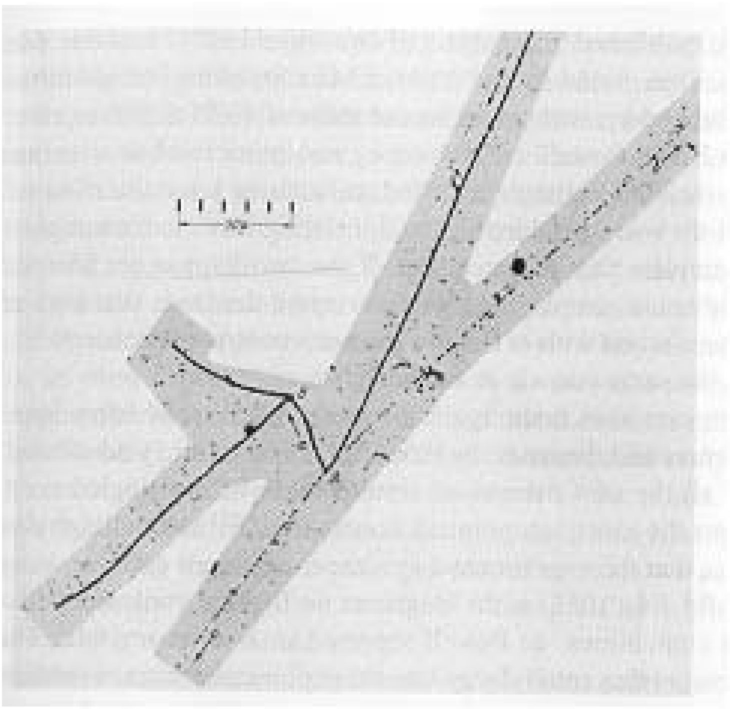

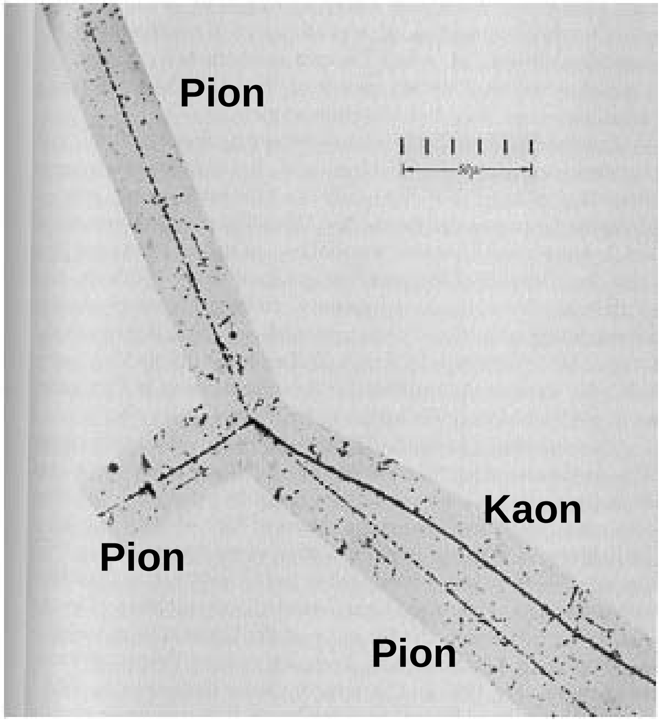

Particles in the mid 50ies

By 1959: 20 particles

e^- : fluorescent screen

n : ionization chamber

7 Cloud Chamber:

e^+

$\square^+$, $\square^-$

K^0

$\square^0$

$\square^-$

$\square^-$

6 Nuclear Emulsion:

$\square^+$, $\square^-$

anti-$\square^0$

$\square^+$

K^+ ,K^-

2 Bubble Chamber:

$\square^0$

$\square^0$

3 with Electronic techniques:

anti-n

anti-p

$\square^0$

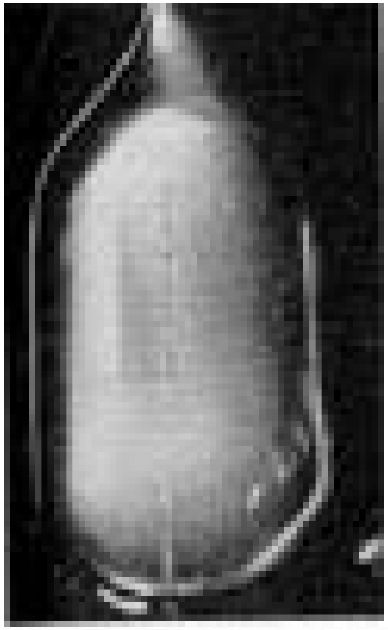

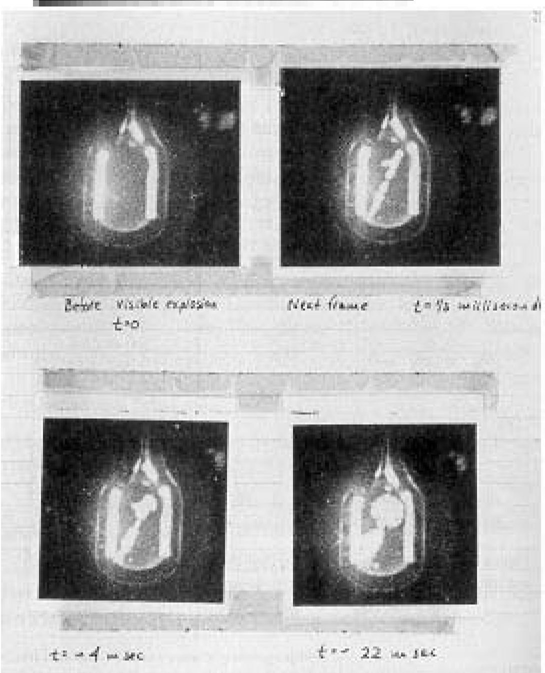

Figure 5.5 Bubble chamber movies (1952). Glaser first filmed distinct track

Bubble Chamber

In the early 1950ies Donald Glaser tried to build on the cloud chamber analogy:

Instead of supersaturating a gas with a vapor one would superheat a liquid. A particle depositing energy along it's path would then make the liquid boil and form bubbles along the track.

In 1952 Glaser photographed first Bubble chamber tracks. Luis Alvarez was one of the main proponents of the bubble chamber.

The size of the chambers grew quickly

1954: 2.5"(6.4cm)
1954: 4" (10cm)
1956: 10" (25cm)
1959: 72" (183cm)
1963: 80" (203cm)
1973: 370cm

Bubble Chamber

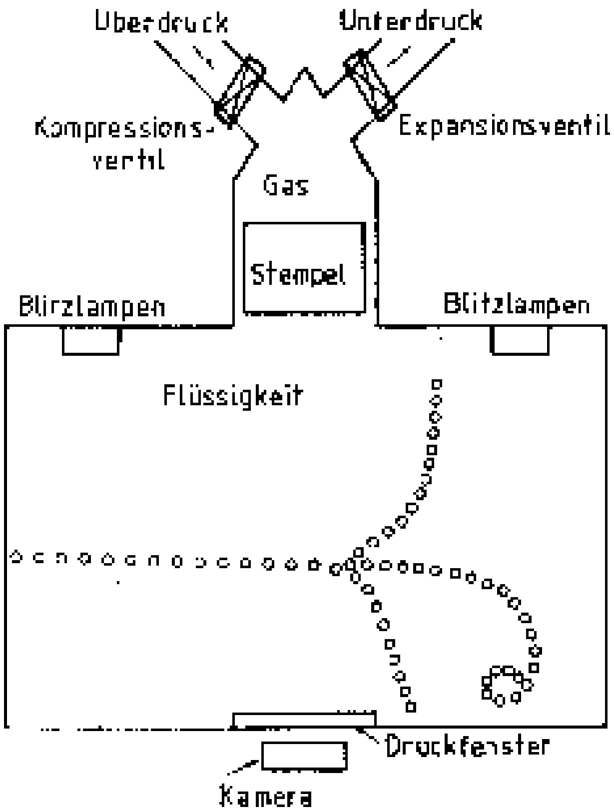

'old bubbles'

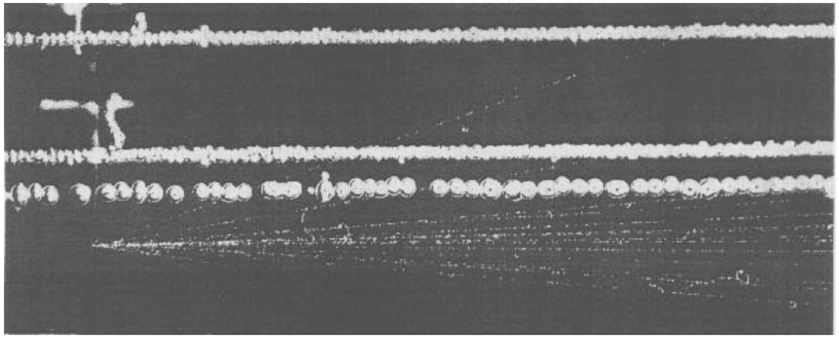

'new bubbles'

Unlike the Cloud Chamber, the Bubble Chamber could not be triggered, i.e. the bubble chamber had to be already in the superheated state when the particle was entering. It was therefore not useful for Cosmic Ray Physics, but as in the 50ies particle physics moved to accelerators it was possible to synchronize the chamber compression with the arrival of the beam.

For data analysis one had to look through millions of pictures.

Bubble Chamber

In the bubble chamber, with a density about 1000 times larger than the cloud chamber, the liquid acts as the target and the detecting medium.

Figure:
A propane chamber with a magnet discovered the $\Sigma°$ in 1956.

A 1300 MeV negative pion hits a proton to produce a neutral kaon and a $\Sigma°$, which decays into a $\Lambda°$ and a photon.

The latter converts into an electron-positron pair.

Bubble Chamber

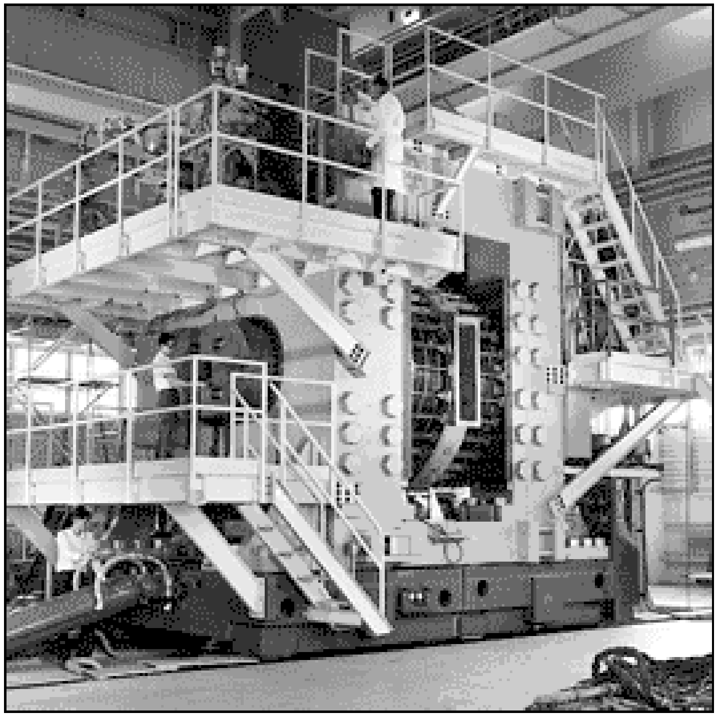

The 80-inch Bubble Chamber

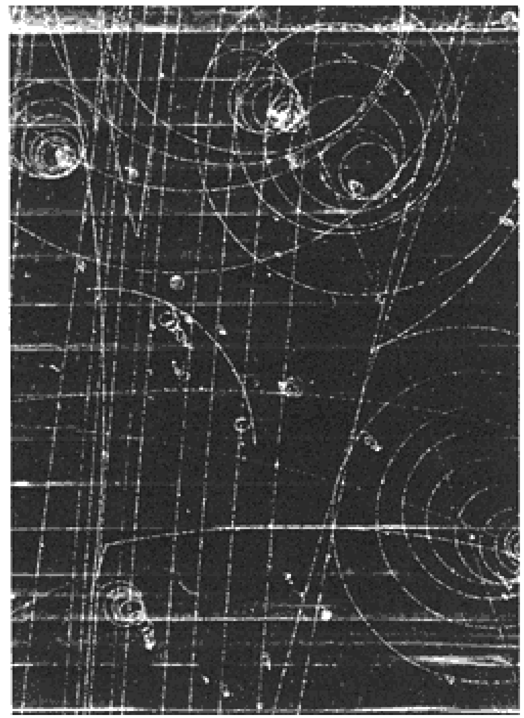

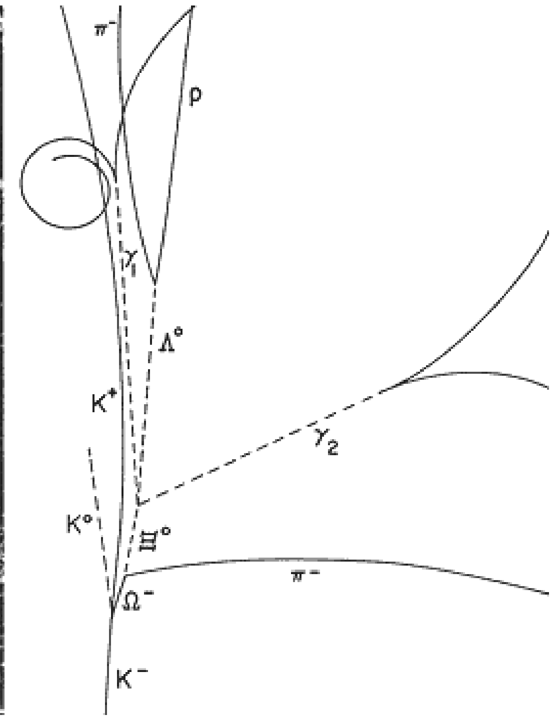

BNL, First Pictures 1963, 0.03s cycle

Discovery of the □ in 1964

Bubble Chamber

Gargamelle, a very large heavy-liquid (freon) chamber constructed at Ecole Polytechnique in Paris, came to CERN in 1970.
It was 2 m in diameter, 4 m long and filled with Freon at 20 atm.

With a conventional magnet producing a field of almost 2 T, Gargamelle in 1973 was the tool that permitted the discovery of neutral currents.

Can be seen outside the Microcosm Exhibition

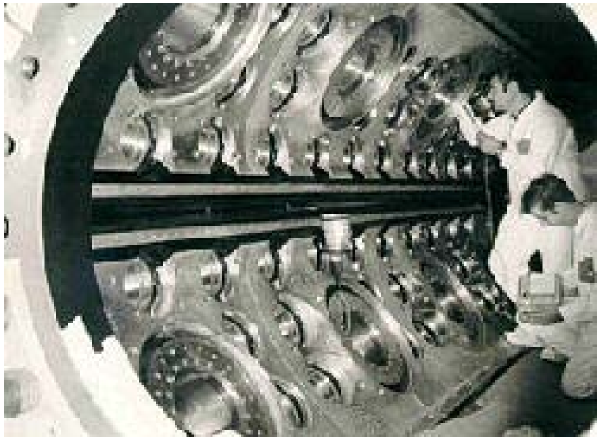

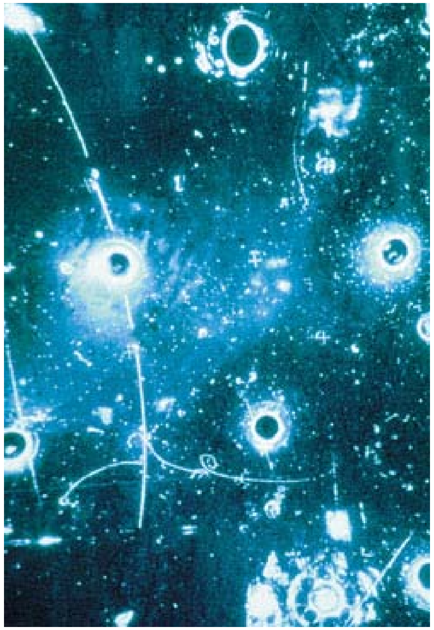

Bubble Chamber

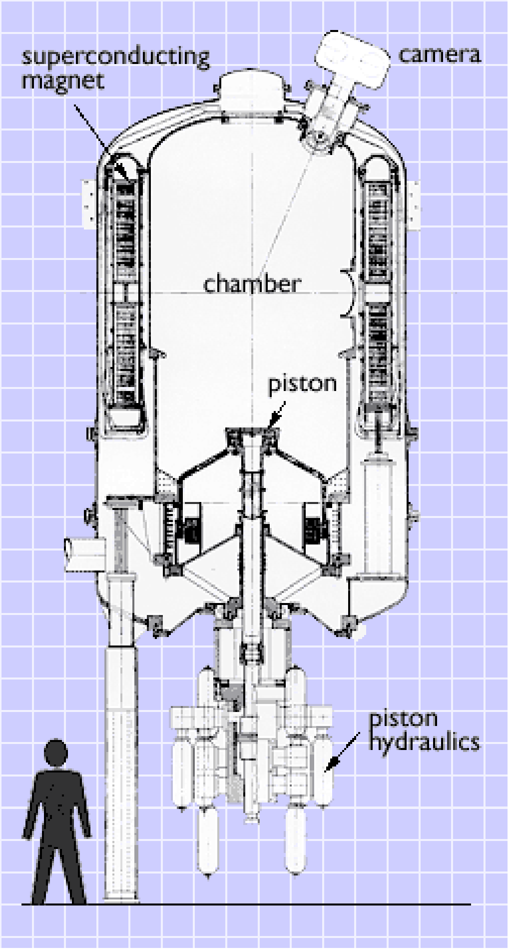

The detector began routine operations in 1974. The following year, the 7-foot chamber was used to discover the charmed baryon, a particle composed of three quarks, one of which was the "charmed" quark.

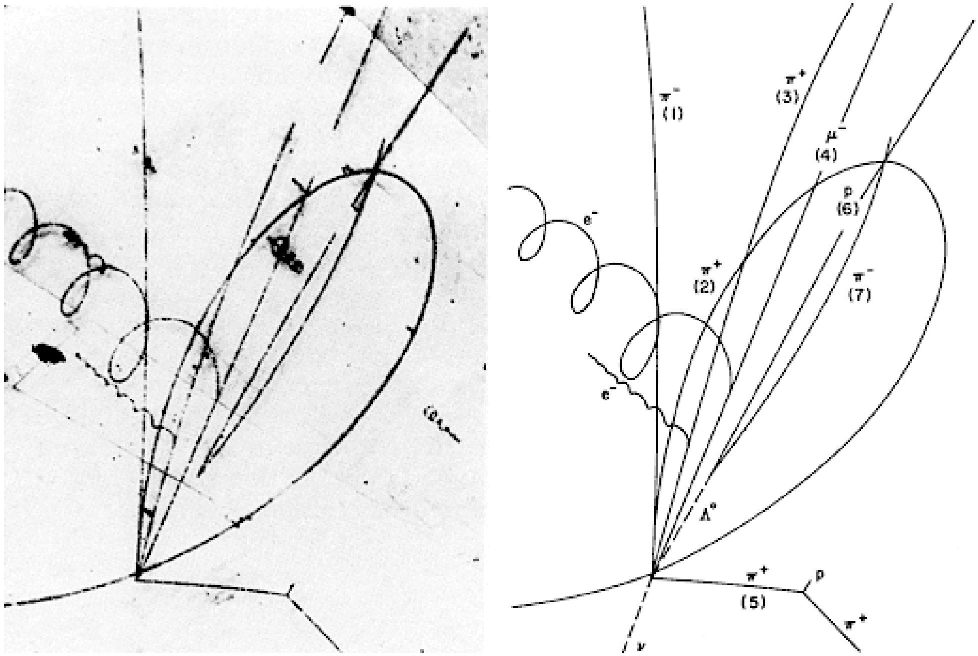

The photograph of the event in the Brookhaven 7-foot bubble chamber which led to the discovery of the charmed baryon (a three-quark particle) is shown at left.

A neutrino enters the picture from below (dashed line) and collides with a proton in the chamber's liquid. The collision produces five charged particles:

A negative muon, three positive pions, and a negative pion and a neutral lambda.

The lambda produces a characteristic 'V' when it decays into a proton and a pi-minus.

The momenta and angles of the tracks together imply that the lambda and the four pions produced with it have come from the decay of a charmed sigma particle, with a mass of about 2.4 GeV.

Bubble Chamber

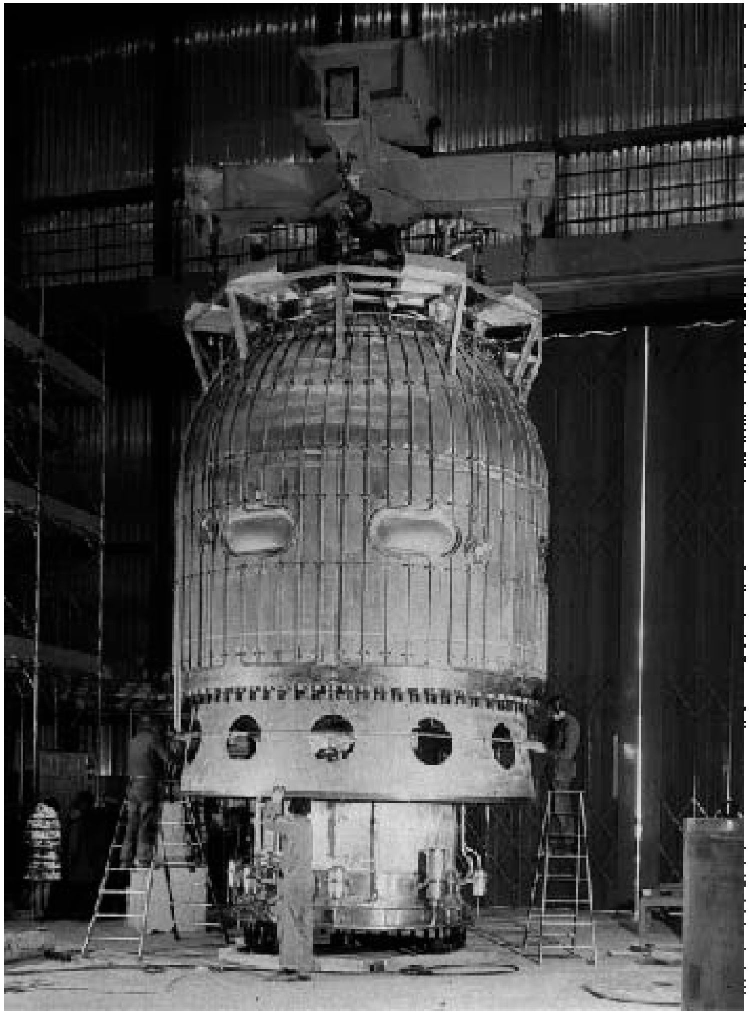

3.7 meter hydrogen bubble chamber at CERN, equipped with the largest superconducting magnet in the world.

During its working life from 1973 to 1984, the "Big European Bubble Chamber" (BEBC) took over 6 million photographs.

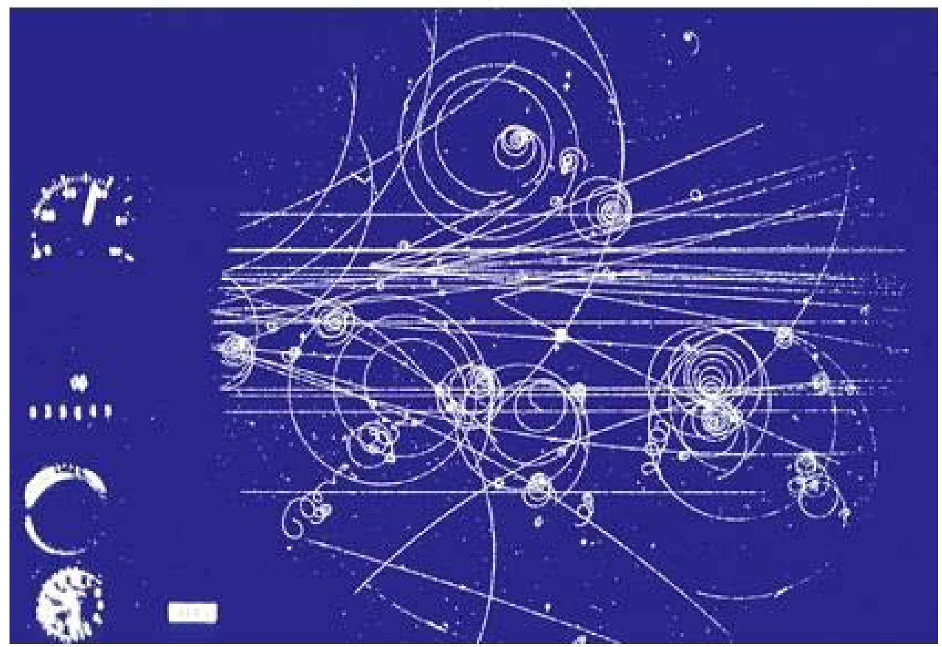

Can be seen outside the Microcosm Exhibition

Bubble Chambers

The excellent position (5μm) resolution and the fact that target and detecting volume are the same (H chambers) makes the Bubble chamber almost unbeatable for reconstruction of complex decay modes.

The drawback of the bubble chamber is the low rate capability (a few tens/ second). E.g. LHC 10^9 collisions/s.

The fact that it cannot be triggered selectively means that every interaction must be photographed.

Analyzing the millions of images by 'operators' was a quite laborious task.

That's why electronics detectors took over in the 70ties.

Logic and Electronics

Early Days of 'Logic Detectors'

Scintillating Screen:

Rutherford Experiment 1911, Zinc Sulfide screen was used as detector.

If an alpha particle hits the screen, a flash can be seen through the microscope.

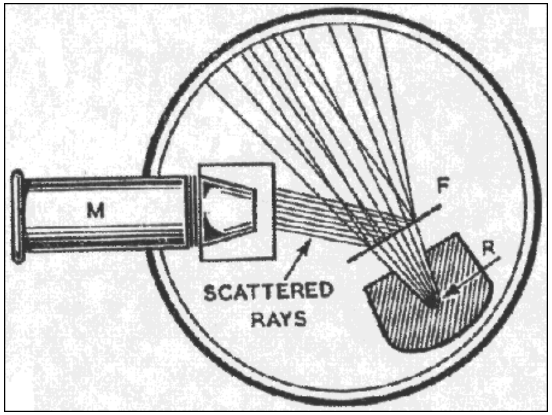

Electroscope:

When the electroscope is given an electric charge the two 'wings' repel each other and stand apart.

Radiation can ionize some of the air in the electroscope and allow the charge to leak away, as shown by the wings slowly coming back together.

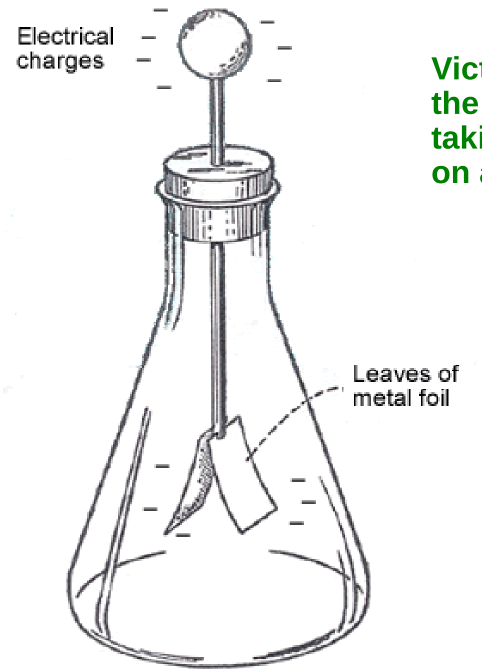

Victor Hess discovered the Cosmic Rays by taking an electroscope on a Balloon

Geiger Rutherford

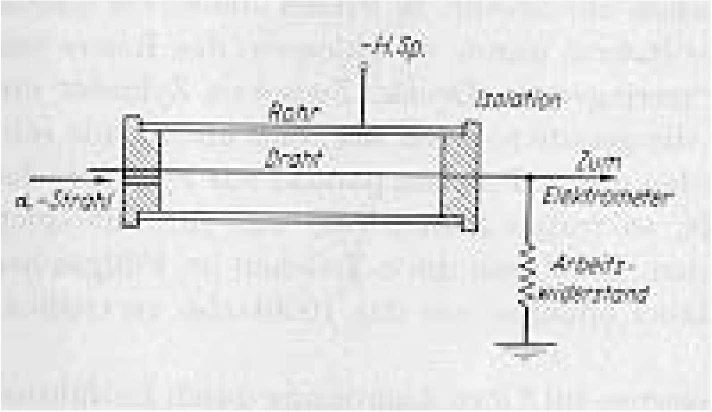

Rutherford and Geiger 1908

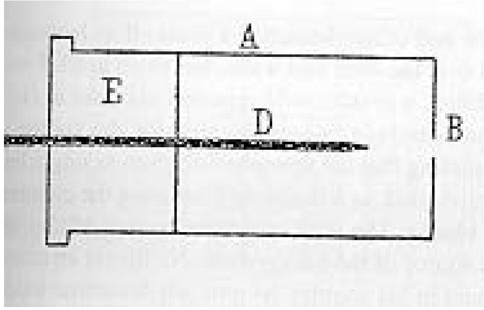

Tip counter, Geiger 1913

In 1908, Rutherford and Geiger developed an electric device to measure alpha particles.

The alpha particles ionize the gas, the electrons drift to the wire in the electric field and they multiply there, causing a large discharge which can be measured by an electroscope.

The 'random discharges' in absence of alphas were interpreted as 'instability', so the device wasn't used much.

As an alternative, Geiger developed the tip counter, that became standard for radioactive experiments for a number of years.

Detector + Electronics 1925

‘Über das Wesen des Compton Effekts’
W. Bothe, H. Geiger, April 1925

Bohr, Kramers, Slater Theorie:

Energy is only conserved statistically testing Compton effect

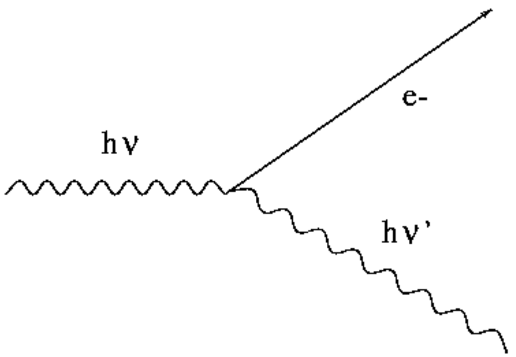

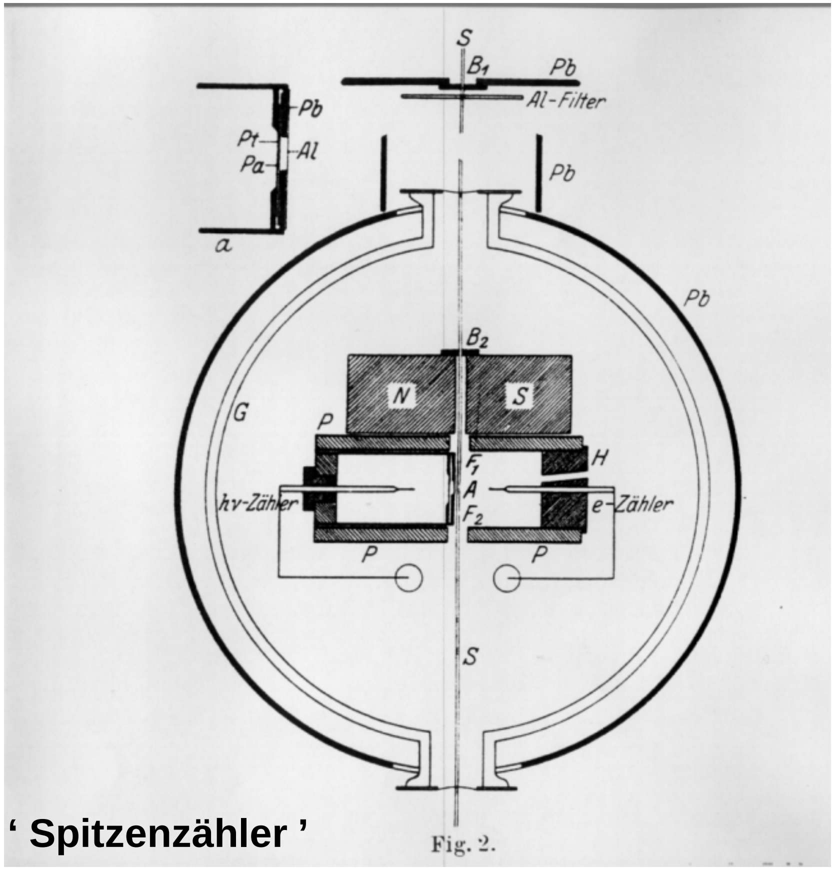

‘ Spitzenzähler ’

Fig. 2.

Detector + Electronics 1925

‘Über das Wesen des Compton Effekts’, W. Bothe, H. Geiger, April 1925

- **‘’Electronics’’:**
  - **Cylinders ‘P’ are on HV.**
  - **The needles of the counters are insulated and connected to electrometers.**
- **Coincidence Photographs:**
  - **A light source is projecting both electrometers on a moving film role.**
  - **Discharges in the counters move the electrometers , which are recorded on the film.**
  - **The coincidences are observed by looking through many meters of film.**

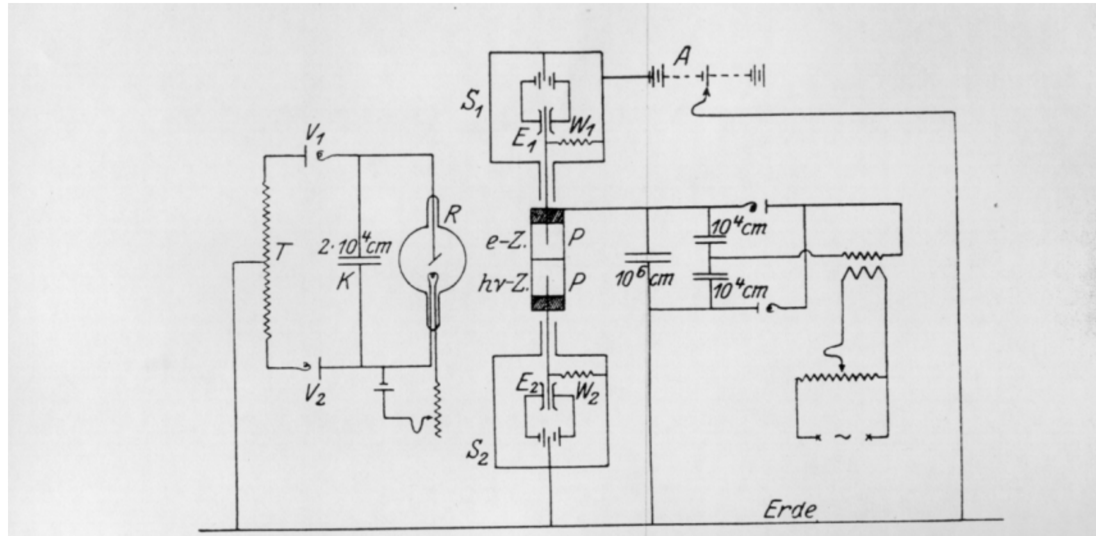

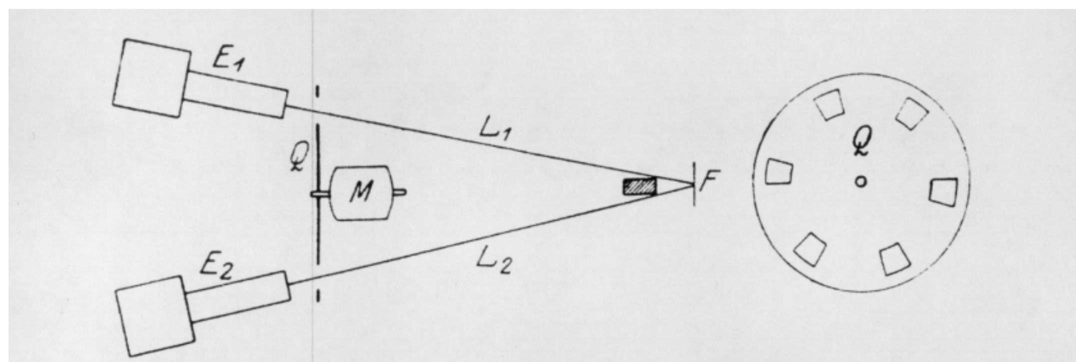

Fig. 4. Photographische Registrierung.

Detector + Electronics 1929

In 1928 Walther Müller started to study the sponteneous discharges systematically and found that they were actually caused by cosmic rays discovered by Victor Hess in 1911.

By realizing that the wild discharges were not a problem of the counter, but were caused by cosmic rays, the Geiger-Müller counter went, without altering a single screw from a device with 'fundametal limits' to the most sensitive intrument for cosmic rays physics.

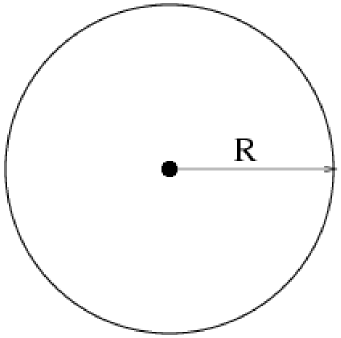

'Zur Vereinfachung von Koinzidenzzählungen'
W. Bothe, November 1929

Coincidence circuit for 2 tubes

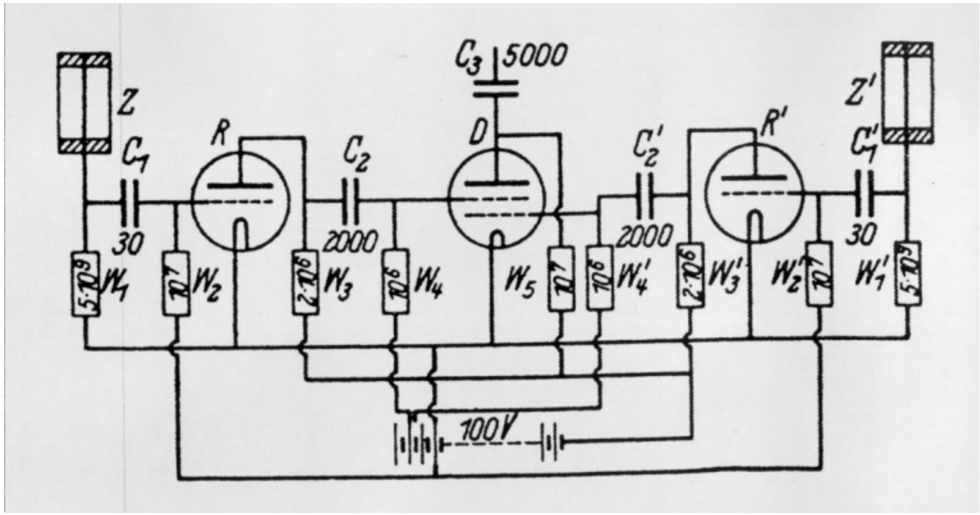

1930 - 1934

Rossi 1930: Coincidence circuit for n tubes

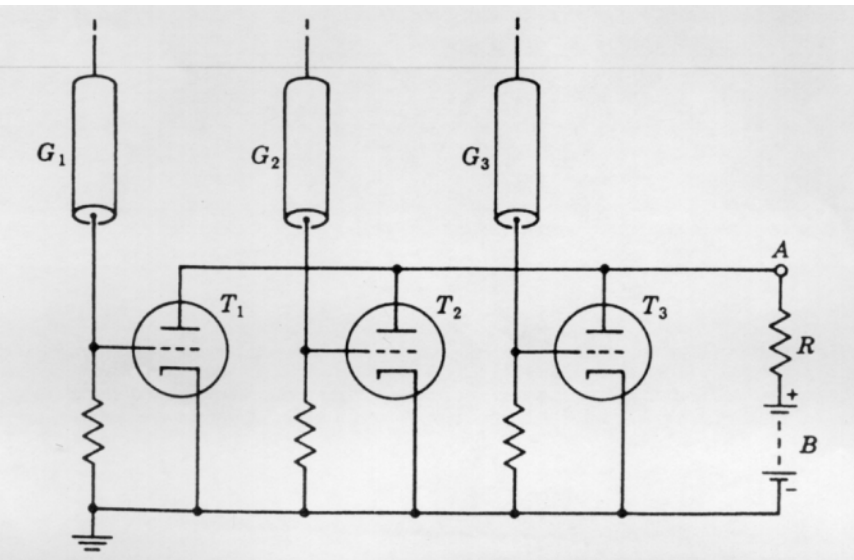

Cosmic ray telescope 1934

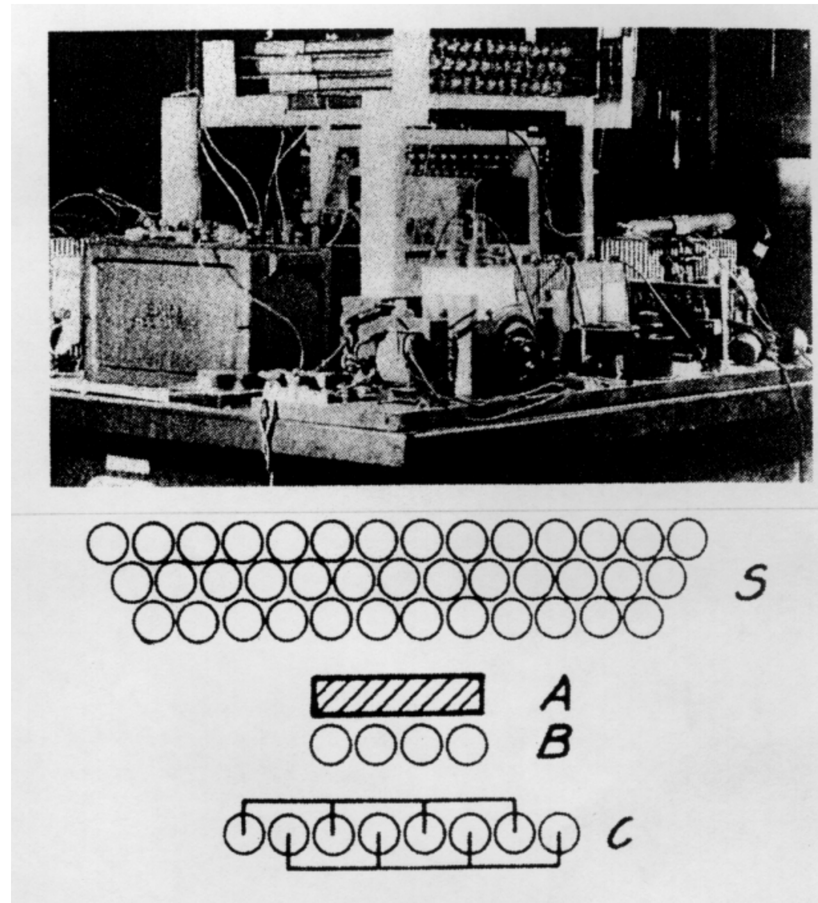

Geiger Counters

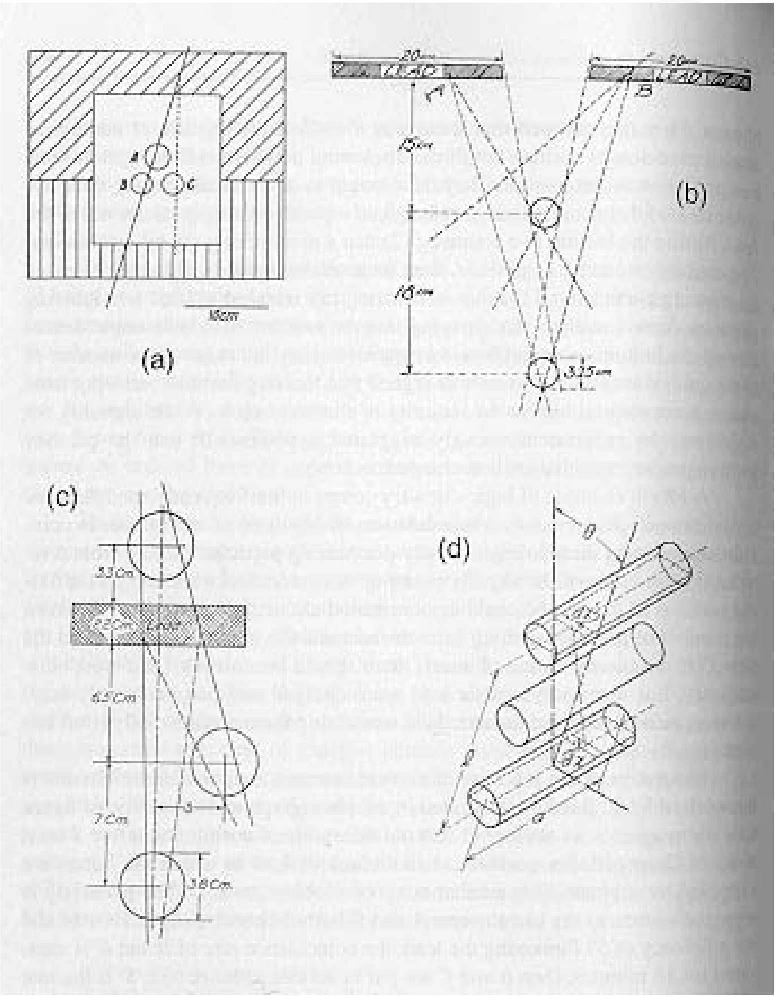

By performing coincidences of Geiger Müller tubes e.g. the angular distribution of cosmic ray particles could be measured.

Scintillators, Cerenkov light, Photomultipliers

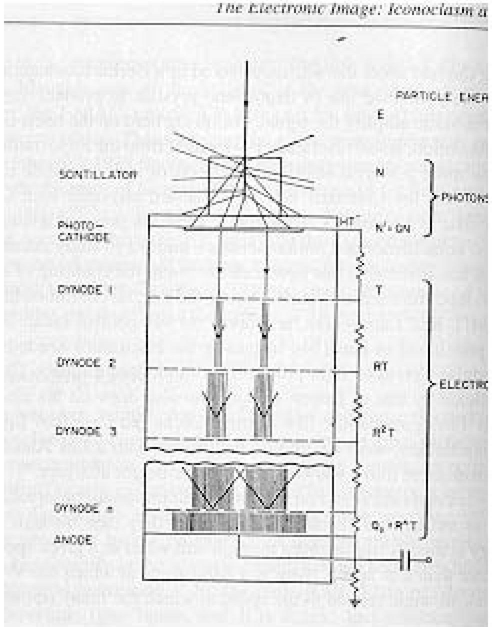

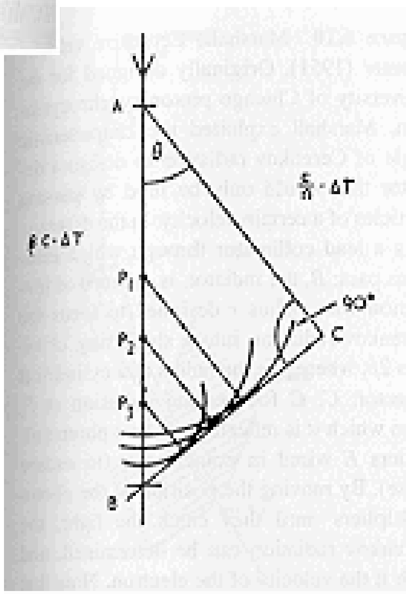

In the late 1940ies, scintillation counters and Cerenkov counters exploded into use.

Scintillation of materials on passage of particles was long known.

By mid 1930 the bluish glow that accompanied the passage of

radioactive particles through liquids was analyzed and largely explained

(Cerenkov Radiation).

Mainly the electronics revolution begun during the war initiated this development.

High-gain photomultiplier tubes, amplifiers, scalers, pulse-height analyzers.

Antiproton

One was looking for a negative particle with the mass of the proton. With a bending magnet, a certain particle momentum was selected (p=mv□).

Since Cerenkov radiation is only emitted if v>c/n, two Cerenkov counters (C1, C2) were set up to measure a velocity comparable with the proton mass.

In addition the time of flight between S1 and S2 was required to be between 40 and 51ns, selecting the same mass.

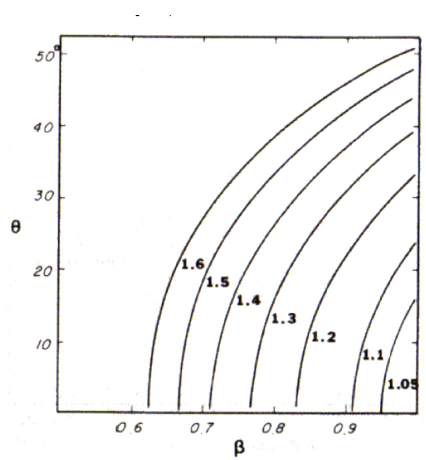

<u>Cerenkov counters:</u>
Use the principle that a particle travelling through a medium faster than the speed of light in that medium emits radiation. Thus they count particles <u>above</u> a certain velocity.

<u>Scintillation counters:</u>
Count amplified radiation bursts emitted when particles pass through. Two were used separated by a large distance to find *distance/time*. Rejecting particles that passed These at the speed of a pion left (hopefully) only antiprotons that registered with this method

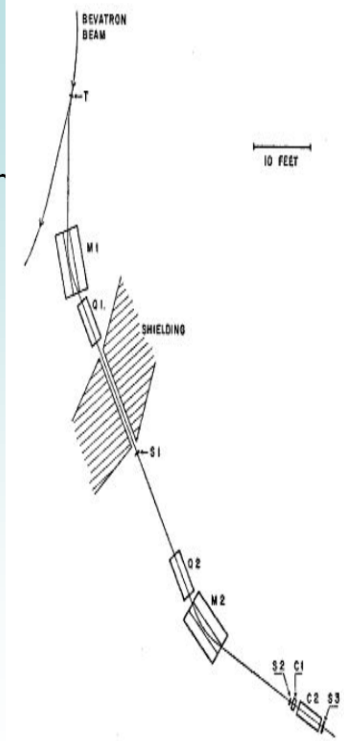

Anti Neutrino Discovery 1959

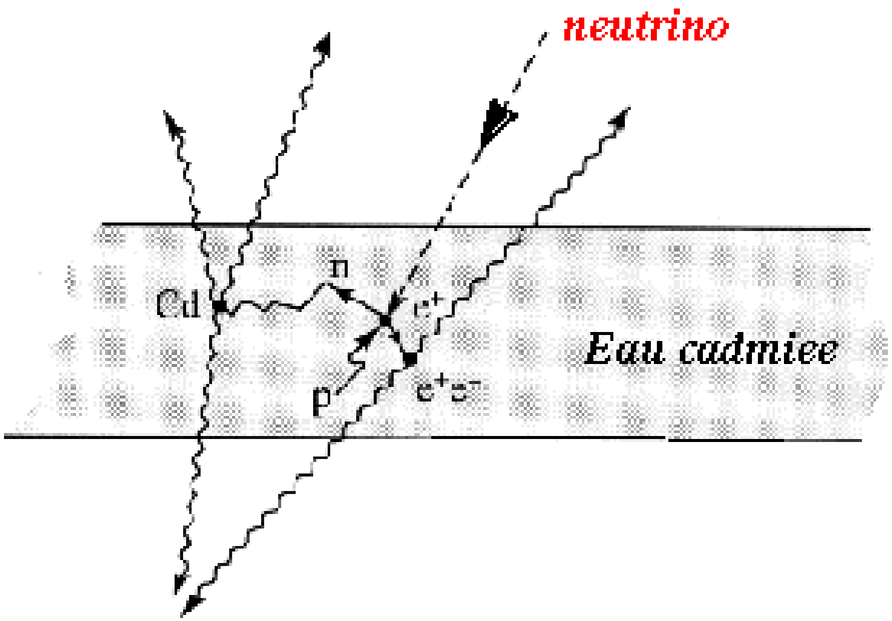

$\overline{\square} + p \rightarrow n + e^{+}$

Reines and Cowan experiment principle consisted in using a target made of around 400 liters of a mixture of water and cadmium chloride.

The anti-neutrino coming from the nuclear reactor interacts with a proton of the target matter, giving a positron and a neutron.

The positron annihilates with an electron of the surrounding material, giving two simultaneous photons and the neutron slows down until it is eventually captured by a cadmium nucleus, implying the emission of photons some 15 microseconds after those of the positron annihilation.

Spark Counters

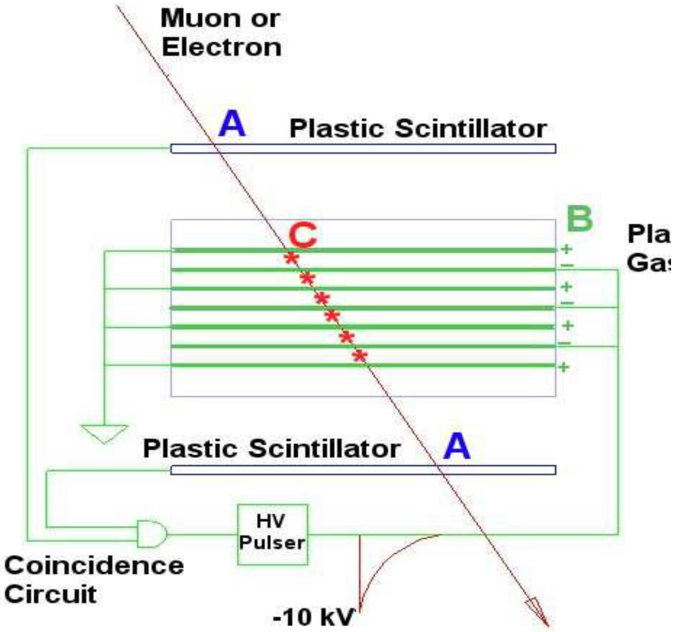

The Spark Chamber was developed in the early 60ies.

Schwartz, Steinberger and Lederman used it in discovery of the muon neutrino

A charged particle traverses the detector and leaves an ionization trail.

The scintillators trigger an HV pulse between the metal plates and sparks form in the place where the ionization took place.

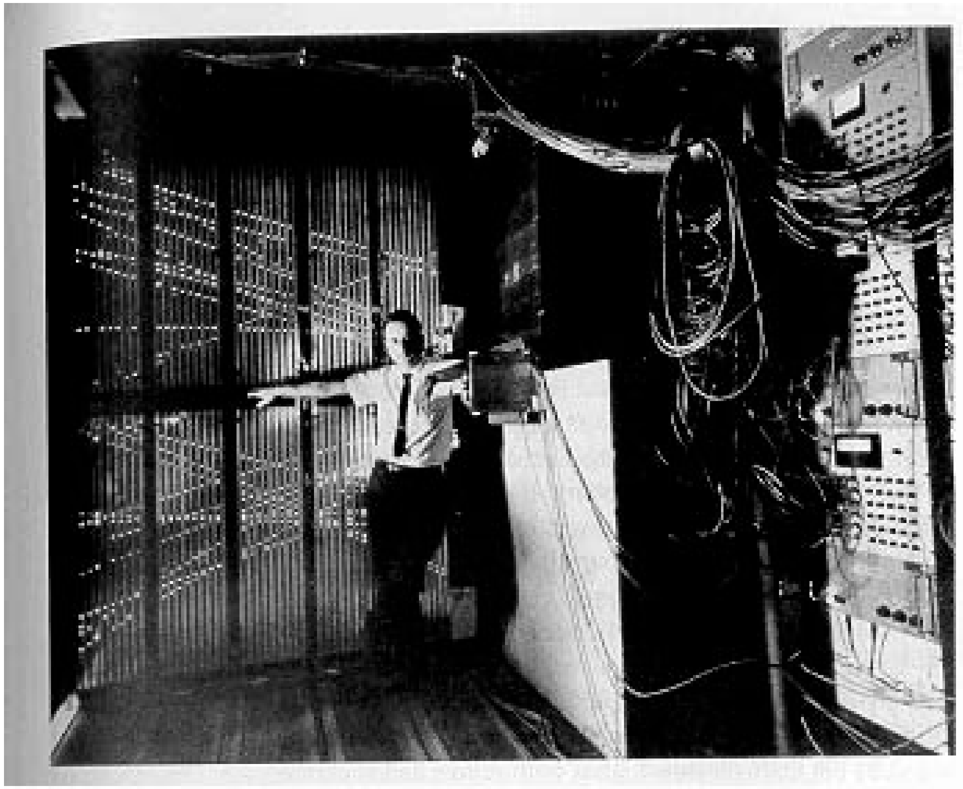

Multi Wire Proportional Chamber

Tube, Geiger- Müller, 1928

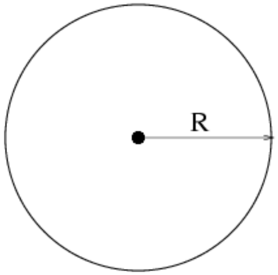

Multi Wire Geometry, in H. Friedmann 1949

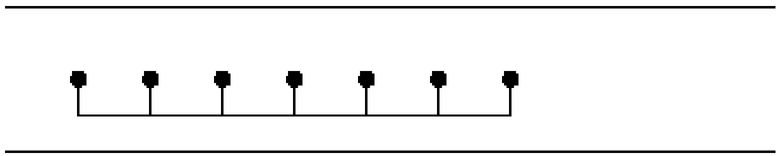

G. Charpak 1968, Multi Wire Proportional Chamber,
readout of individual wires and proportional mode working point.

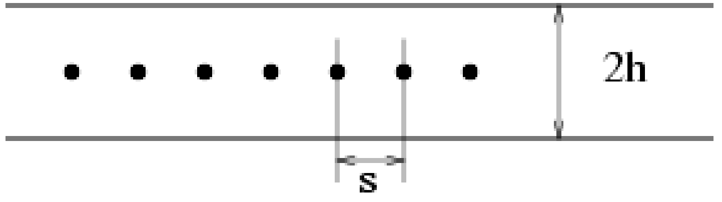

MWPC

Individual wire readout: A charged particle traversing the detector leaves a trail of electrons and ions. The wires are on positive HV. The electrons drift to the wires in the electric field and start to form an avalanche in the high electric field close to the wire. This induces a signal on the wire which can be read out by an amplifier.

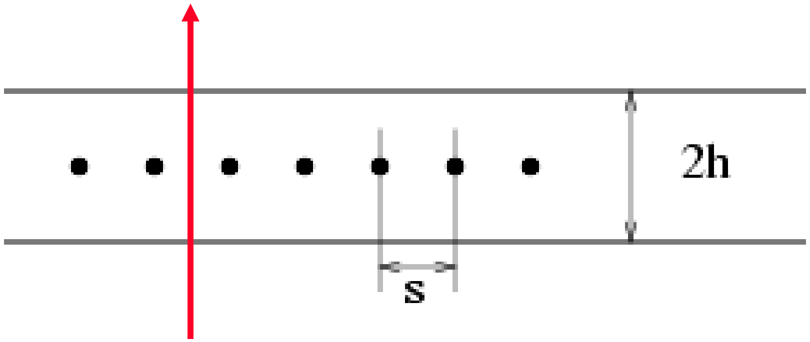

Measuring this drift time, i.e. the time between passage of the particle and the arrival time of the electrons at the wires, made this detector a precision positioning device.

The Electronic Image

During the 1970ies, the Image and Logic devices merged into ‘Electronics Imaging Devices’

W, Z-Discovery 1983/84

UA1 used a very large wire chamber.

Can now be seen in the CERN Microcosm Exhibition

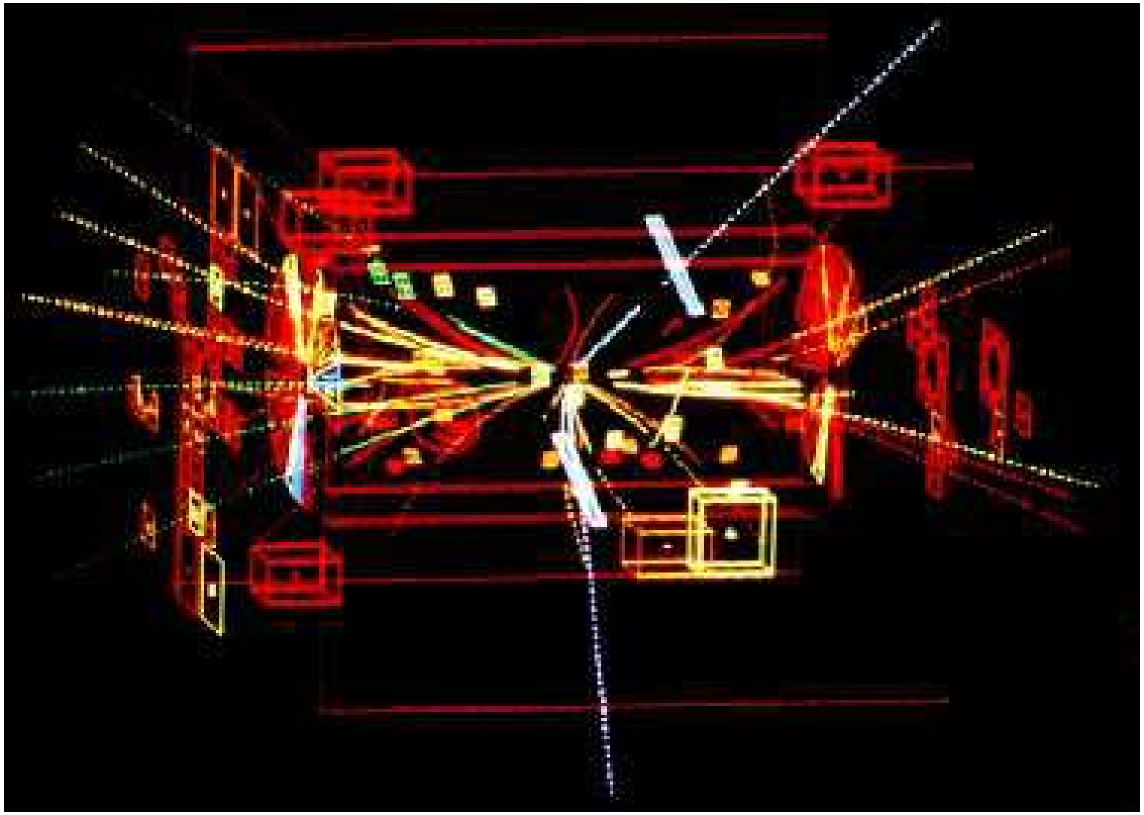

This computer reconstruction shows the tracks of charged particles from the proton-antiproton collision. The two white tracks reveal the Z's decay. They are the tracks of a high-energy electron and positron.

LEP 1988-2000

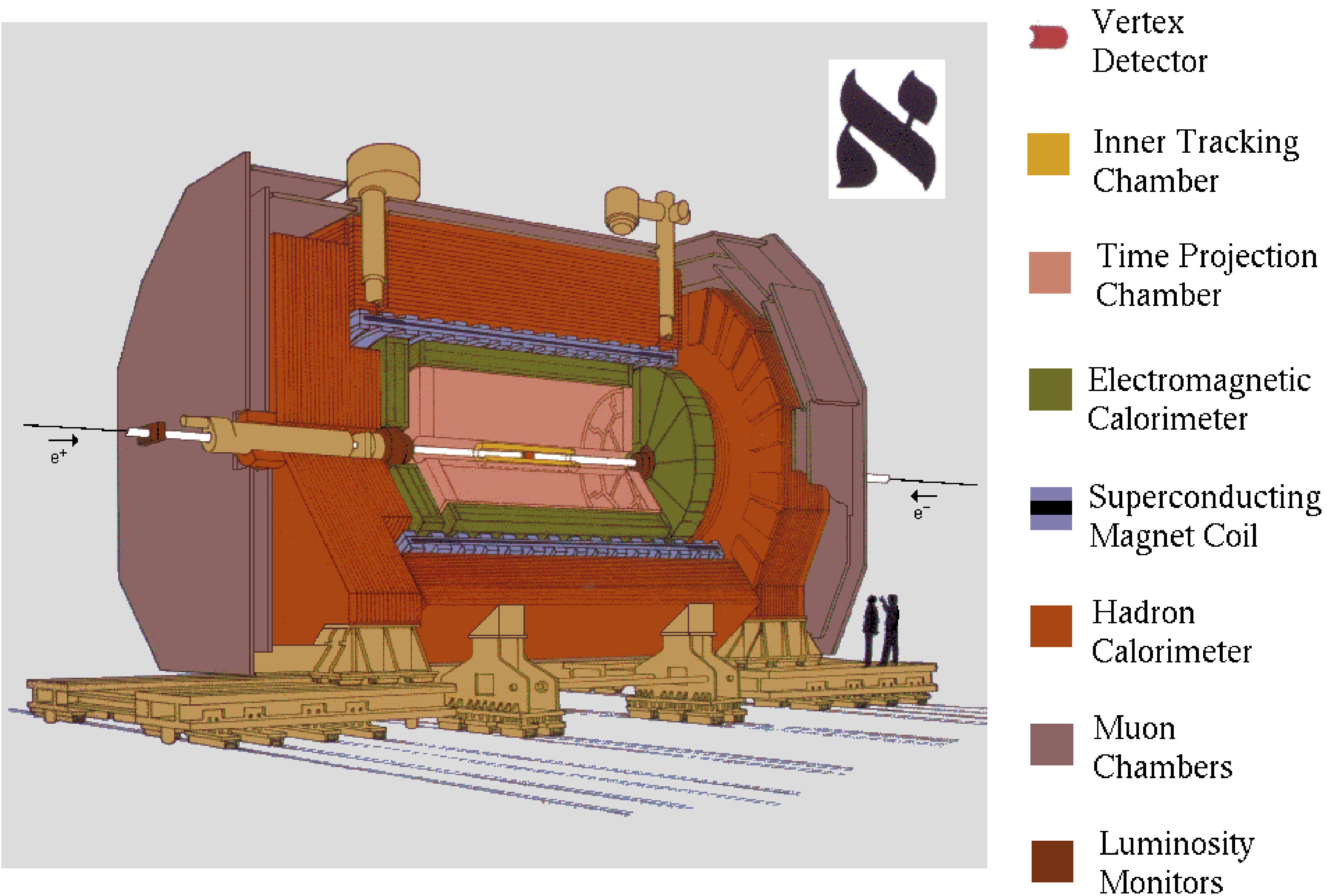

The ALEPH Detector

All Gas Detectors

LEP 1988-2000

Aleph Higgs Candidate Event: $e^+ e^- \rightarrow HZ \rightarrow b\bar{b} + jj$

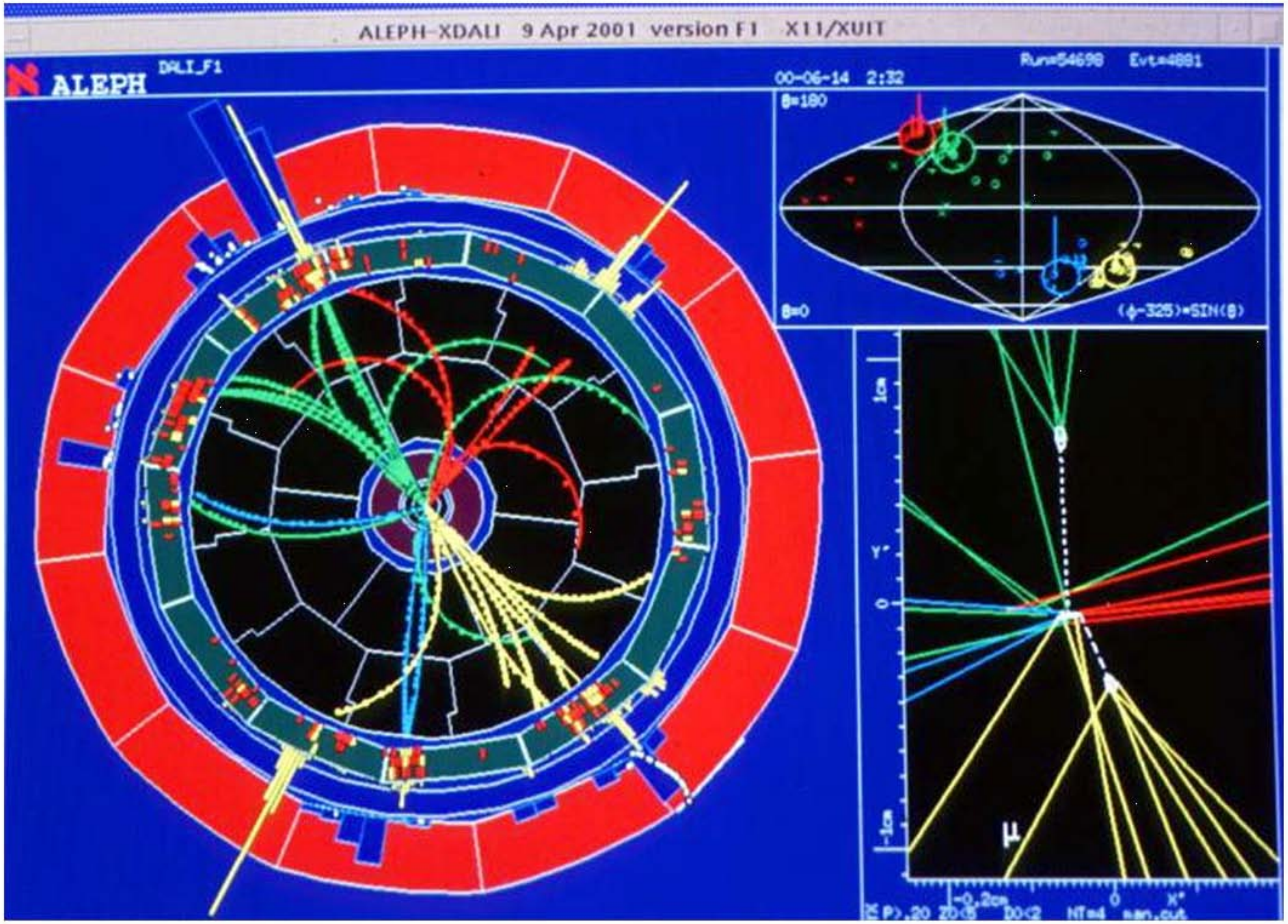

Increasing Multiplicities in Heavy Ion Collisions

e+ e- collision in the ALEPH Experiment/LEP.

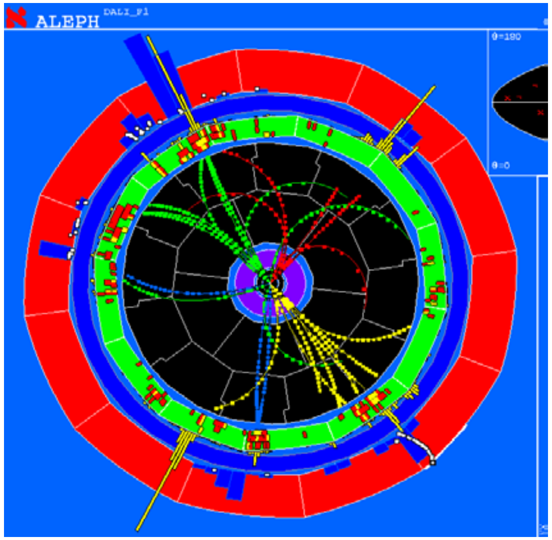

Au+ Au+ collision in the STAR Experiment/RHIC

Up to 2000 tracks

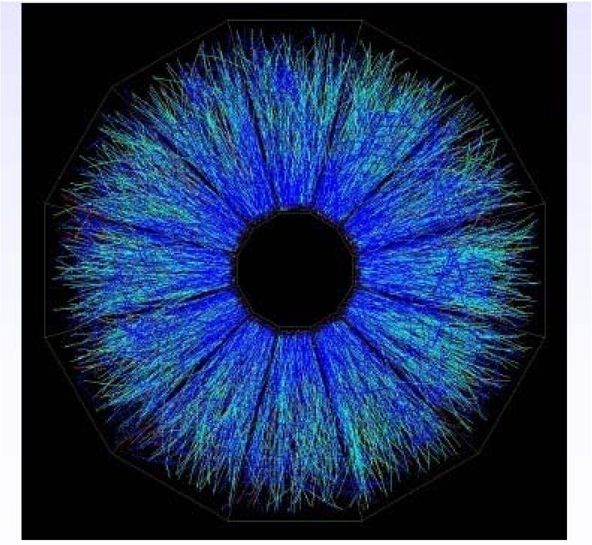

Pb+ Pb+ Kollision in the ALICE Experiment/LHC

Simulation for

Angle Θ=60 to 62º

Up to 40 000 tracks/collision

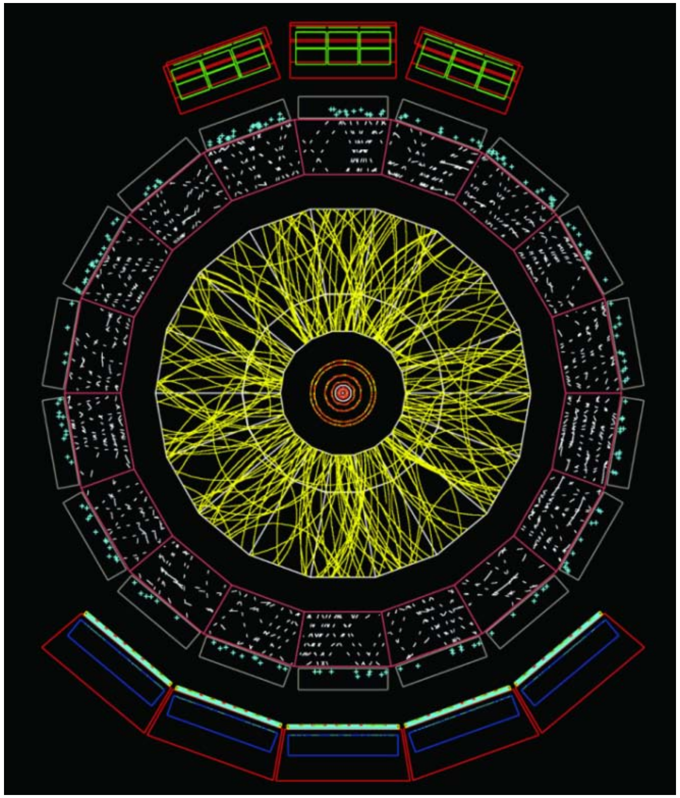

ATLAS at LHC

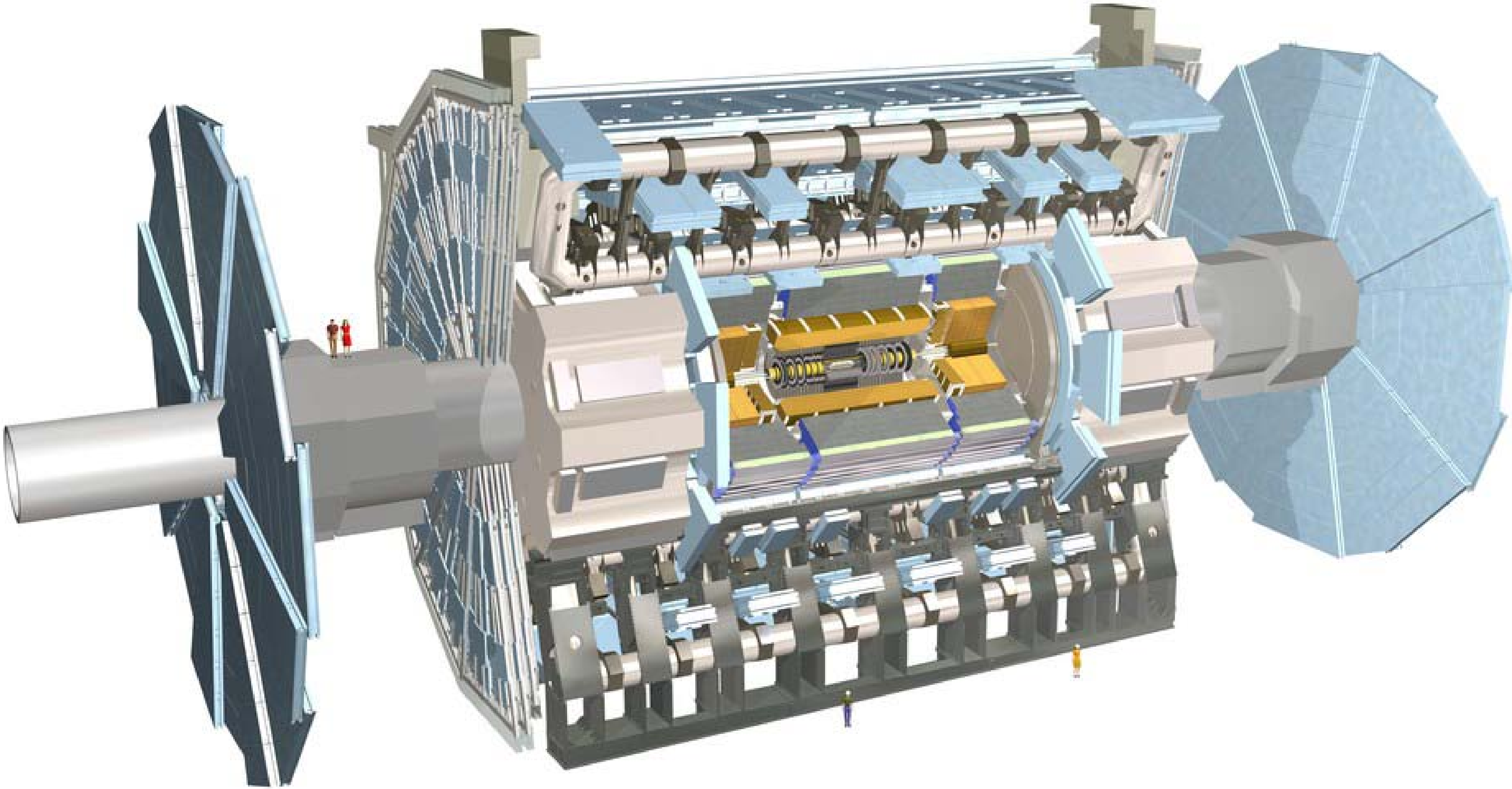

Large Hadron Collider at CERN.

The ATLAS detector uses more than 100 million detector channels.

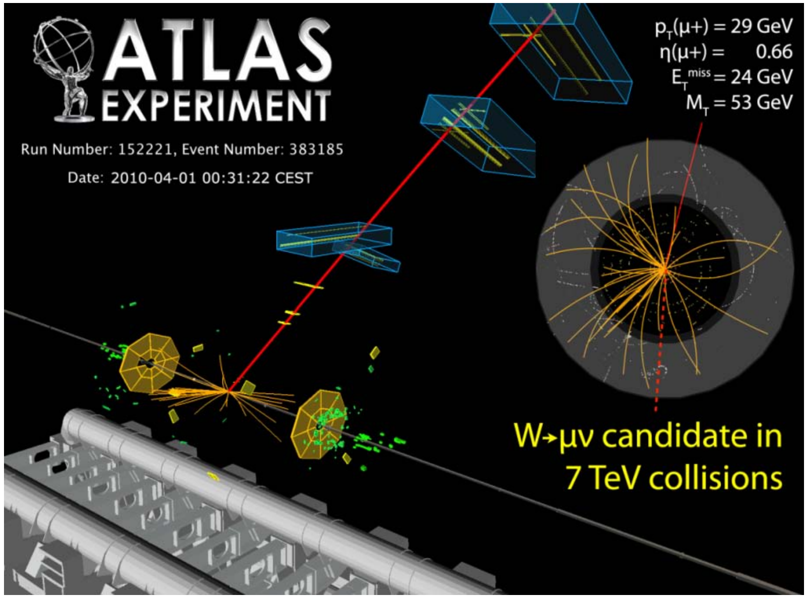
ATLAS EXPERIMENT
Run Number: 152221, Event Number: 383185
Date: 2010-04-01 00:31:22 CEST
$p_T(\mu+)$ = 29 GeV
$\eta(\mu+)$ = 0.66
E_T^{miss} = 24 GeV
M_T = 53 GeV
W→μν candidate in
7 TeV collisions

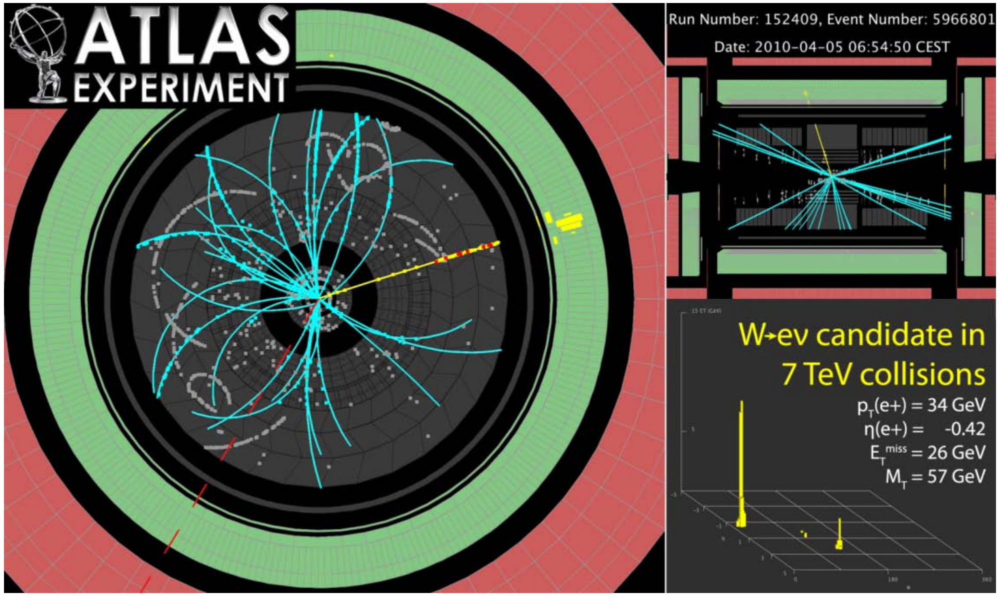
ATLAS EXPERIMENT
Run Number: 152409, Event Number: 5966801
Date: 2010-04-05 06:54:50 CEST
W→eν candidate in
7 TeV collisions
$p_T(e+)$ = 34 GeV
$\eta(e+)$ = -0.42
E_T^{miss} = 26 GeV
M_T = 57 GeV

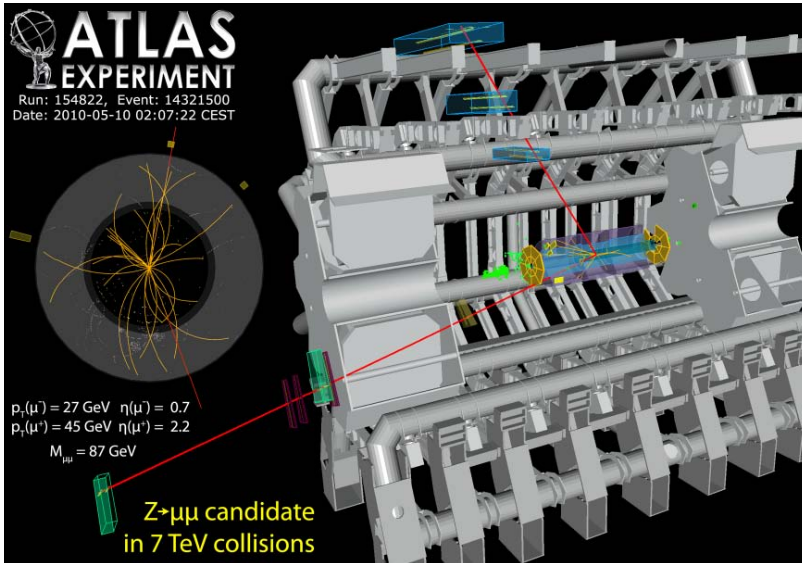
ATLAS EXPERIMENT
Run: 154822, Event: 14321500
Date: 2010-05-10 02:07:22 CEST
$p_T(\mu^-)$ = 27 GeV $\eta(\mu^-)$ = 0.7
$p_T(\mu^+)$ = 45 GeV $\eta(\mu^+)$ = 2.2
$M_{\mu\mu}$ = 87 GeV
Z→μμ candidate
in 7 TeV collisions

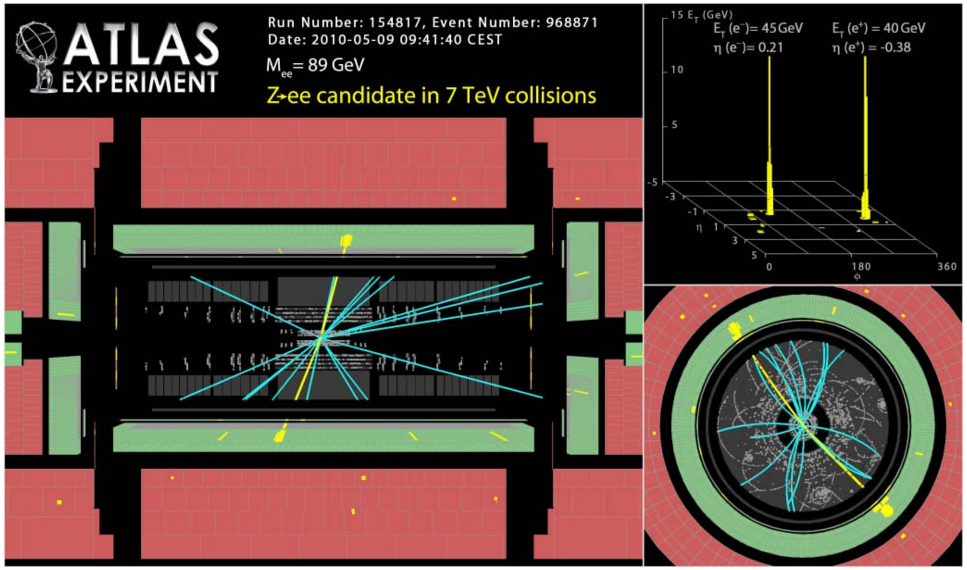
ATLAS EXPERIMENT
Run Number: 154817, Event Number: 968871
Date: 2010-05-09 09:41:40 CEST
M_{ee} = 89 GeV
Z→ee candidate in 7 TeV collisions
E_T (GeV)
$E_T(e^-)$= 45 GeV
$\eta(e^-)$= 0.21
$E_T(e^+)$ = 40 GeV
$\eta(e^+)$ = -0.38
η
φ

Near Future: CMS Experiment at LHC

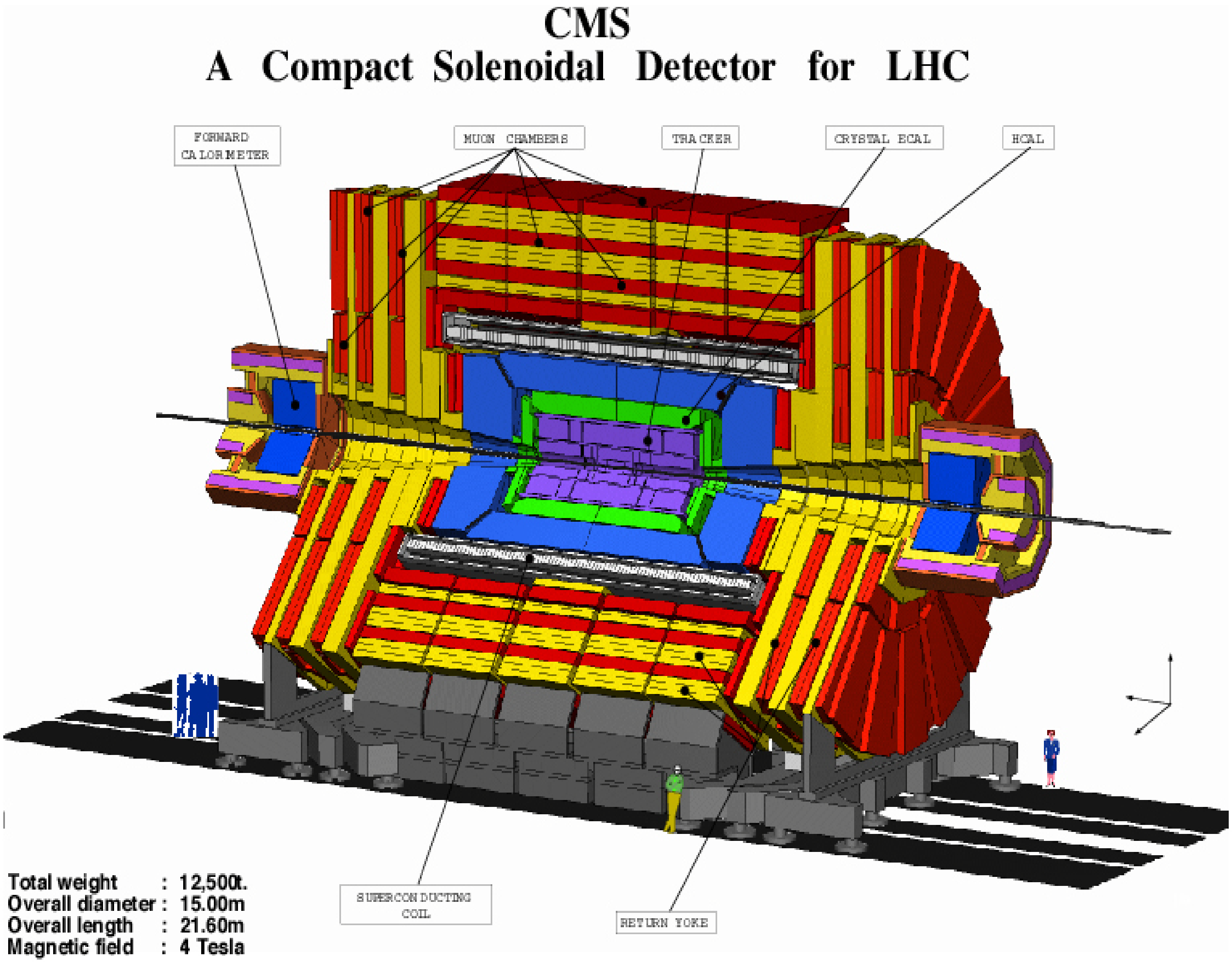

Summary

- Particle physics, 'born' with the discovery of radioactivity and the electron at the end of the 19^{th} century, has become 'Big Science' during the last 100 years.

- A large variety of instruments and techniques were developed for studying the world of particles.

- Imaging devices like the cloud chamber, emulsion and the bubble chamber took photographs of the particle tracks.

- Logic devices like the Geiger Müller counter, the scintillator or the Cerenkov detector were (and are) widely used.

- Through the electronic revolution and the development of new detectors, both traditions merged into the 'electronics image' in the 1970ies.

- Particle detectors with over 100 million readout channels are operating at this moment.

Signal Formation in Particle Detectors

Werner Riegler, CERN, werner.riegler@cern.ch

II Seminario Nazionale Rivelatori Innovativi

18-22 October 2010, Trieste

Lecture2/3

Signal Theorems

Signals in Detectors

Although the principles and formulas are well known since a long time, there exists considerable confusion about this topic.

This is probably due to different vocabulary in different detector traditions and also due to the fact that the signal explanations in many (or most !) textbooks on particle detectors are simply wrong.

Creation of the Signal

From a modern detector text book:

… It is important to realize that the signals from wire chambers operating in proportional mode are primarily generated by *induction* due to the moving charges rather than by the *collection* of these charges on the electrodes …

… When a charged […] particle traverses the gap, it ionizes the atoms […]. Because of the presence of an electric field, the electrons and ions created in this process drift to their respective electrodes. The charge collected at these electrodes forms the […] signal, in contrast to gaseous detectors described above, where the signal corresponds to the current *induced* on the electrodes by the drifting charges (ions). …

These statements are completely wrong !

***All* signals in particle detectors are due to *induction* by moving charges. Once the charges have arrived at the electrodes the signals are 'over'.**

Signals in Detectors

Signals induced on grounded electrodes:

S. Ramo, Currents induced by electron motion, Proc. IRE 27 (1939)

W. Shockley, 1938, Currents to Conductors Induced by a Moving Point Charge, Journal of Applied Physics, vol. 9 (1938) 635

Signals induced on electrodes connected by impedance elements:

E. Gatti, G. Padovini and V. Radeka, Signal evaluation in multielectrode radiation detectors by means of a time dependent weighting vector, Nucl. Instr. and Meth. 193 (1982) 651

Signals induced on electrodes embedded in materials with finite conductivity and connected with arbitrary impedance elements:

W. Riegler, Extended theorems for signal induction in particle detectors, Nucl. Instr. and Meth. A 535 (2004) 287.

Creation of the Signal

Charged particles leave a trail of charges (and excited atoms) along their path: Electron-Ion pairs in gases and liquids, electron hole pairs in solids.

Photons from de-excitation are usually converted to electrons for detection.

The produced charges can be registered → Position measurement → Time measurement → Tracking Detectors ....

Cloud Chamber: Charges create drops → photography.
Bubble Chamber: Charges create bubbles → photography.
Emulsion: Charges 'blacked' the film.
Spark Chamber: Charges produce a conductive channel that create a discharge → photography

Gas and Solid State Detectors: Moving Charges (electric fields) induce electronic signals on metallic electrodes that can be read by dedicated electronics.

→In solid state detectors the charge created by the incoming particle is sufficient (not exactly correct, in Avalanche Photo Diodes one produces avalanches in a solid state detector)

→In gas detectors (e.g. wire chamber) the charges are internally multiplied in order to provide a measurable signal.

Cloud Chamber, C.T.R. Wilson 1910

Charges act as condensation nuclei in supersaturated water vapor

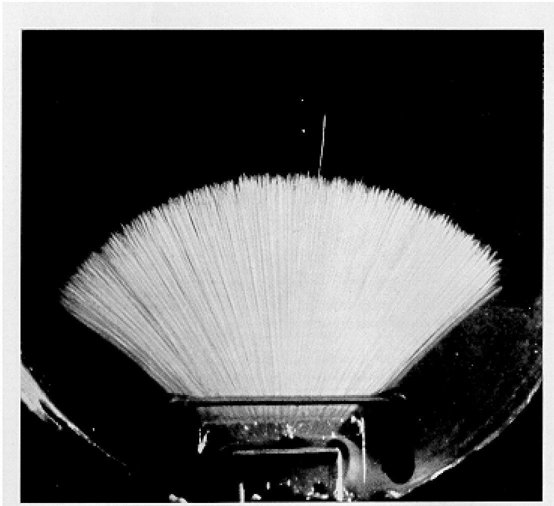

Fig. 13. K. Philipp, Naturwiss. 14, 1203 (1926).

Alphas, Philipp 1926

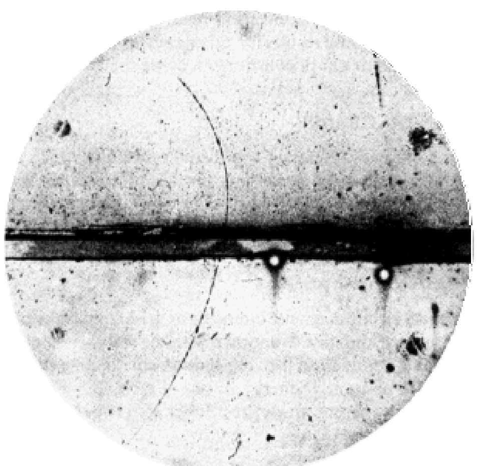

Positron discovery, Carl Andersen 1933

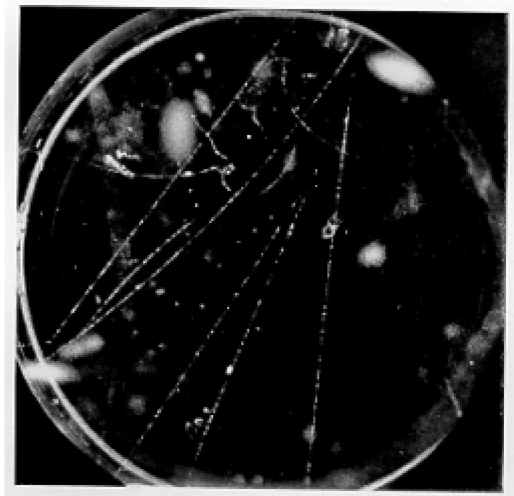

Plate 115

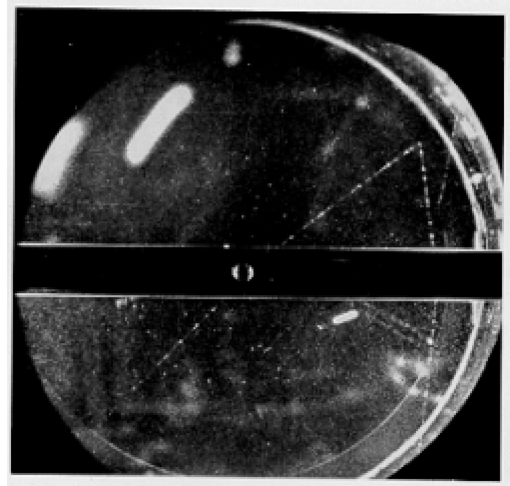

Plate 116

V- particles, Rochester and Wilson, 1940ies

Nuclear Emulsion, M. Blau 1930ies

Charges initiate a chemical reaction that blackens the emulsion (film)

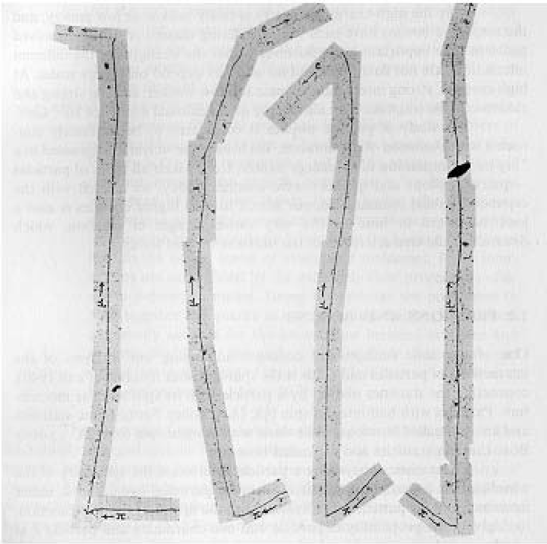

C. Powell, Discovery of muon and pion, 1947

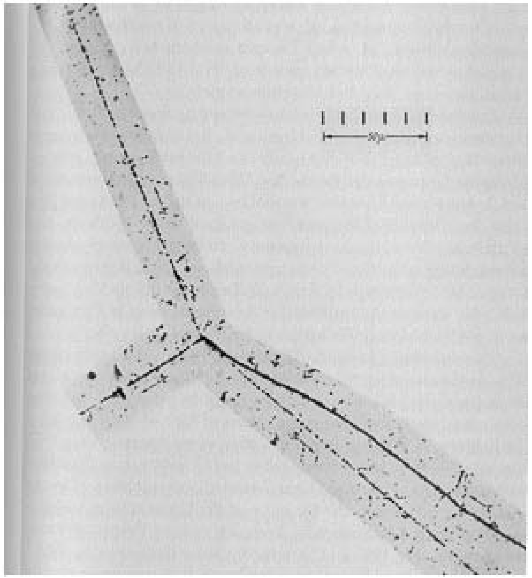

Kaon Decay into 3 pions, 1949

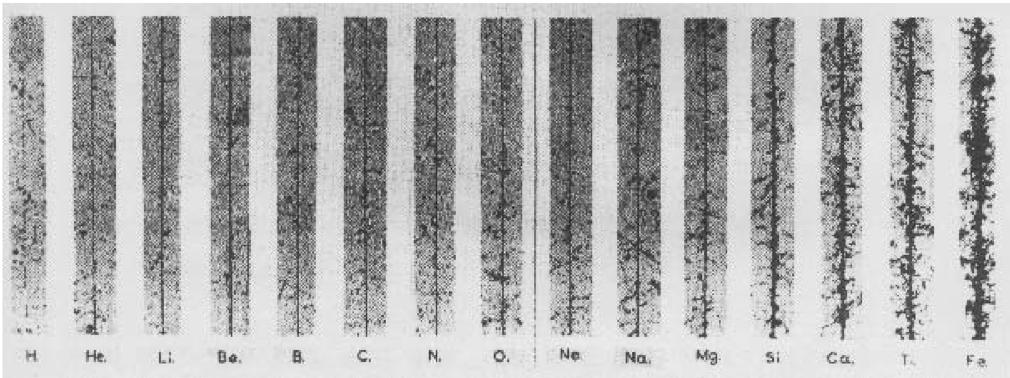

Cosmic Ray Composition

Bubble Chamber, D. Glaser 1952

Charges create bubbles in superheated liquid, e.g. propane or Hydrogen (Alvarez)

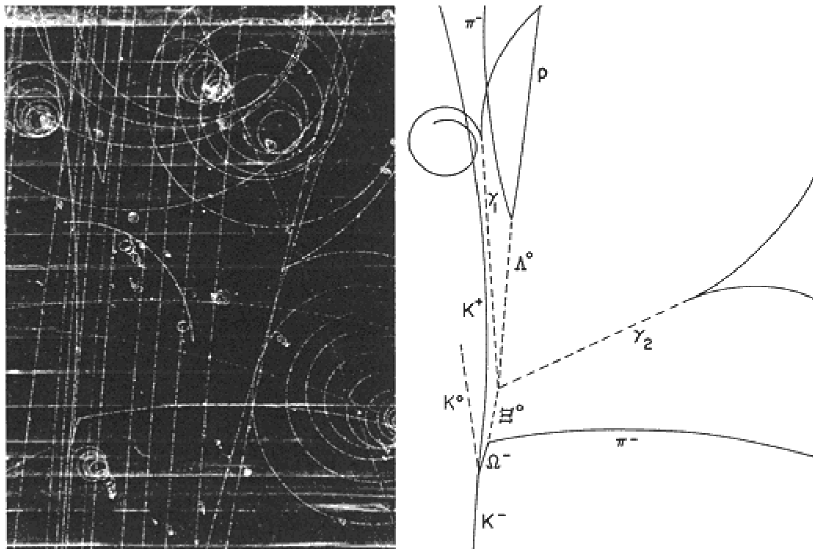

Discovery of the Ω^- in 1964

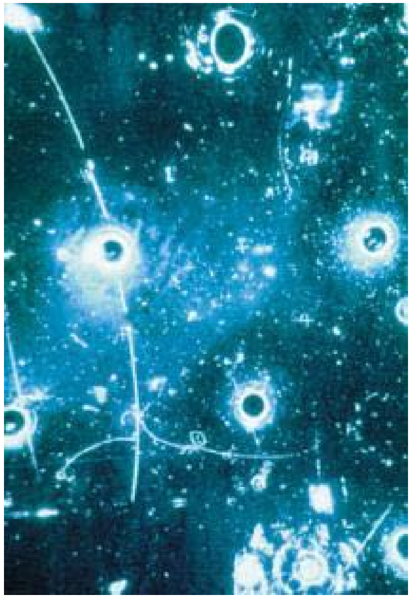

Neutral Currents 1973

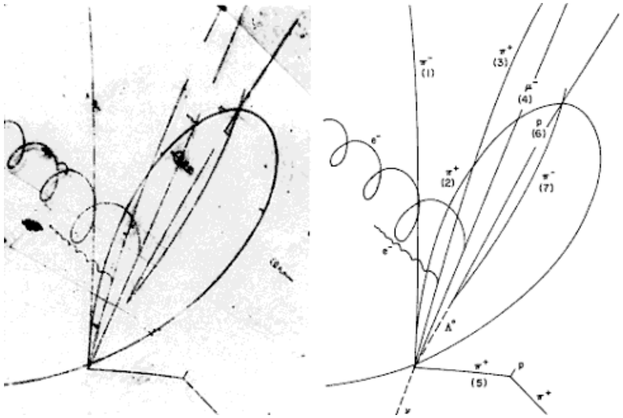

Charmed Baryon, 1975

Spark Chamber, 1960ies

Charges create 'conductive channel' which initiates a spark in case HV is applied.

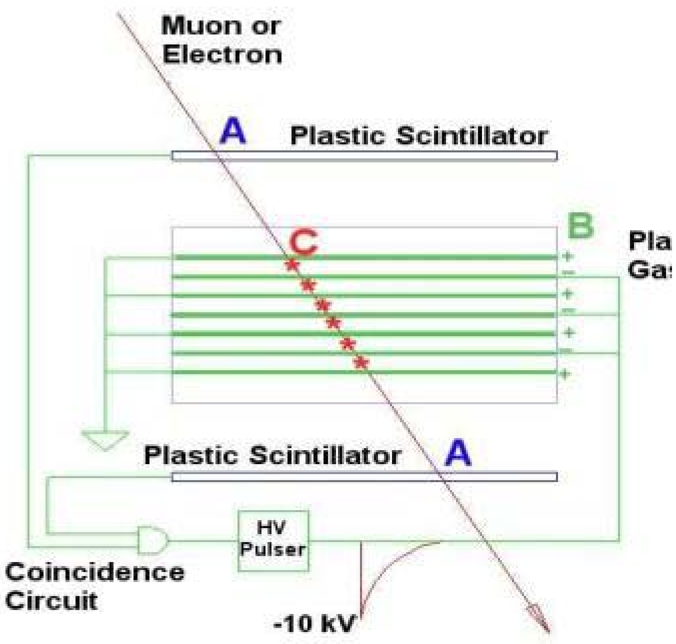

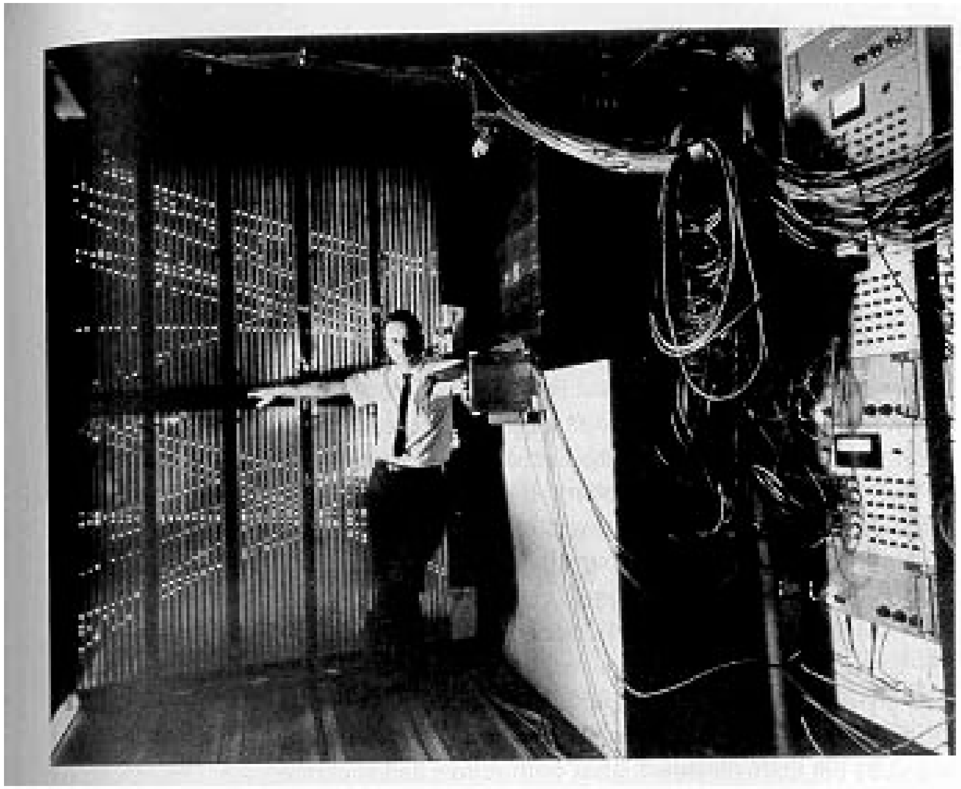

Discovery of the Muon Neutrino 1960ies

Tip Counter, Geiger 1914

Charges create a discharge of a needle which is at HV with respect to a cylinder.

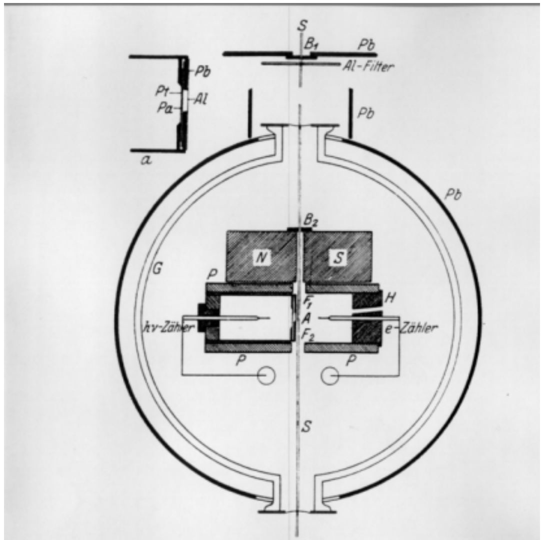

Fig. 2.

The needle is connected to an electroscope that can detect the produced charge.

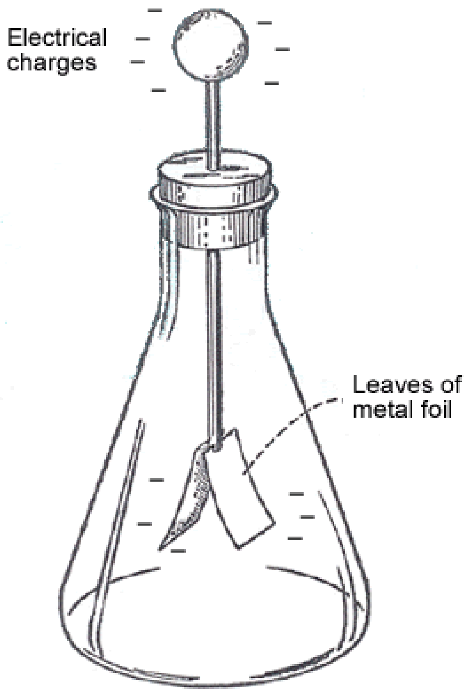

Electric Registration of Geiger Müller Tube Signals

Charges create a discharge in a cylinder with a thin wire set to HV. The charge is measured with a electronics circuit consisting of tubes → electronic signal.

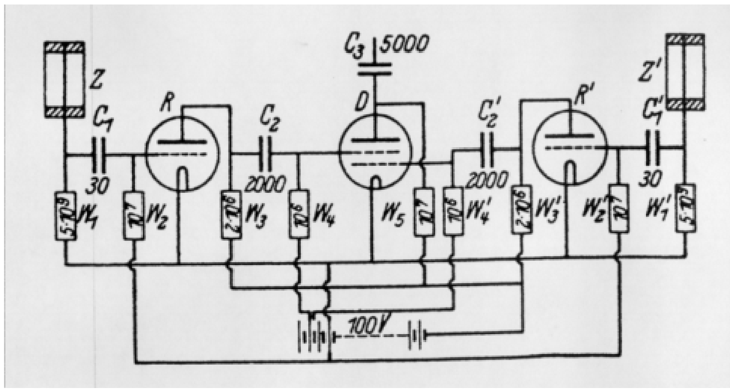

W. Bothe, 1928

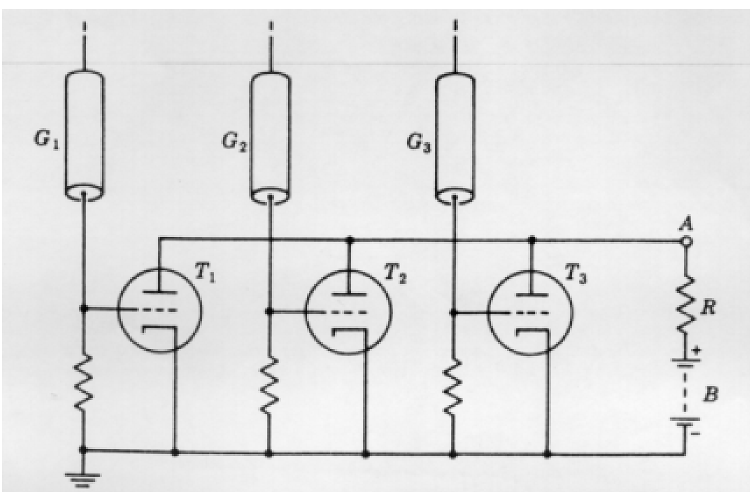

B. Rossi, 1932

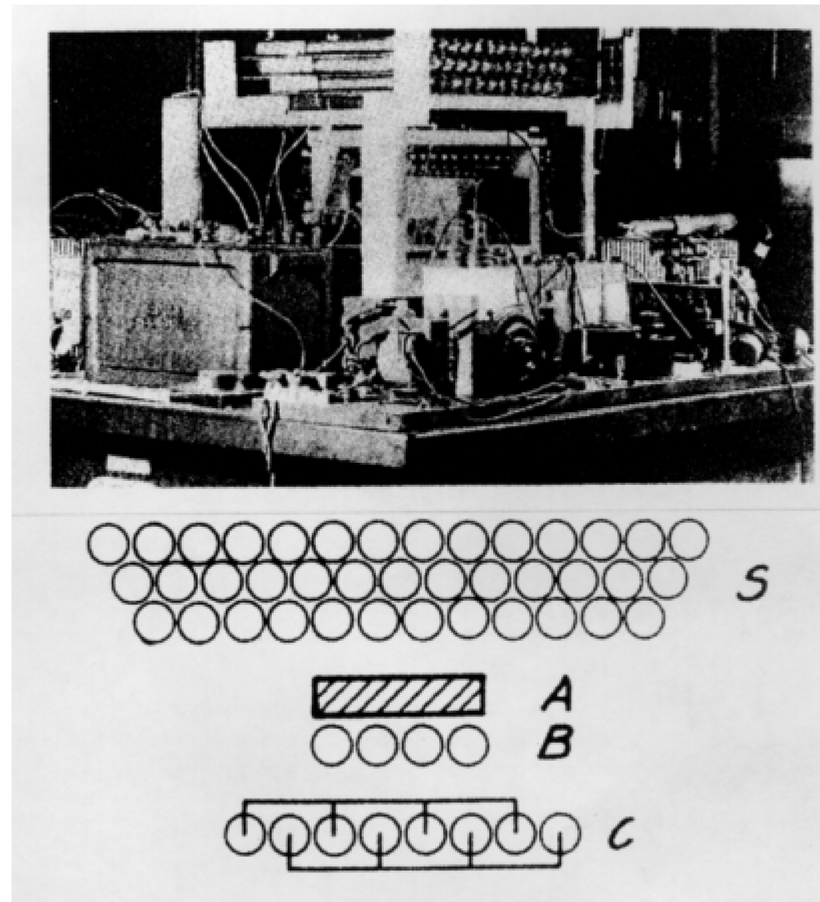

Cosmic Ray Telescope 1930ies

Ionization Chambers, Wire Chambers, Solid State Detectors

!The movement of charges in electric fields induces signals on readout electrodes (No discharge, there is no charge flowing from cathode to Anode) !

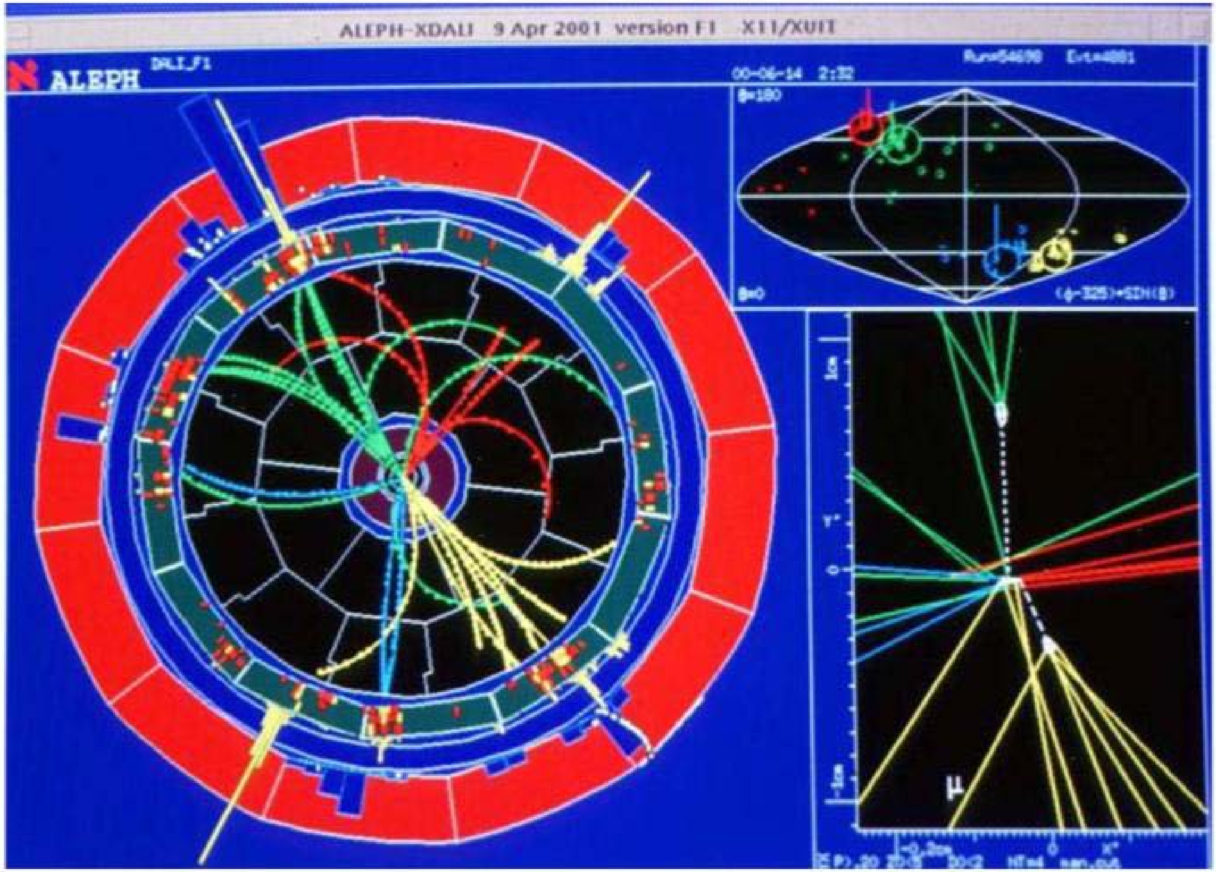

The Principle of Signal Induction on Metal Electrodes by Moving Charges

More on signal theorems, readout electronics etc. can be found in this book →

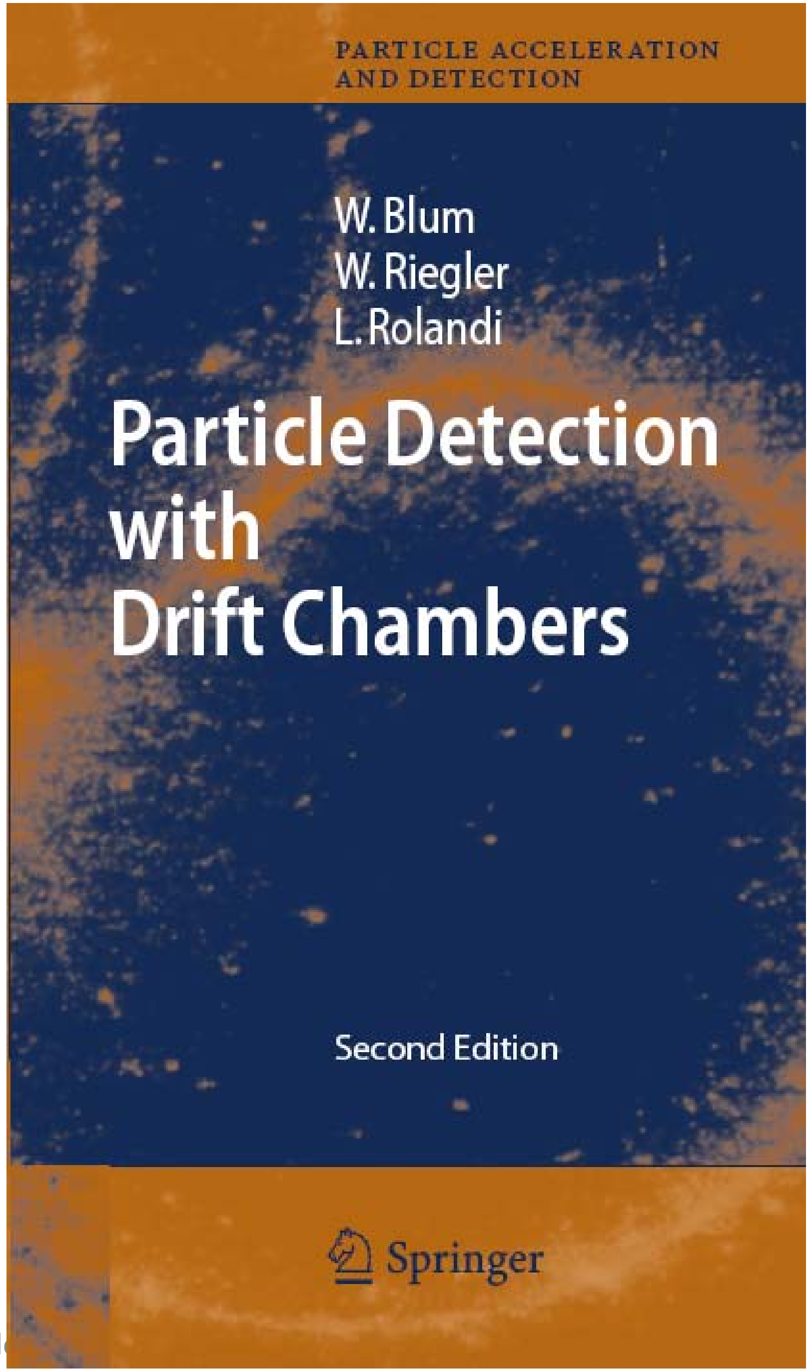

Induced Charges

A point charge q at a distance z_0 above a grounded metal plate 'induces' a surface charge.

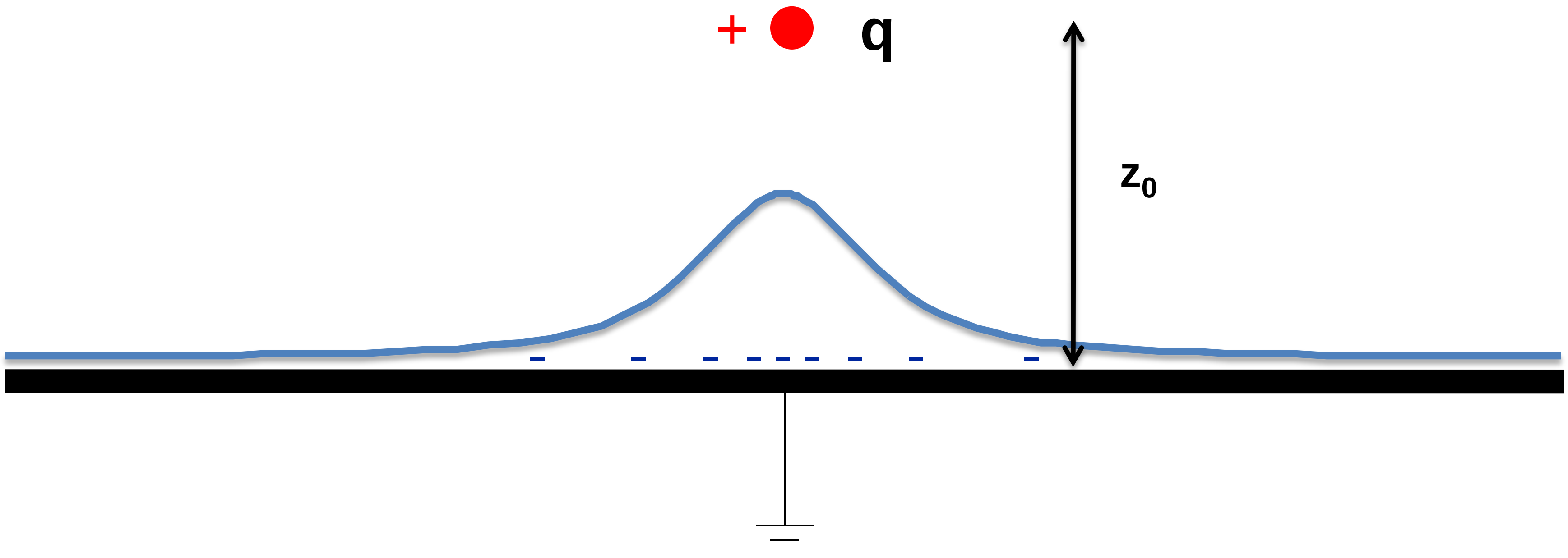

Electrostatics, things we know

Poisson Equation:

$$\Delta\varphi = -\frac{\rho}{\varepsilon_0} \qquad \vec{E} = -\vec{\nabla}\varphi$$

Gauss Law:

$$\oint \vec{E}\, d\vec{A} = \frac{1}{\varepsilon_0}\oint \rho\, dV$$

→ Metal Surface: Electric Field is perpendicular to the surface. Charges are only on the surface. Surface Charge Density ♦ and electric E field on the surface are related by

$$E\,A = \frac{1}{\varepsilon_0}\sigma\,A \qquad \rightarrow \qquad \sigma = \varepsilon_0 E$$

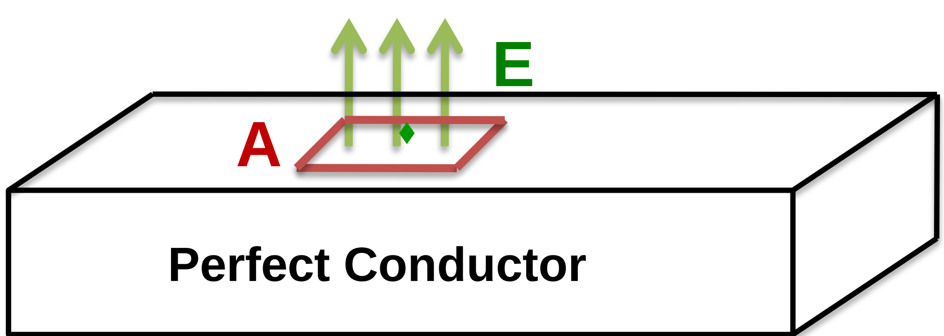

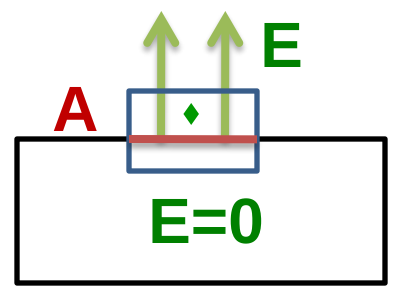

Induced Charges

In order to find the charge induced on an electrode we therefore have to

a) **Solve the Poisson equation with boundary condition that $\varphi=0$ on the conductor surface.**

b) **Calculate the electric field E on the surface of the conductor**

c) **Integrate e_0E over the electrode surface.**

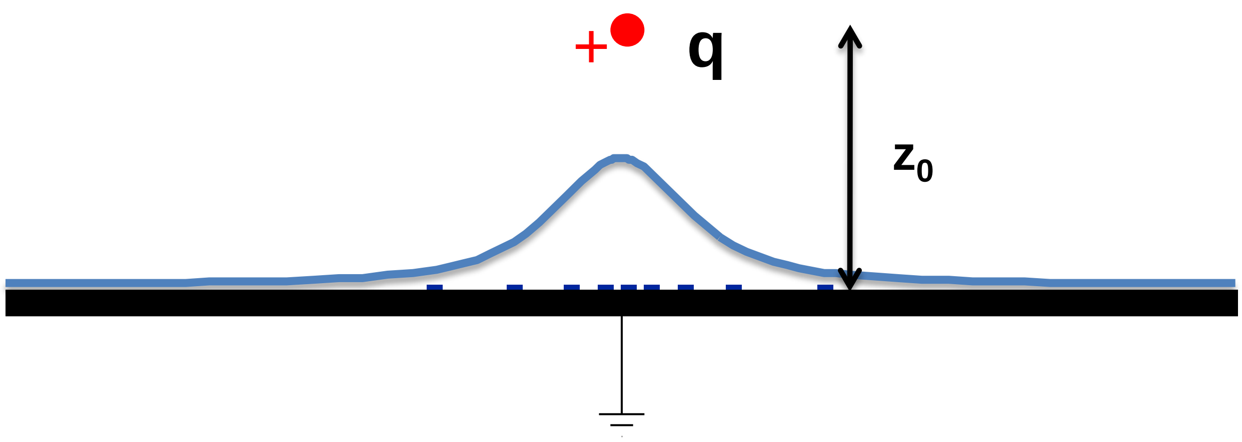

Induced Charges

The solution for the field of a point charge in front of a metal plate is equal to the solution of the charge together with a (negative) mirror charge at $z=-z_0$.

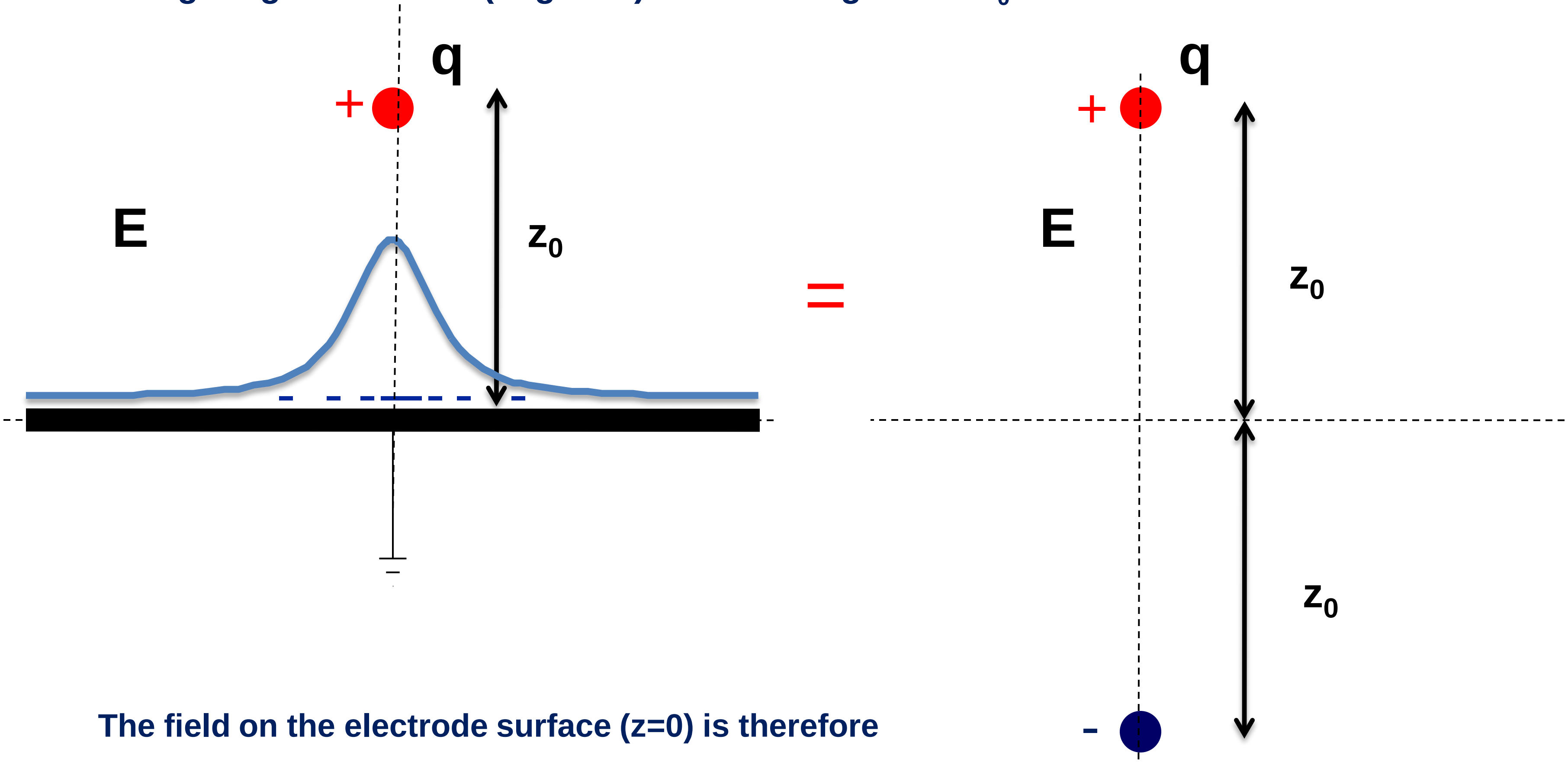

The field on the electrode surface (z=0) is therefore

$$E_z(x,y) = -\frac{q z_0}{2\pi\varepsilon_0 (x^2+y^2+z_0^2)^{\frac{3}{2}}} \qquad E_x = E_y = 0$$

Induced Charges

We therefore find a surface charge density of

$$\sigma(x,y) = \varepsilon_0 E_z(x,y) = -\frac{q z_0}{2\pi(x^2+y^2+z_0^2)^{\frac{3}{2}}}$$

And therefore a total induced charge of

$$Q = \int_{-\infty}^{\infty}\int_{-\infty}^{\infty} \sigma(x,y)\,dx\,dy = -q$$

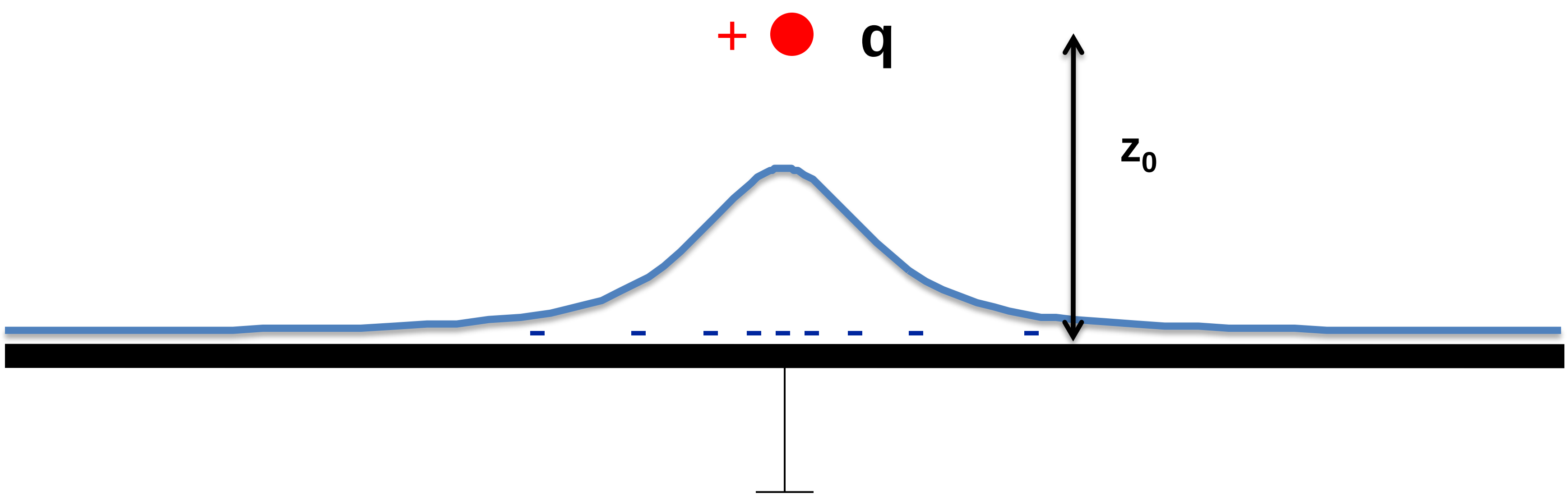

Induced Charges

The total charge induced by a point charge q on an infinitely large grounded metal plate is equal to –q, independent of the distance of the charge from the plate.

The surface charge distribution is however depending on the distance z_0 of the charge q.

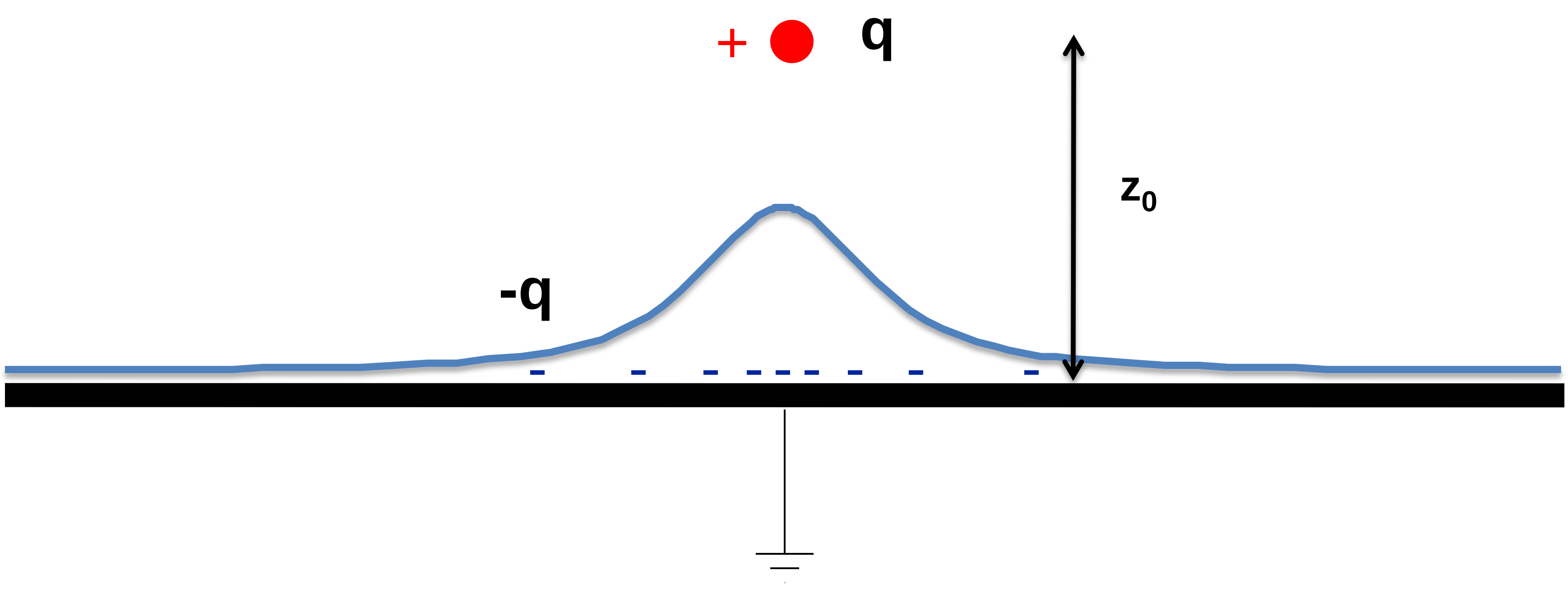

Induced Charges

Moving the point charge closer to the metal plate, the surface charge distribution becomes more peaked, the total induced charge is however always equal to –q.

$$\sigma(x,y) = -\frac{q z_0}{2\pi(x^2+y^2+z_0^2)^{\frac{3}{2}}}$$

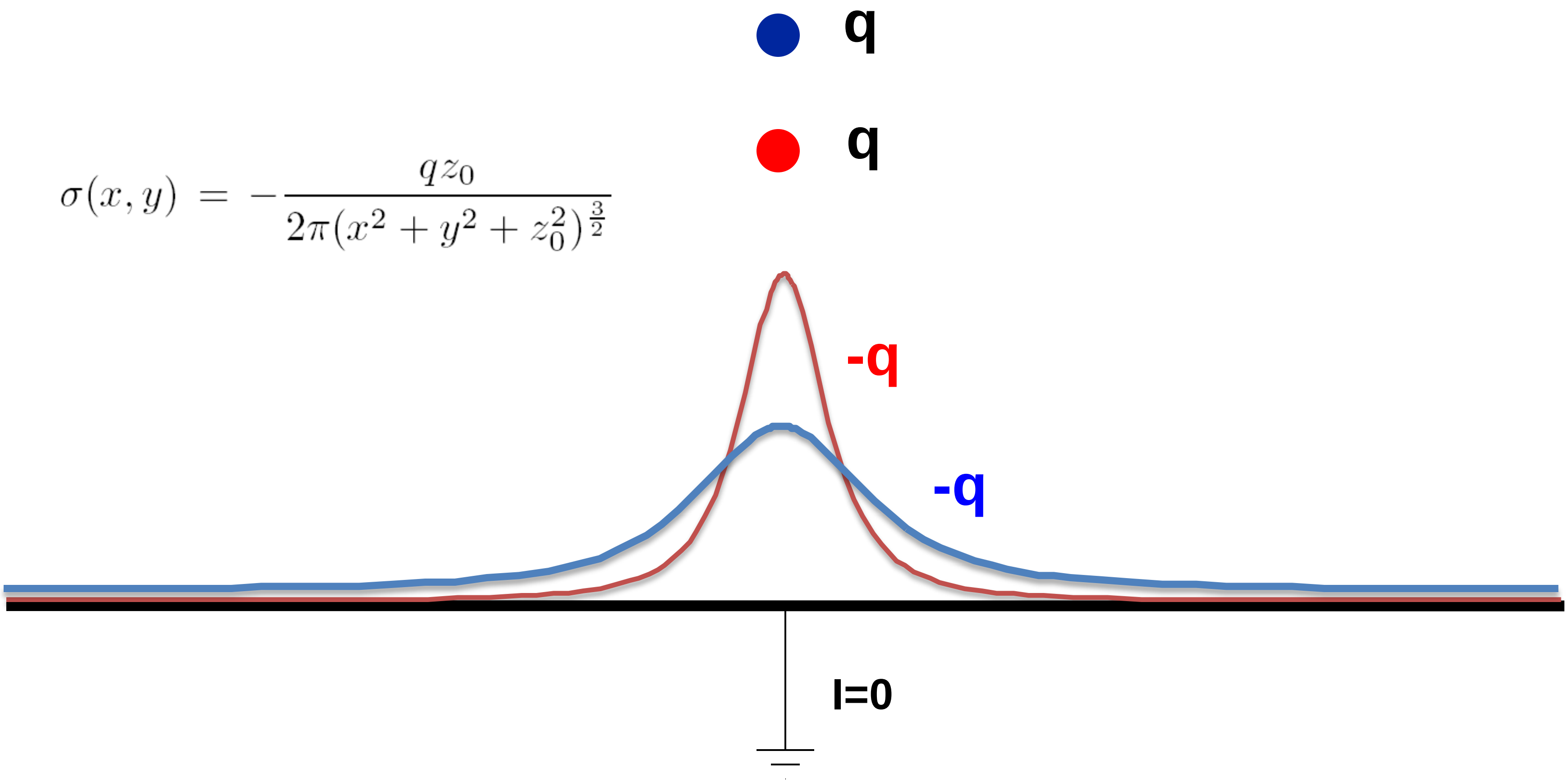

Signal Induction by Moving Charges

If we segment the grounded metal plate and if we ground the individual strips, the surface charge density doesn't change with respect to the continuous metal plate.

The charge induced on the individual strips is now depending on the position z_0 of the charge.

If the charge is moving there are currents flowing between the strips and ground.

→ The movement of the charge induces a current.

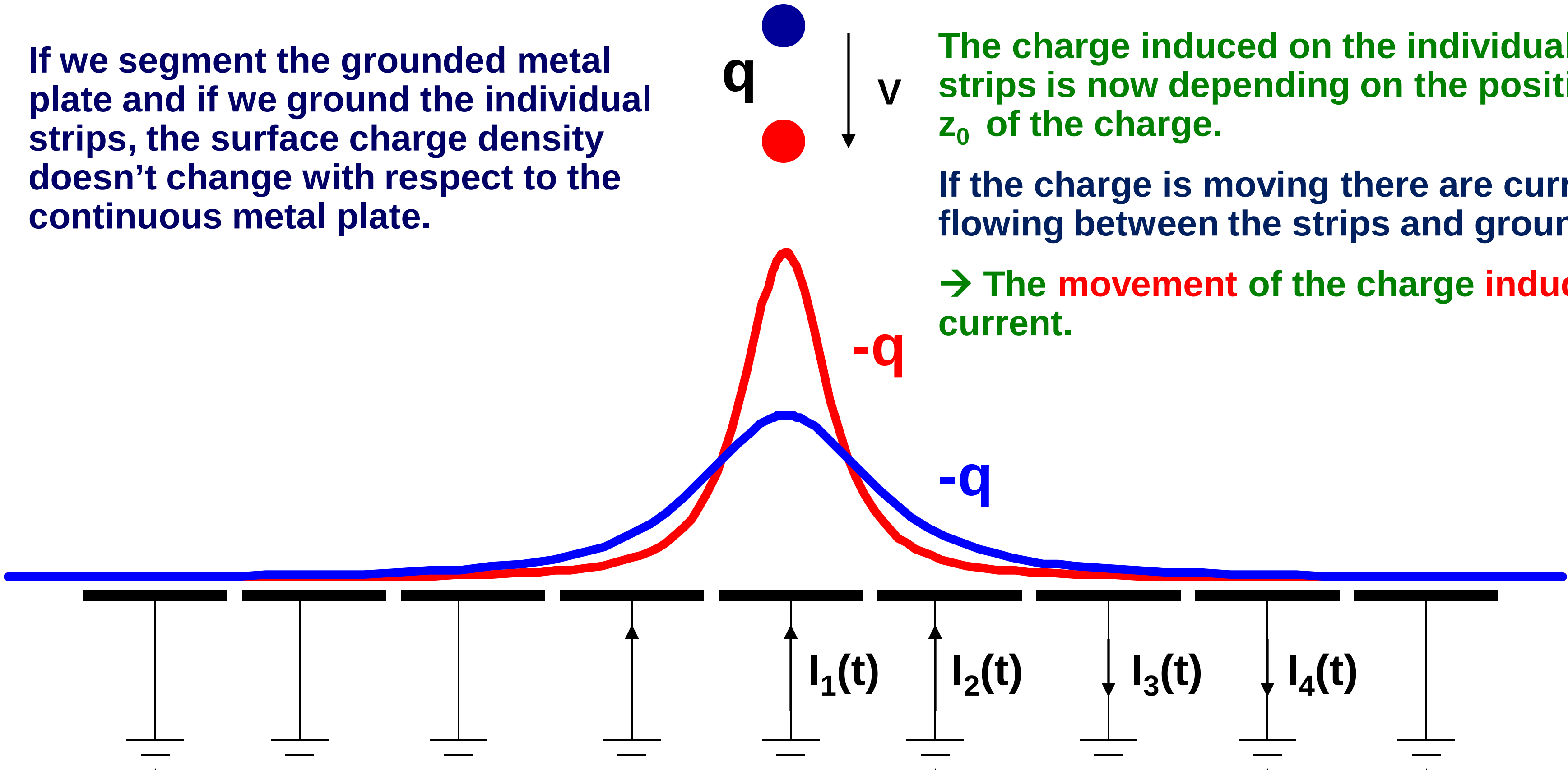

$$Q_1(z_0) = \int_{-\infty}^{\infty}\int_{-w/2}^{w/2} \sigma(x,y)\,dx\,dy = -\frac{2q}{\pi}\arctan\left(\frac{w}{2z_0}\right) \qquad z_0(t) = z_0 - vt$$

$$I_1^{ind}(t) = -\frac{d}{dt}Q_1[z_0(t)] = -\frac{\partial Q_1[z_0(t)]}{\partial z_0}\frac{dz_0(t)}{dt} = \frac{4qw}{\pi[4z_0(t)^2 + w^2]}v$$

Formulation of the Problem

In a real particle detector, the electrodes (wires, cathode strips, silicon strips, plate electrodes …) are not grounded but they are connected to readout electronics and interconnected by other discrete elements.

We want to answer the question:

What are the voltages induced on metal electrodes by a charge q moving along a trajectory x(t), in case these metal electrodes are connected by arbitrary linear impedance components ?

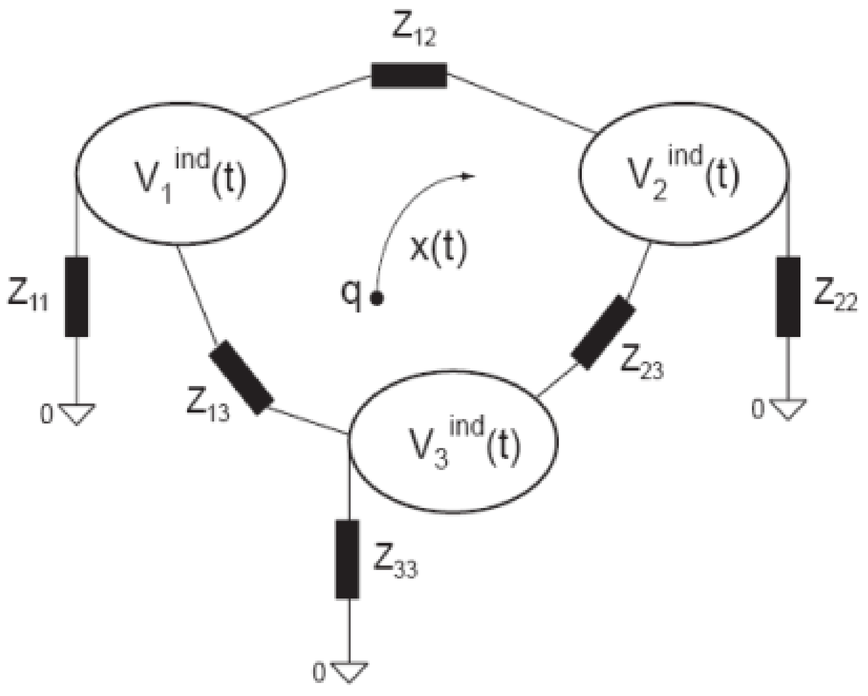

Formulation of the Problem

We will divide the problem into two parts:

We first calculate the currents induced on grounded electrodes.

Another theorem, states that we then have to place these currents as ideal current sources on a circuit containing the discrete components and the mutual electrode capacitances (see e.g. Blum, Riegler, Rolandi, Particle Detection with Drift Chambers).

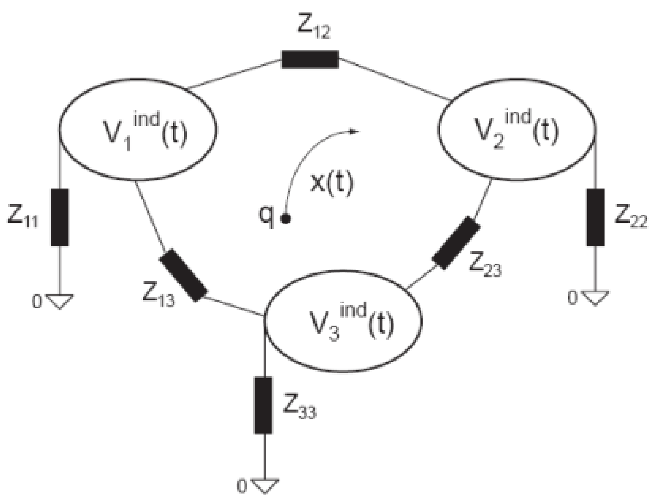

=

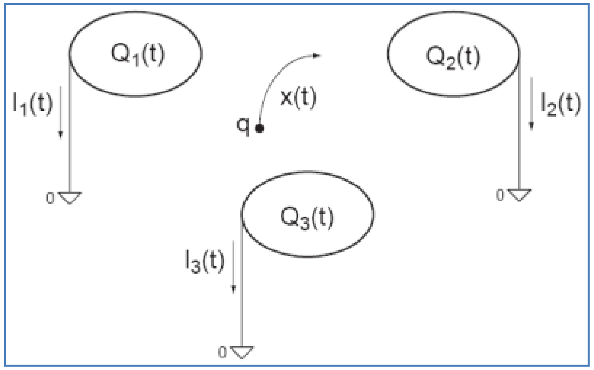

+

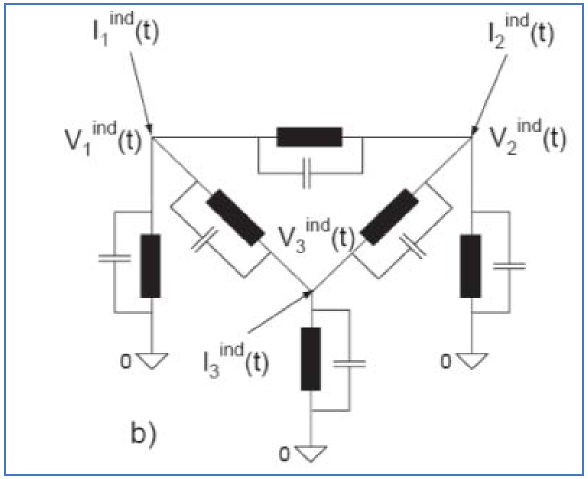

The second step is typically performed by using an analog circuit simulation program. We will focus on the induced currents.

Currents on Grounded Electrodes

We can imagine this case by reading the signal with an ideal current amplifier of zero input impedance

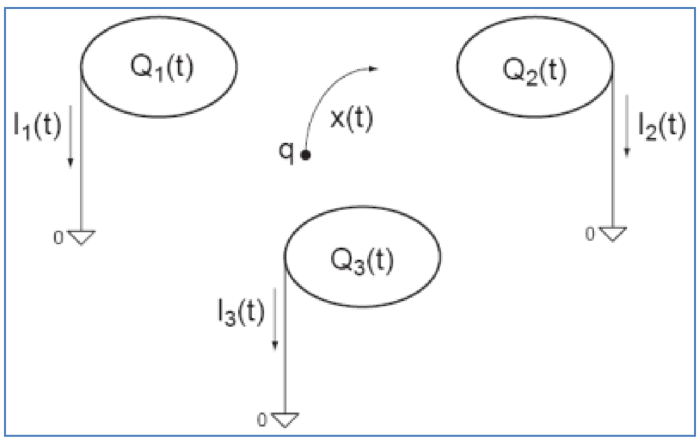

=

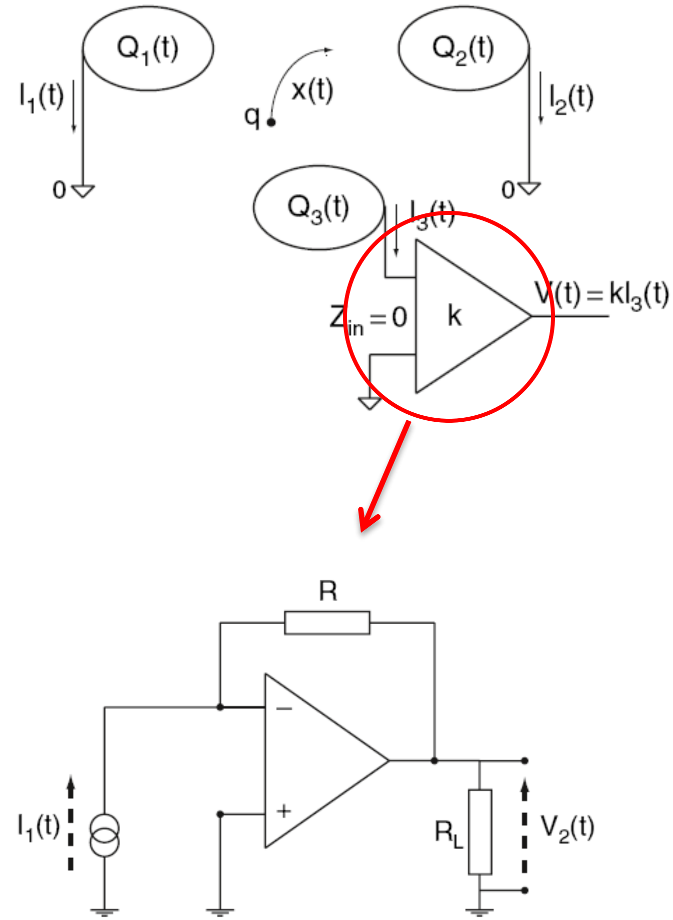

$$V_2(t) = -R\, I_1(t)$$

Parallel Plate Chamber

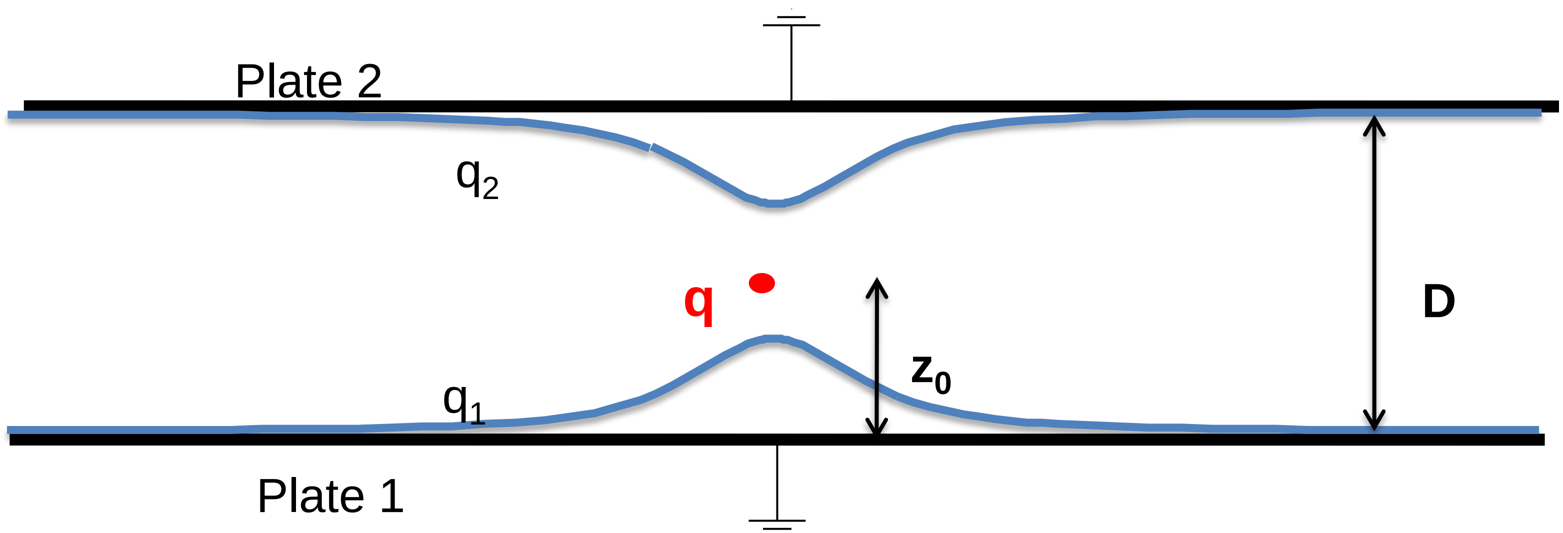

$$\phi(r,z) = \frac{q}{\varepsilon_0 \pi D} \sum_{n=1}^{\infty} \sin\left(\frac{n\pi}{D} z\right) \sin\left(\frac{n\pi}{D} z_0\right) K_0\left(\frac{n\pi}{D} r\right)$$ [5]

$$E(r,z) = \frac{q}{\varepsilon_0 \pi D} \sum_{n=1}^{\infty} \frac{n\pi}{D} \cos\left(\frac{n\pi}{D} z\right) \sin\left(\frac{n\pi}{D} z_0\right) K_0\left(\frac{n\pi}{D} r\right)$$

$$\sigma_1(r) = \varepsilon_0 E(r, z=0) = \frac{q}{\pi D} \sum_{n=1}^{\infty} \frac{n\pi}{D} \sin\left(\frac{n\pi}{D} z_0\right) K_0\left(\frac{n\pi}{D} r\right)$$

[5] C. Y. Fong, C. Kittel, Induced Charge on Capacitor Plates, Am. J . Phys. 35(1967)1091.

Parallel Plate Chamber

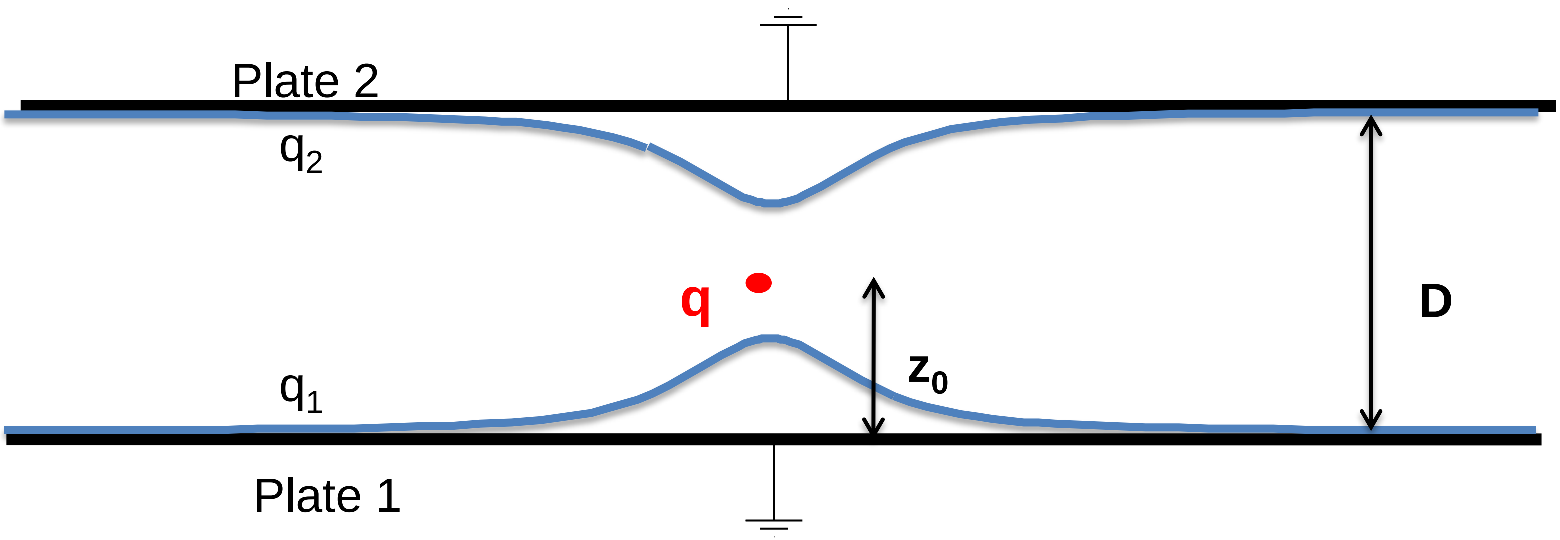

$$q_1 = \int_0^\infty 2r\pi\sigma(r)dr = \frac{q}{\pi D}\sum_{n=1}^{\infty}\frac{n\pi}{D}\sin\left(\frac{n\pi}{D}z_0\right)\int_0^\infty 2r\pi K_0\left(\frac{n\pi}{D}r\right)dr = \frac{2q}{\pi}\sum_{n=1}^{\infty}\frac{1}{n}\sin\left(\frac{n\pi}{D}z_0\right) =$$

$$= -q\left(1-\frac{z_0}{D}\right)$$

$$q_2 = \ldots = -q\,\frac{z_0}{D}$$

$$q_1 + q_2 = -q$$

Parallel Plate Chamber

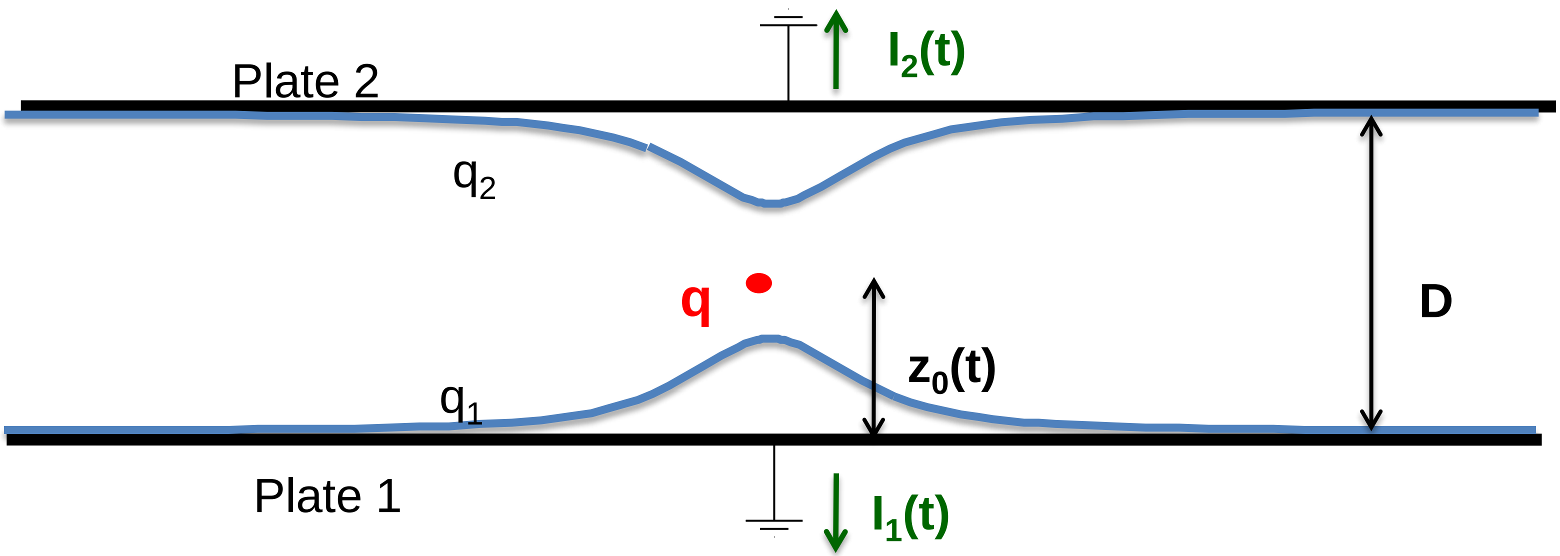

$$q_1 = -q\left(1 - \frac{z_0}{D}\right) \qquad q_2 = -q\frac{z_0}{D} \qquad z_0(t) = vt$$

$$q_1(t) = -q\left(1 - \frac{vt}{D}\right) \qquad q_2(t) = -q\frac{vt}{D} \qquad q_1(t) + q_2(t) = q$$

$$I_1(t) = -\frac{dq_1(t)}{dt} = -\frac{qv}{D} \qquad I_2(t) = -\frac{dq_2(t)}{dt} = +\frac{qv}{D} \qquad I_1(t) + I_2(t) = 0$$

Parallel Plate Chamber

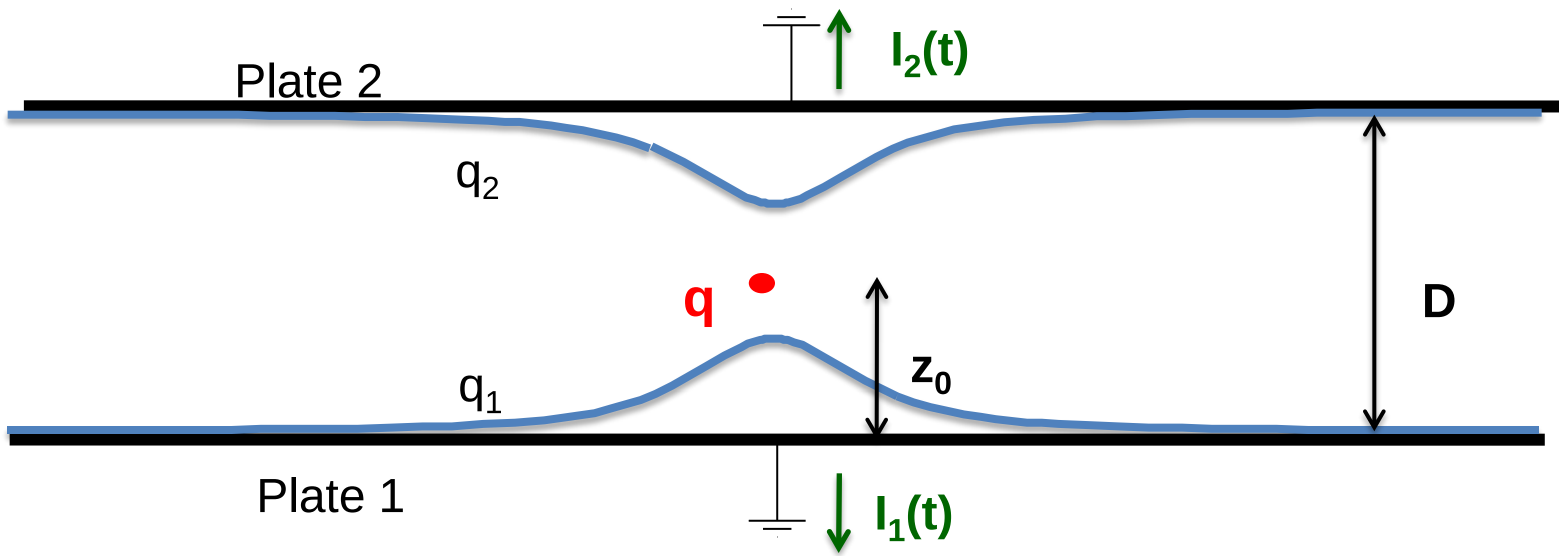

$$q_1(t) = -q\left(1 - \frac{vt}{D}\right) \qquad q_2(t) = -q\frac{vt}{D} \qquad I_1(t) = -\frac{dq_1(t)}{dt} = -\frac{qv}{D} \qquad I_2(t) = -\frac{dq_2(t)}{dt} = +\frac{qv}{D}$$

The sum of all induced charges is equal to the moving charge at any time.

The sum of the induced currents is zero at any time.

The field calculation is complicated, the formula for the induced signal is however very simple – there might be an easier way to calculate the signals ?

→ Ramo-Shockley theorem !

Signal Polarity Definition

$$I(t) = -\frac{dQ(t)}{dt}$$

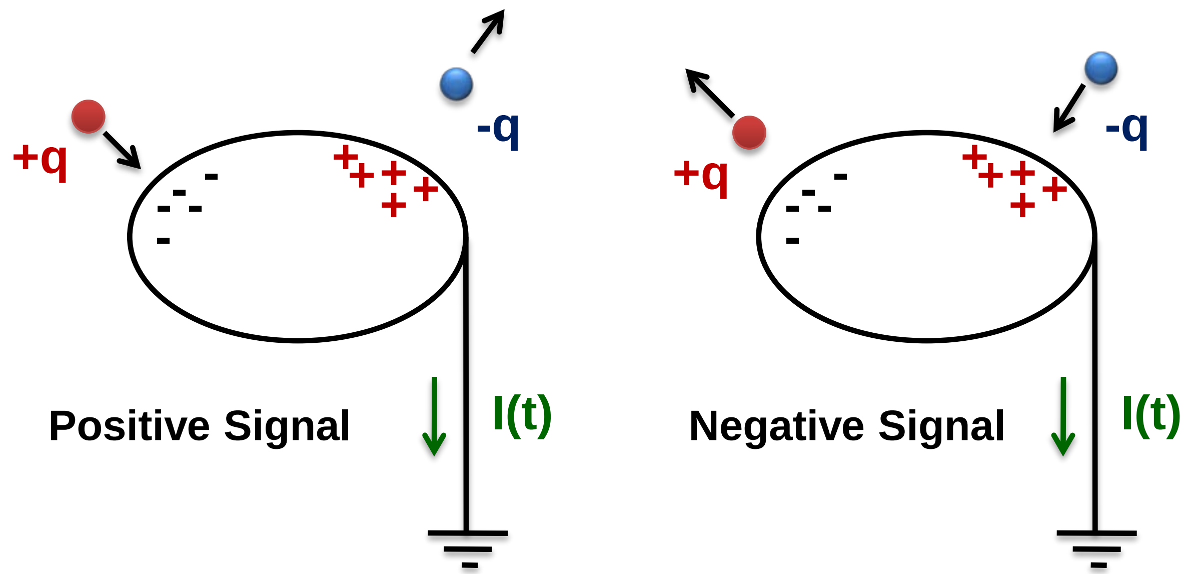

The definition of I=-dQ/dt states that the positive current is pointing away from the electrode.

The signal is positive if:
Positive charge is moving from electrode to ground or
Negative charge is moving from ground to the electrode

The signal is negative if:
Negative charge is moving from electrode to ground or
Positive charge is moving from ground to the electrode

Signal Polarity Definition

$$I(t) = -\frac{dQ(t)}{dt}$$

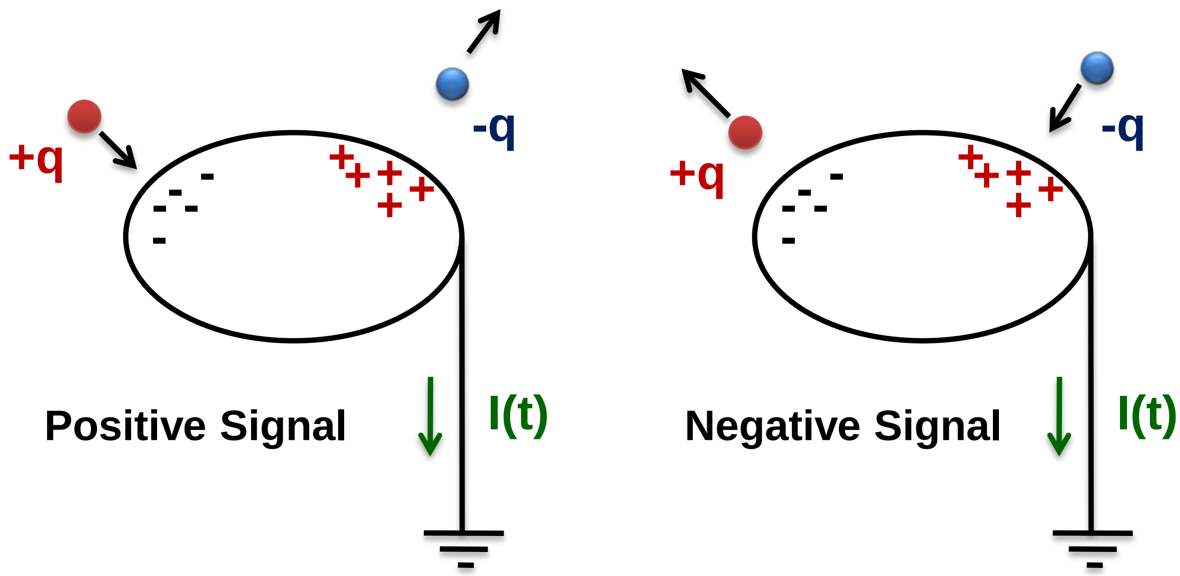

By this we can guess the signal polarities:

In a wire chamber, the electrons are moving towards the wire, which means that they attract positive charges that are moving from ground to the electrode. The signal of a wire that collects electrons is therefore negative.

Sum of Induced Charges and Currents

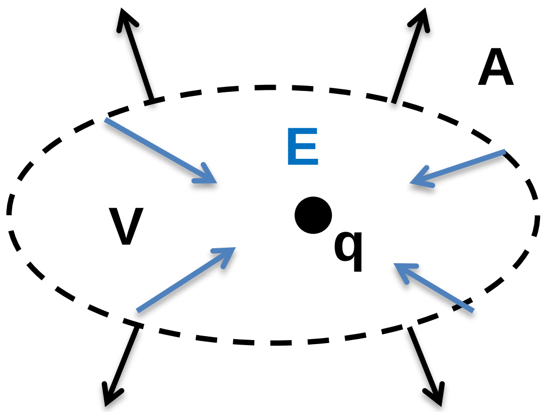

$$\oint_{\vec{A}} \vec{E}\,d\vec{A} = \frac{1}{\varepsilon_0}\oint_V \rho\,dV = \frac{q}{\varepsilon_0}$$

The surface A must be oriented towards the outside of the volume V.

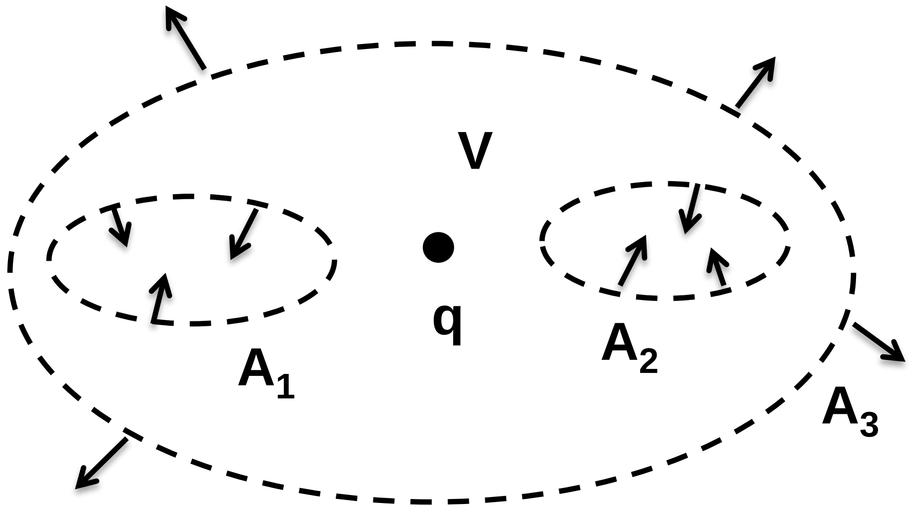

$A=A_1+A_2+A_3$

$$\oint_{\vec{A}} \vec{E}\,d\vec{A} = \oint_{\vec{A}_1} \vec{E}\,d\vec{A} + \oint_{\vec{A}_2} \vec{E}\,d\vec{A} + \oint_{\vec{A}_3} \vec{E}\,d\vec{A} = \frac{q}{\varepsilon_0}$$

Sum of Induced Charges and Currents

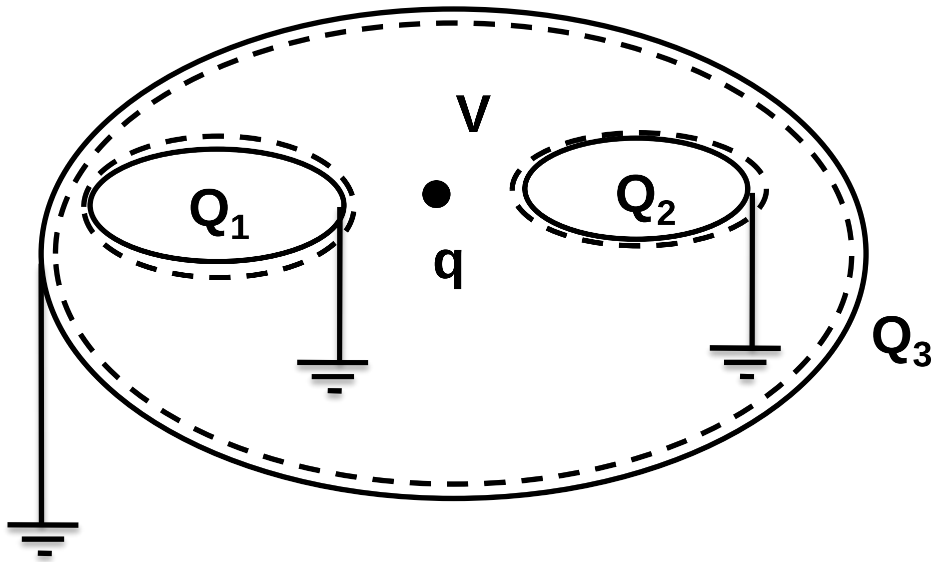

$$\oint_{\vec{A}} \vec{E}\, d\vec{A} = \oint_{\vec{A}_1} \vec{E}\, d\vec{A} + \oint_{\vec{A}_2} \vec{E}\, d\vec{A} + \oint_{\vec{A}_3} \vec{E}\, d\vec{A} = \frac{q}{\varepsilon_0}$$

In case the surfaces are metal electrodes we know that

$$Q_1 = -\oint_{\vec{A}_1} \varepsilon_0 \vec{E}\, d\vec{A} \qquad Q_2 = -\oint_{\vec{A}_2} \varepsilon_0 \vec{E}\, d\vec{A} \qquad Q_3 = -\oint_{\vec{A}_3} \varepsilon_0 \vec{E}\, d\vec{A}$$

And we therefore have

$$Q_1 + Q_2 + Q_3 = -q$$

In case there is one electrode enclosing all the others, the sum of all induced charges is always equal to the point charge.

The sum of all induced currents is therefore zero at any time !

Sum of Induced Charges and Currents

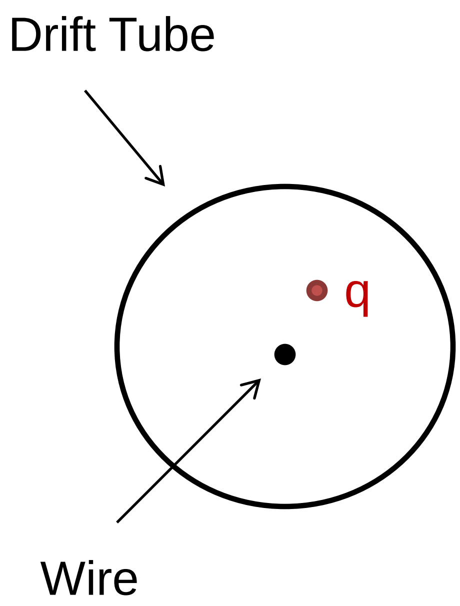

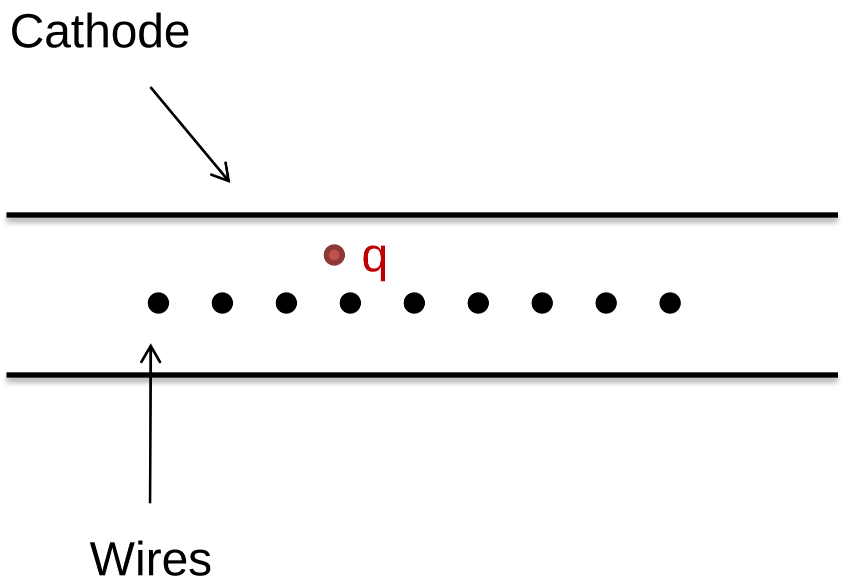

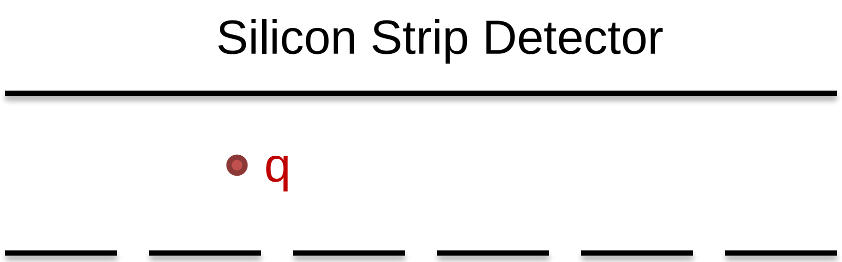

The sum of all induced currents is therefore zero at any time !

Charged Electrodes

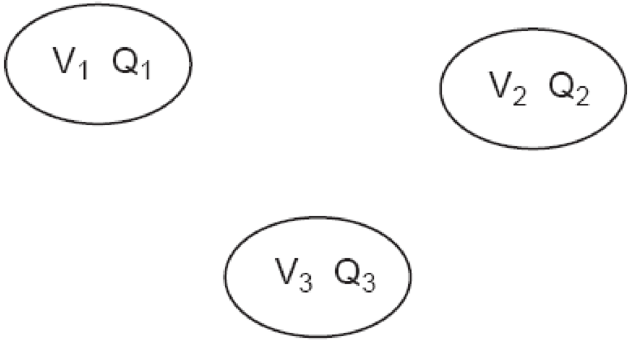

Setting the three electrodes to potentials V_1, V_2, V_3 results in charges Q_1, Q_2, Q_3. In order to find them we have to solve the Laplace equation

$$\Delta\varphi = 0$$

with boundary condition

$$\varphi|_{\vec{A}_1} = V_1 \qquad \varphi|_{\vec{A}_2} = V_2 \qquad \varphi|_{\vec{A}_3} = V_3$$

And the calculate

$$Q_1 = \oint_{\vec{A}_1} -\vec{\nabla}\varphi \, d\vec{A} \qquad Q_2 = \oint_{\vec{A}_2} -\vec{\nabla}\varphi \, d\vec{A} \qquad Q_3 = \oint_{\vec{A}_3} -\vec{\nabla}\varphi \, d\vec{A}$$

Green's Second Theorem

Gauss Law which is valid for any Vector Field and Volume V surrounded by the Surface A:

$$\oint_{\vec{A}} \vec{E}\, d\vec{A} = \oint_{V} \vec{\nabla}\vec{E}\, dV$$

By setting

$$\vec{E} = \varphi\vec{\nabla}\psi \qquad \oint_{\vec{A}} \varphi\vec{\nabla}\psi\, d\vec{A} = \oint_{V} \vec{\nabla}\varphi\vec{\nabla}\psi\, dV + \oint_{V} \varphi\Delta\psi\, dV$$

and setting

$$\vec{E} = \psi\vec{\nabla}\varphi \qquad \oint_{\vec{A}} \psi\vec{\nabla}\varphi\, d\vec{A} = \oint_{V} \vec{\nabla}\psi\vec{\nabla}\varphi\, dV + \oint_{V} \psi\Delta\varphi\, dV$$

and subtracting the two expressions we get Green's second theorem:

$$\oint_{\vec{A}} \left(\varphi\vec{\nabla}\psi - \psi\vec{\nabla}\varphi\right)\, d\vec{A} = \oint_{V} \left(\varphi\Delta\psi - \psi\Delta\varphi\right) dV$$

Green's Theorem, Reciprocity

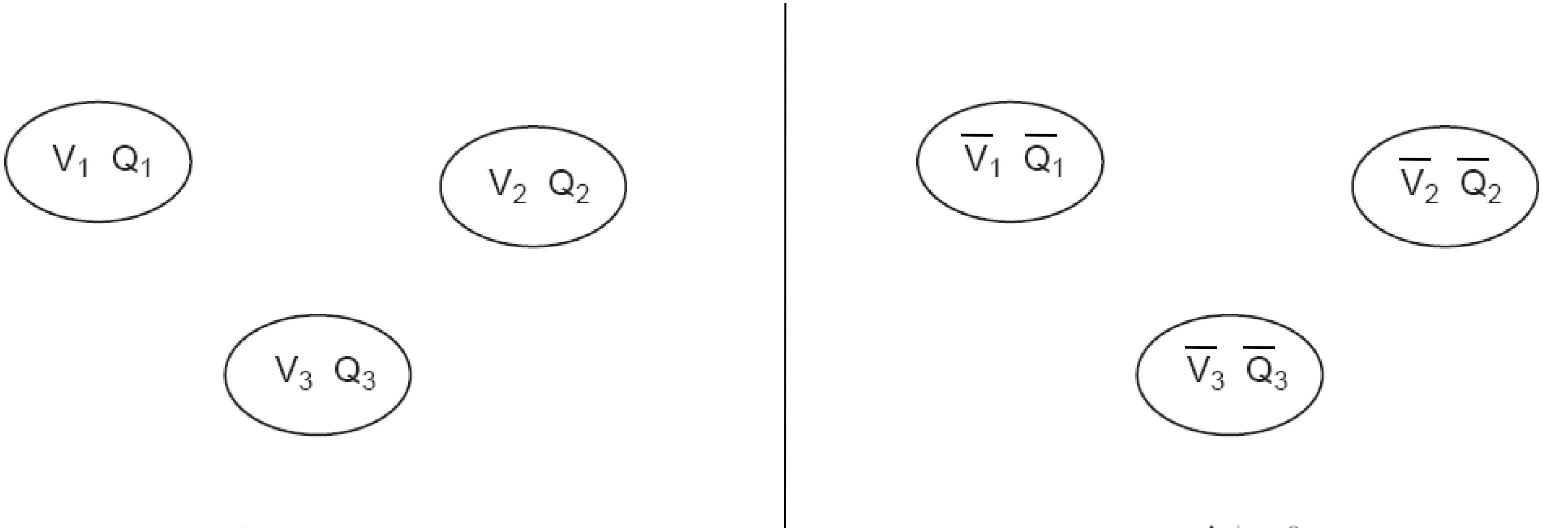

$$\Delta\varphi = 0 \qquad\qquad \Delta\psi = 0$$

$$\varphi|_{\vec{A}_1} = V_1 \qquad \varphi|_{\vec{A}_2} = V_2 \qquad \varphi|_{\vec{A}_3} = V_3 \qquad\qquad \psi|_{\vec{A}_1} = \overline{V}_1 \qquad \psi|_{\vec{A}_2} = \overline{V}_2 \qquad \psi|_{\vec{A}_3} = \overline{V}_3$$

$$Q_1 = \oint_{\vec{A}_1} -\vec{\nabla}\varphi\, d\vec{A} \qquad Q_2 = \oint_{\vec{A}_2} -\vec{\nabla}\varphi\, d\vec{A} \qquad Q_3 = \oint_{\vec{A}_3} -\vec{\nabla}\varphi\, d\vec{A}$$

$$\overline{Q}_1 = \oint_{\vec{A}_1} -\vec{\nabla}\psi\, d\vec{A} \qquad \overline{Q}_2 = \oint_{\vec{A}_2} -\vec{\nabla}\psi\, d\vec{A} \qquad \overline{Q}_3 = \oint_{\vec{A}_3} -\vec{\nabla}\psi\, d\vec{A}$$

$$\oint_{\vec{A}} \left(\varphi\vec{\nabla}\psi - \psi\vec{\nabla}\varphi\right) d\vec{A} = \oint_V (\varphi\Delta\psi - \psi\Delta\varphi)\, dV$$

$$\longrightarrow \quad \sum_{n=1}^{N} Q_n \overline{V}_n = \sum_{n=1}^{N} \overline{Q}_n V_n$$

Reciprocity Theorem

It related two electrostatic states, i.e. two sets of voltages and charges

Electrostatics, Capacitance Matrix

From the reciprocity theorem it follows that the voltages of the electrodes and the charges on the electrodes are related by a matrix

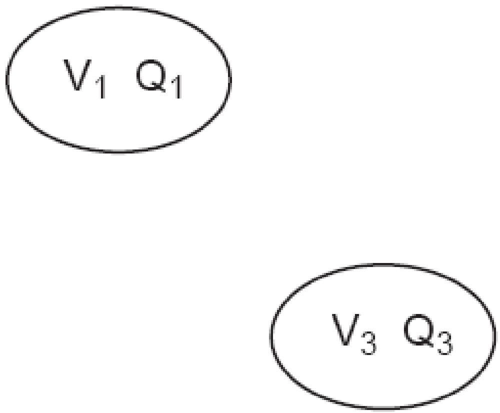

$$Q_n = \sum_{m=1}^{N} c_{nm} V_m$$

The matrix c_{nm} is called the capacitance matrix with the important properties

$$c_{nm} = c_{mn} \qquad c_{nm} < 0 \qquad \sum_{m=1}^{N} c_{nm} > 0$$

The capacitance matrix elements are not to be confused with the electrode capacitances of the equivalent circuit. They are related by

$$C_{nm} = -c_{nm} \quad n \neq m \qquad C_{nn} = \sum_{m=1}^{N} c_{nm}$$

Induced Charge

We assume three grounded electrodes and a point charge in between. We want to know the charges induced on the grounded electrodes. We assume the point charge to be an very small metal electrode with charge q, so we have a system of 4 electrodes with V_1=0, V_2=0, V_3=0, Q_0=q.

We can now assume another set of voltages and charges where we remove the charge from electrode zero, we put electrode 1 to voltage V_w and keep electrodes 2 and 3 grounded.

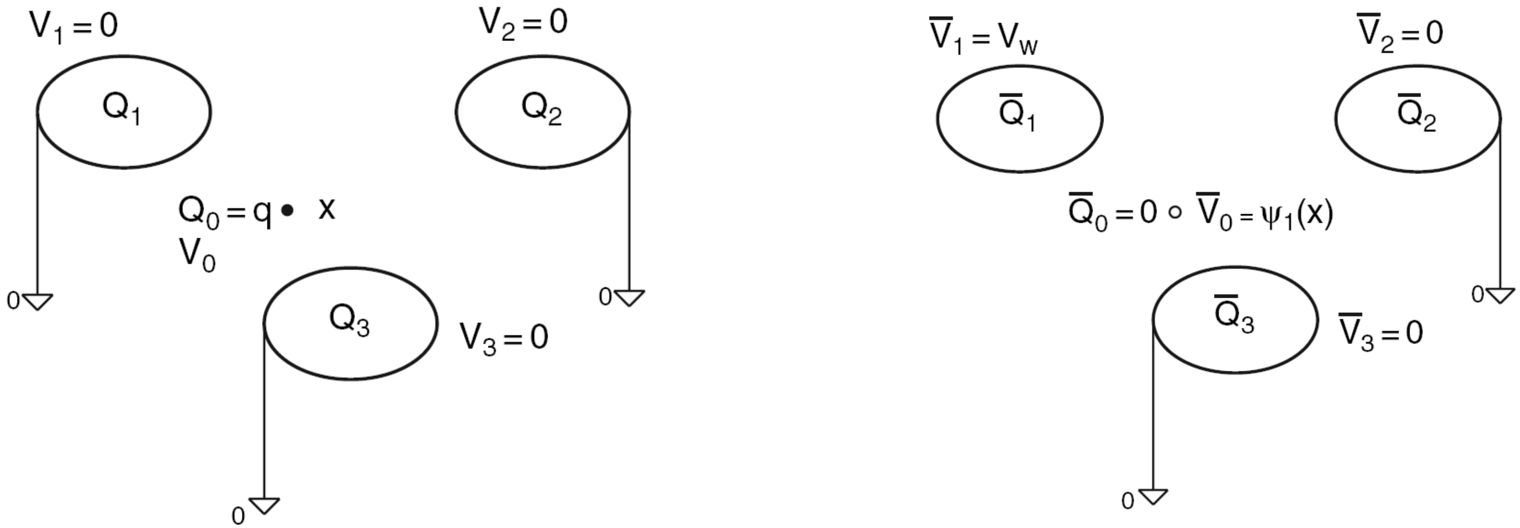

Using the reciprocity theorem $\sum_{n=1}^{N} Q_n \overline{V}_n = \sum_{n=1}^{N} \overline{Q}_n V_n$ **we get**

$$q\overline{V}_0 + Q_1 V_w = 0 \qquad \rightarrow \qquad Q_1 = -q\frac{\overline{V}_0}{V_w}\,.$$

Induced Charge

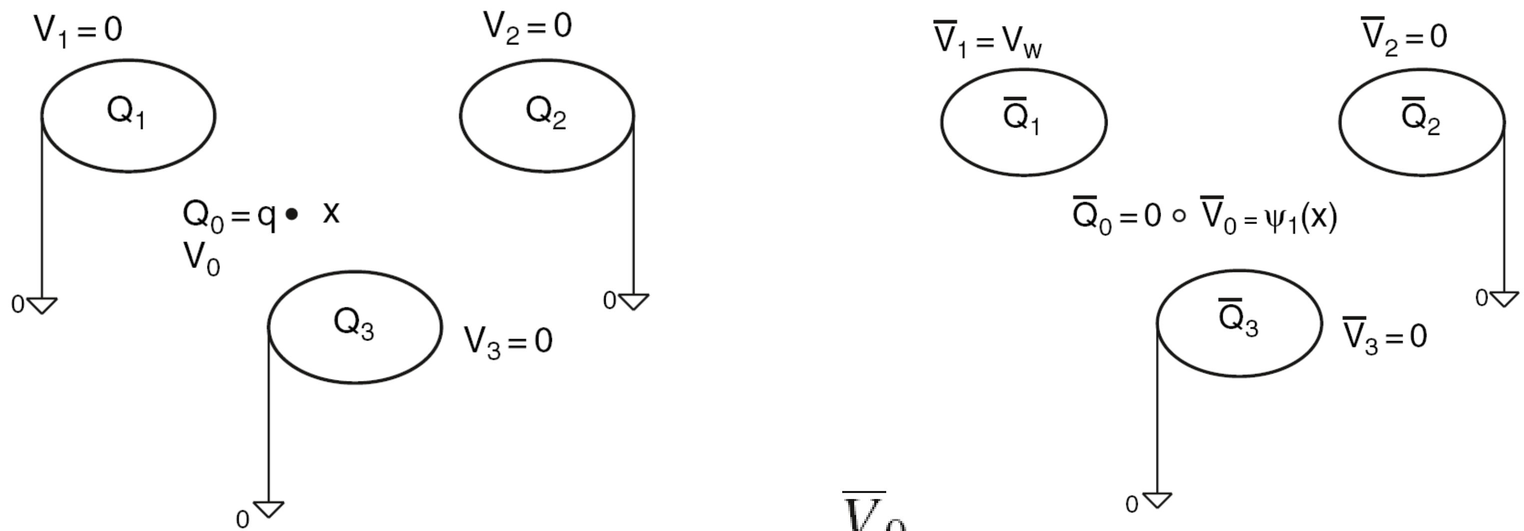

$$Q_1 = -q\frac{\overline{V}_0}{V_w}$$

The voltage $\overline{V}_0$ is the voltage of the small uncharged electrode for the second electrostatic state, and because a small uncharged electrode is equal to having no electrode, $\overline{V}_0$ is the voltage at the place x of the point charge in case the charge is removed, electrode 1 is put to voltage V_w and the other electrodes are grounded.

We call the potential ⍓(x) the weighting potential of electrode 1.

Induced Charge

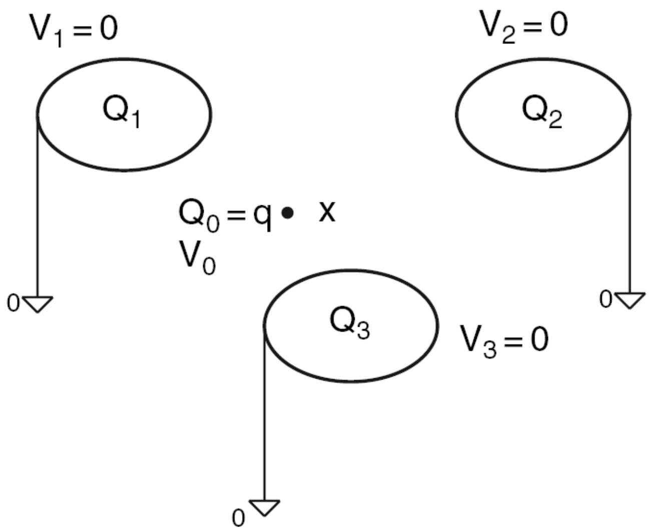

$$Q = -\frac{q}{V_w}\psi(\vec{x})$$

The charge induced by a point charge q at position x on a grounded electrode can be calculated the following way: One removes the point charge, puts the electrode in question to potential V_w while keeping the other electrodes grounded.

This defines the potential 'weighting potential' ψ(x) from which the induced charge can be calculated by the above formula.

Induced Current, Ramo Shockley Theorem

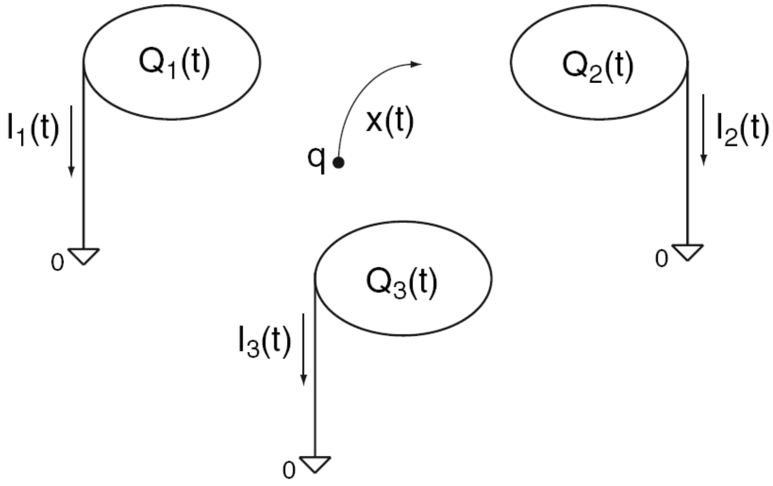

$$Q = -\frac{q}{V_w}\,\psi(\vec{x})$$

In case the charge is moving along a trajectory x(t), the time dependent induced charge is

$$Q(t) = -\frac{q}{V_w}\,\psi\,(\vec{x}(t))$$

And the induced current is

$$I(t) = -\frac{dQ}{dt} = \frac{q}{V_w}\,\vec{\nabla}\psi\,(\vec{x}(t))\,\frac{d\vec{x}(t)}{dt} = -\frac{q}{V_w}\,\vec{E}\,(\vec{x}(t))\,\vec{v}(t)$$

Induced Current, Ramo Shockley Theorem

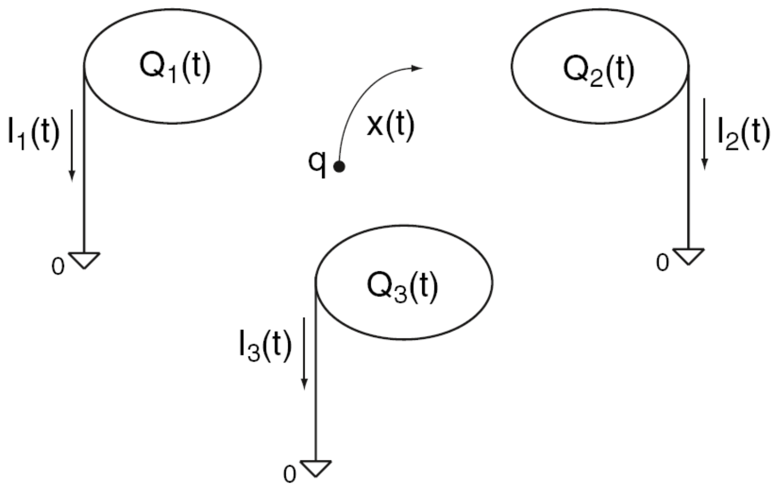

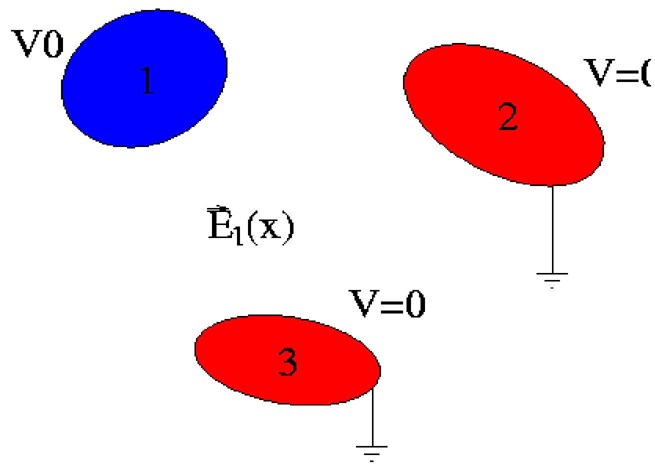

The current induced on a grounded electrode n by a moving point charge q is given by

$$I_n(t) == -\frac{q}{V_w} \vec{E_n}\left(\vec{x}(t)\right) \vec{v}(t)$$

Where the weighting field E_n is defined by removing the point charge, setting the electrode in question to potential V_w and keeping the other electrodes grounded.

Removing the charge means that we just have to solve the Laplace equation and not the Poisson equation !

Parallel Plate Chamber

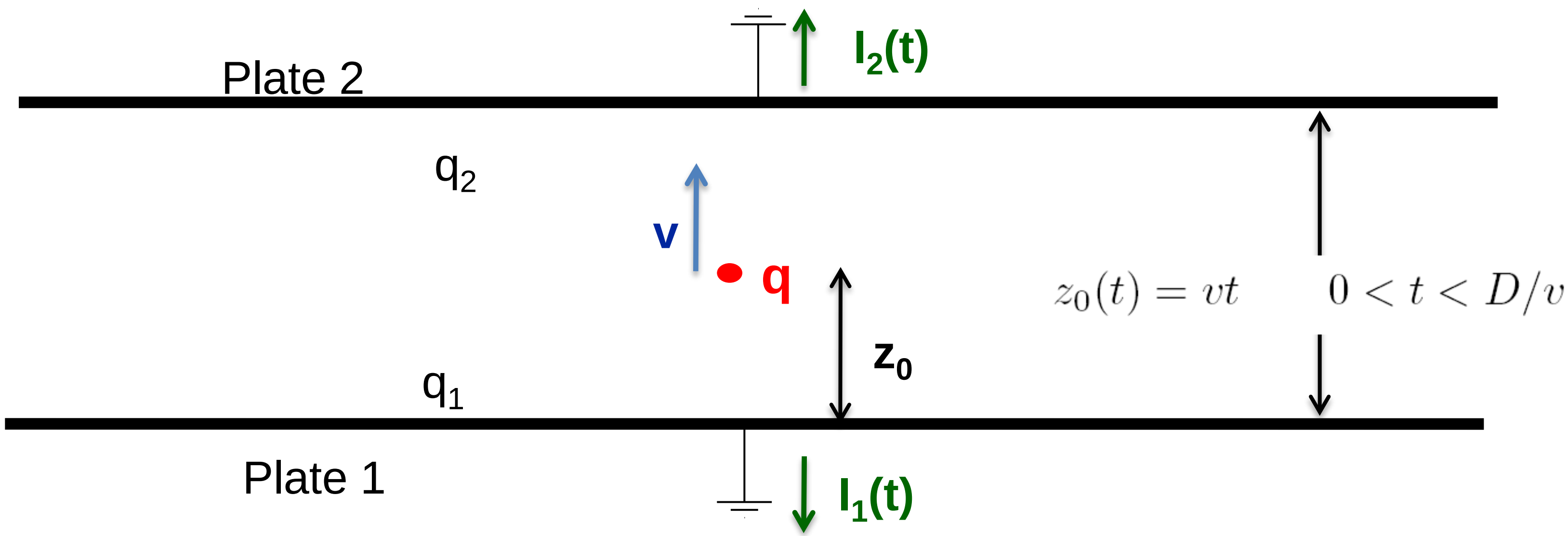

Weighting field E_1 of plate 1: Remove charge, set plate1 to V_w and keep plate2 grounded

$$E_1 = \frac{V_w}{D}$$

Weighting field E_2 of plate 2: Remove charge, set plate2 to V_w and keep plate1 grounded

$$E_2 = -\frac{V_w}{D}$$

So we have the induced currents

$$I_1 = -\frac{q}{V_w}\frac{V_w}{D}E_1\,v = -\frac{qv}{D} \qquad\qquad I_2 = -\frac{q}{V_w}\frac{V_w}{D}E_2\,v = \frac{qv}{D}$$

Arguing with Energy ? Not a good Idea !

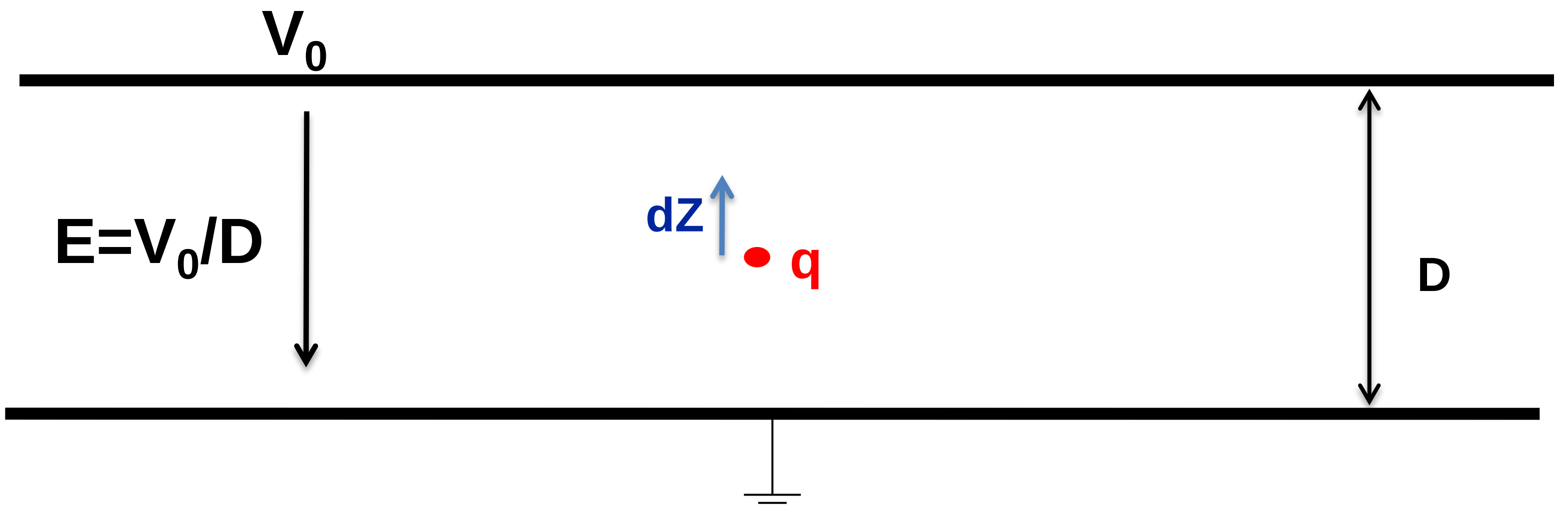

$$Energy = \frac{1}{2}CV_0^2 = \frac{1}{2}\frac{Q^2}{C} \qquad dW = qEdz = \frac{qV_0}{D}dz$$

$$d(Energy) = dW \qquad d\frac{1}{2}\frac{Q^2}{C} = \frac{qV_0}{D}dz$$

$$\frac{1}{2}\frac{1}{C}QdQ = \frac{qV_0}{D}dz \qquad dQ = \frac{q}{D}dz$$

This argument gives the correct result, it is however only correct for a 2 electrode system because there the weighting field and the real field are equal. In addition the argument is very misleading.

Arguing with Energy ? Not a good Idea !

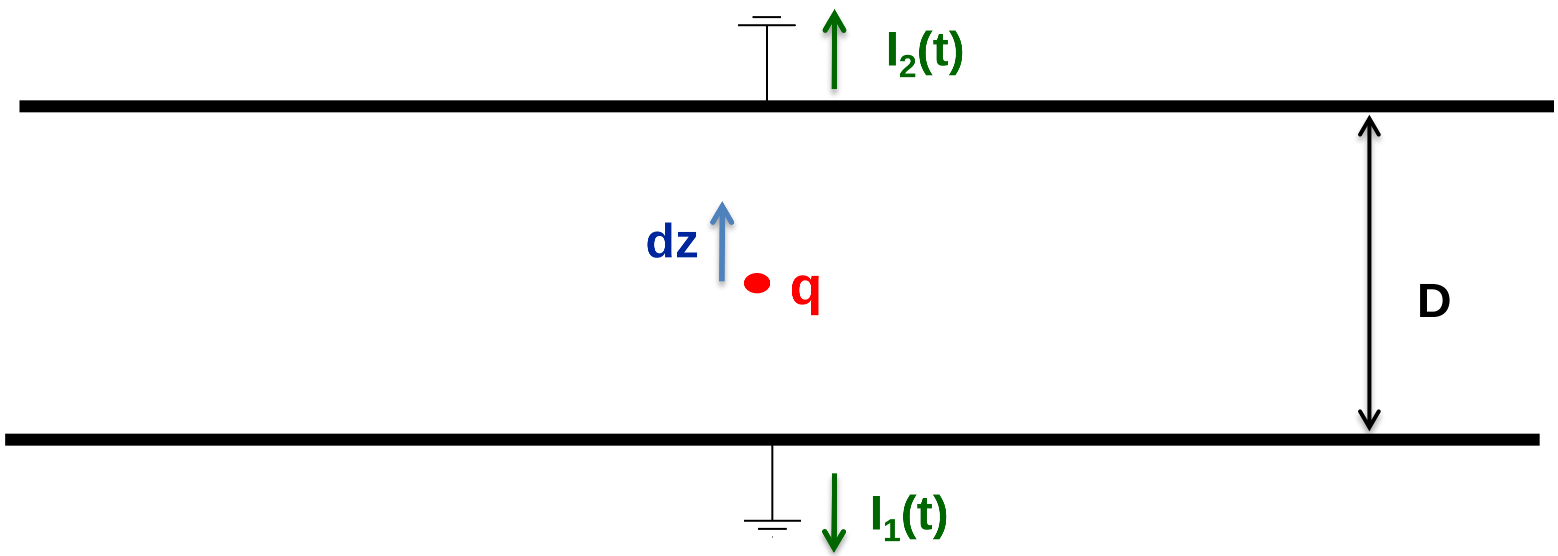

An induced current signal has nothing to do with Energy. In a gas detector the electrons are moving at constant speed in a constant electric field, so the energy gained by the electron in the electric field is lost into collisions with the gas, i.e. heating of the gas.

In absence of an electric field, the charge can be moved across the gap without using any force and currents are flowing.

The electric signals are due to induction !

Total Induced Charge

If a charge is moving from point x_0 to point x_1, the induced charge is

$$Q_n^{ind} = \int_{t_0}^{t_1} I_n^{ind}(t)dt = -\frac{q}{V_w}\int_{t_0}^{t_1} \boldsymbol{E}_n[\boldsymbol{x}(t)]\,\dot{\boldsymbol{x}}(t)dt = \frac{q}{V_w}[\psi_n(\boldsymbol{x}_1) - \psi_n(\boldsymbol{x}_0)]$$

If a pair of charges +q and -q is produced at point x_0 and q moves to x_1 while –q moves to x_2 , the charge induced on electrode n is given by

$$Q_n^{ind} = \int_{t_0}^{t_1} I_n^{ind}(t)dt = \frac{q}{V_w}[\psi_n(\boldsymbol{x}_1) - \psi_n(\boldsymbol{x}_2)]$$

If the charge q moves to electrode n while the charge –q moves to another electrode, the total induced charge on electrode n is q, because the ψ_n is equal to V_w on electrode n and equal to zero on all other electrodes.

In case both charges go to different electrodes the total induced charge is zero.

After ALL charges have arrived at the electrodes, the total induced charge on a given electrode is equal to the charge that has ARRIVED at this electrode.

Current signals on electrodes that don't receive a charge are therefore strictly bipolar.

Induced Charge, ‘Collected’ Charge

The fact that the total induced charge on an electrode, once ALL charges have arrived at the electrodes, is equal to the actual charge that has ARRIVED at the electrode, leads to very different ‘vocabulary for detectors in different detectors.

In wire chambers the ions take hundreds of microseconds to arrive at the cathodes. Because the electronics ‘integration time’ is typically much shorter than this time, the reality that the signal is ‘induced’ is very well known for wire chambers, and the signal shape is dominated by the movement of the ions.

The longer the amplifier integration time, the more charge is integrated, which is sometimes called ‘collected’ , but it has nothing to do with collecting charge from the detector volume …

In Silicon Detectors, the electrons and holes take only a few ns to arrive at their electrodes, so e.g. for typical ‘integration times’ of amplifiers of 25ns, the shape is dominated by the amplifier response. The peak of the amplifier output is the proportional to the primary charge, and all the charge is ‘collected’

Still, the signal is not due to charges entering the amplifier from the detector, it is due to induction by the moving charge. Once the charge has actually arrived at the electrode, the signal is over !

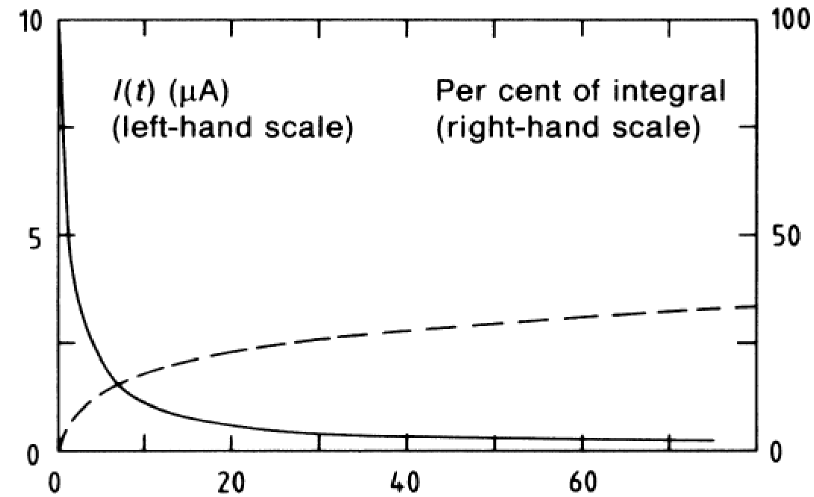

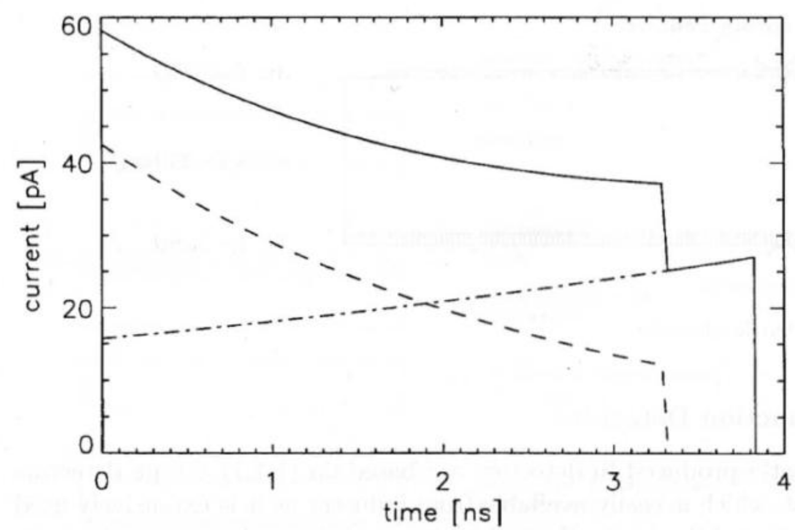

Total Induced Charge

Imagine avalanche in a drift tube, caused by a single electron.
Let's assume that the gas gain is 10^4.
We read out the wire signal with an ideal integrator

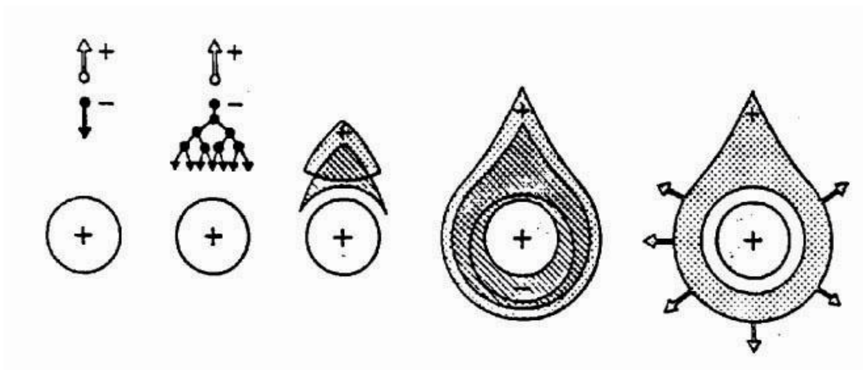

The 10^4 electrons arrive at the wire within <1ns, so the integrator should instantly see the full charge of $-10^4\ e_0$ electrons ?

No ! The ions close to the wire induce the opposite charge on the wire, so in the very beginning there is zero charge on the integrator and only once the Ions have moved away from the wire the integrator measures the full $-10^4\ e_0$

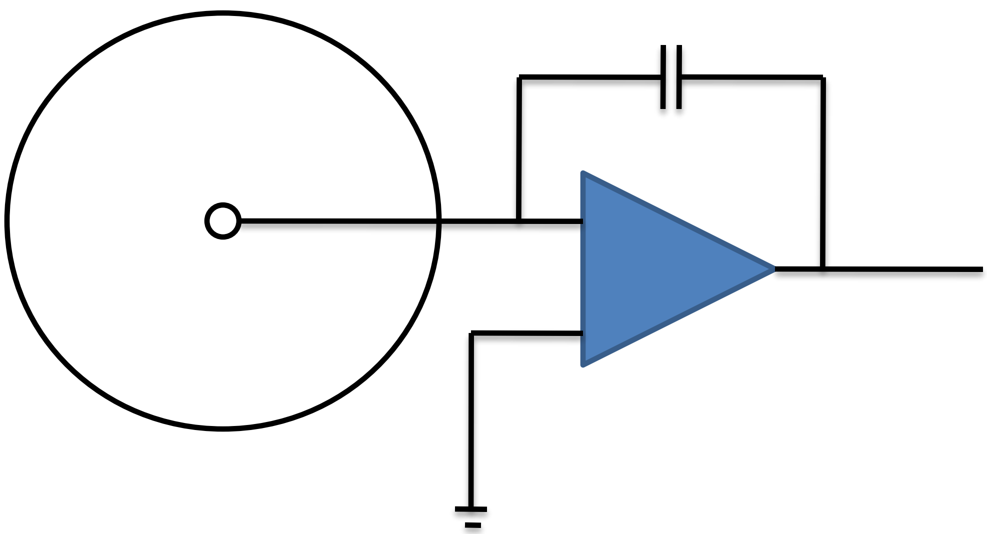

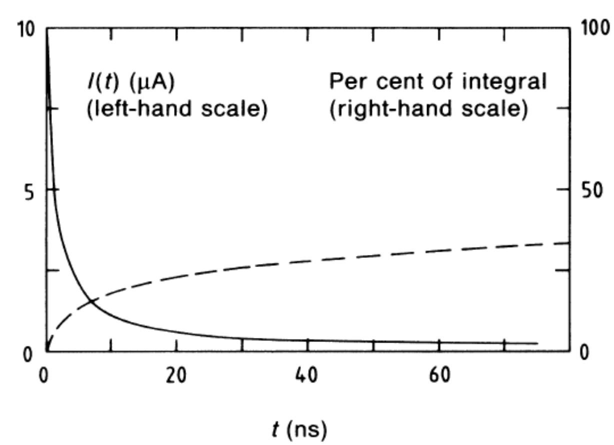

Signal Calculation in 3 Steps

What are the signals induced by a moving charge on electrodes that are connected with arbitrary linear impedance elements ?

1) Calculate the particle trajectory in the 'real' electric field.

2) Remove all the impedance elements, connect the electrodes to ground and calculate the currents induced by the moving charge on the grounded electrodes.

The current induced on a grounded electrode by a charge q moving along a trajectory x(t) is calculated the following way (Ramo Theorem):

One removes the charge q from the setup, puts the electrode to voltage V_0 while keeping all other electrodes grounded. This results in an electric field $E_n(x)$, the Weighting Field, in the volume between the electrodes, from which the current is calculated by

$$I_n(t) = -\frac{q}{V_0}\vec{E}_n[\vec{x}(t)]\frac{d\vec{x}(t)}{dt} = -\frac{q}{V_0}\vec{E}_n[\vec{x}(t)]\vec{v}(t)$$

3) These currents are then placed as ideal current sources on a circuit where the electrodes are 'shrunk' to simple nodes and the mutual electrode capacitances are added between the nodes. These capacitances are calculated from the weighting fields by

$$c_{nm} = \frac{\varepsilon_0}{V_w}\oint_{\boldsymbol{A}_n} \boldsymbol{E}_m(\boldsymbol{x})dA \qquad C_{nn} = \sum_m c_{nm} \qquad C_{nm} = -c_{nm} \quad n \neq m$$

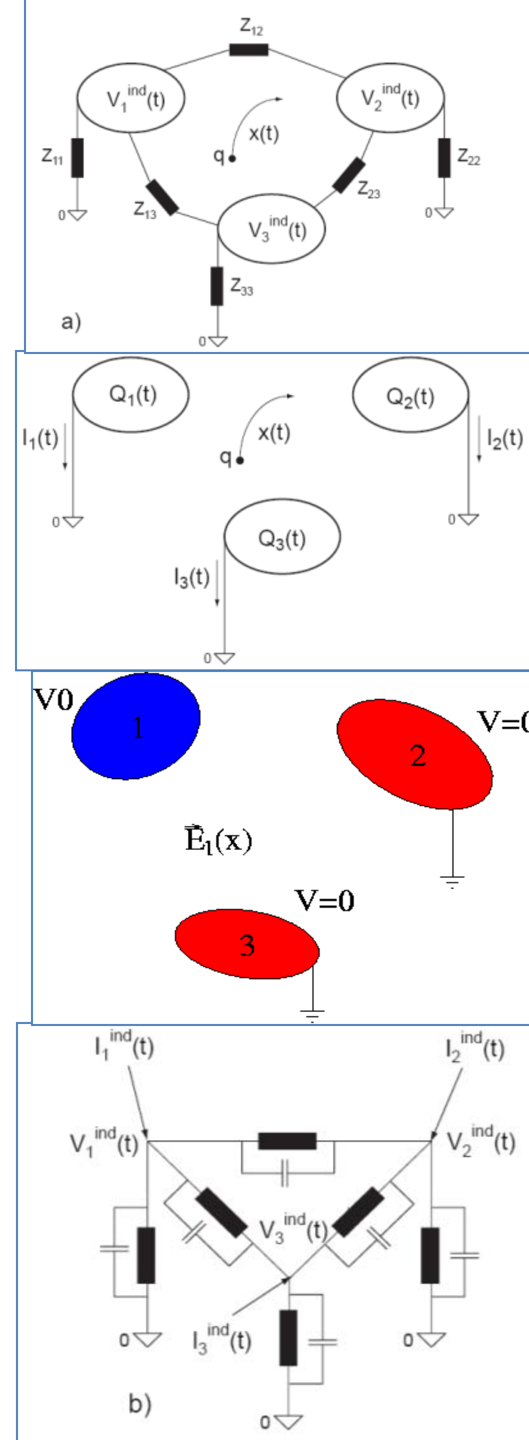

General Signal Theorems

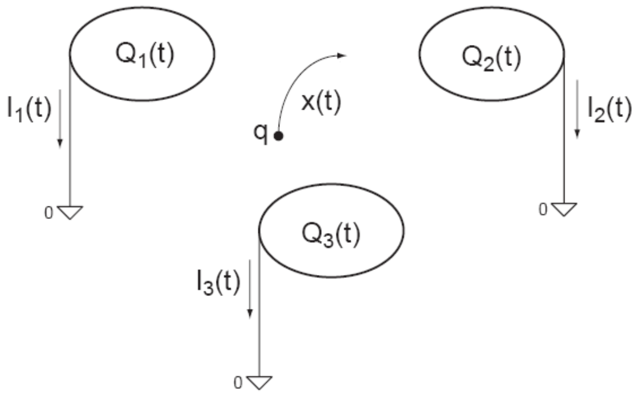

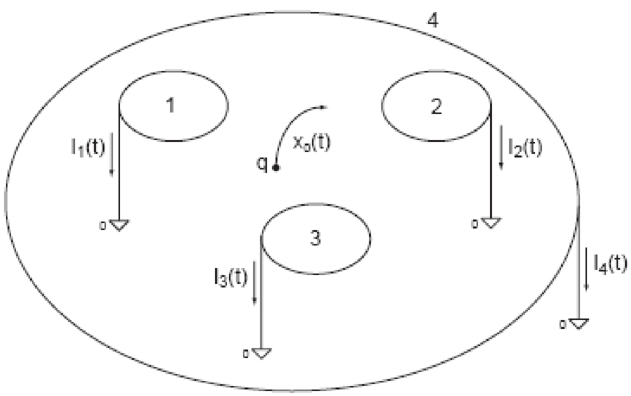

The following relations hold for the induced currents:

1) The charge induced on an electrode in case a charge in between the electrode has moved from a point x_0 to a point x_1 is

$$Q_n^{ind} = \int_{t_0}^{t_1} I_n^{ind}(t)dt = -\frac{q}{V_w}\int_{t_0}^{t_1} \boldsymbol{E}_n[\boldsymbol{x}(t)]\,\dot{\boldsymbol{x}}(t)dt = \frac{q}{V_w}[\psi_n(\boldsymbol{x}_1) - \psi_n(\boldsymbol{x}_0)]$$

and is independent on the actual path.

2) Once ALL charges have arrived at the electrodes, the total induced charge in the electrodes is equal to the charge that has ARRIVED at this electrode.

3) In case there is one electrode enclosing all the others, the sum of all induced currents is zero at any time.

Conclusion

This principle of signal generation is identical for Solid State Detectors, Gas Detectors and Liquid Detectors.

The signals are due to charges (currents) induced on metal electrodes by moving charges.

The easiest way to calculate signals induced by moving charges on metal electrodes is the use of Weighting fields (Ramo – Shockley theorem) for calculation of currents induced on grounded electrodes.

These currents can then be placed as ideal current sources on an equivalent circuit diagram representing the detector.

Signal Formation in Particle Detectors

Werner Riegler, CERN, werner.riegler@cern.ch

II Seminario Nazionale Rivelatori Innovativi

18-22 October 2010, Trieste

Lecture3/3

Signals in Detectors

Signal Calculation in 3 Steps

What are the signals induced by a moving charge on electrodes that are connected with arbitrary linear impedance elements ?

1) Calculate the particle trajectory in the 'real' electric field.

2) Remove all the impedance elements, connect the electrodes to ground and calculate the currents induced by the moving charge on the grounded electrodes.

The current induced on a grounded electrode by a charge q moving along a trajectory x(t) is calculated the following way (Ramo Theorem):

One removes the charge q from the setup, puts the electrode to voltage V_0 while keeping all other electrodes grounded. This results in an electric field $E_n(x)$, the Weighting Field, in the volume between the electrodes, from which the current is calculated by

$$I_n(t) = -\frac{q}{V_0}\vec{E_n}[\vec{x}(t)]\frac{d\vec{x}(t)}{dt} = -\frac{q}{V_0}\vec{E_n}[\vec{x}(t)]\vec{v}(t)$$

3) These currents are then placed as ideal current sources on a circuit where the electrodes are 'shrunk' to simple nodes and the mutual electrode capacitances are added between the nodes. These capacitances are calculated from the weighting fields by

$$c_{nm} = \frac{\varepsilon_0}{V_w}\oint_{\boldsymbol{A}_n}\boldsymbol{E}_m(\boldsymbol{x})d\boldsymbol{A} \qquad C_{nn} = \sum_m c_{nm} \qquad C_{nm} = -c_{nm} \quad n \neq m$$

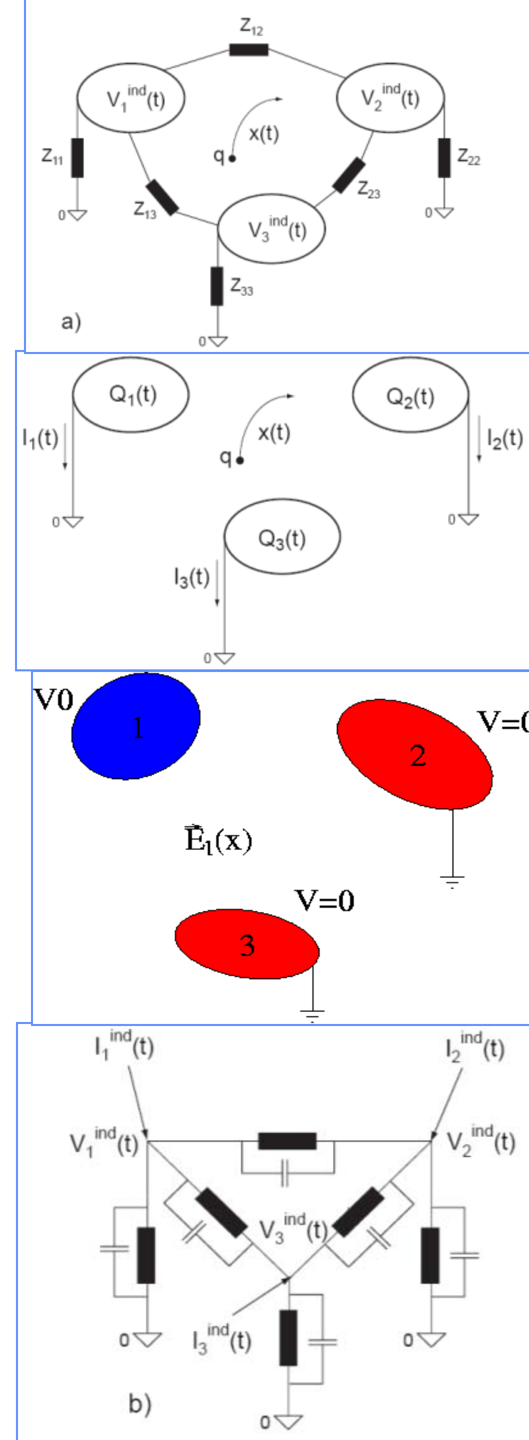

Gas Detectors with internal Electron Multiplication

Principle: At sufficiently high electric fields (100kV/cm) the electrons gain energy in excess of the ionization energy → secondary ionzation etc. etc.

$dN = N \alpha \, dx$ α…Townsend Coefficient

$N(x) = N_0 \exp(\alpha x)$ $N/N_0 = A$ (Amplification, Gas Gain)

Avalanche in a homogeneous field:

Problem: High field on electrode surface → breakdown

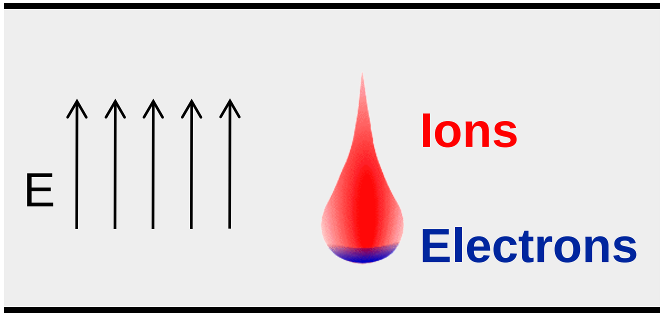

In an inhomogeneous Field: $\alpha(E)$ → $N(x) = N_0 \exp [\int \alpha(E(x'))dx']$

W. Riegler/CERN

Wire Chamber Signals

Wire with radius (10-25μm) in a tube of radius b (1-3cm):

$$E(r) = \frac{\lambda}{2\pi\varepsilon_0}\frac{1}{r} = \frac{V_0}{\ln\frac{b}{a}}\frac{1}{r}, \qquad V(r) = \frac{V_0}{\ln\frac{b}{a}}\ln\frac{r}{a},$$

Electric field close to a thin wire (100-300kV/cm). E.g. V_0=1000V, a=10μm, b=10mm, E(a)=150kV/cm

The electric field is large enough to accelerate electrons to energies which are sufficient to produce secondary ionization → electron avalanche → signal.

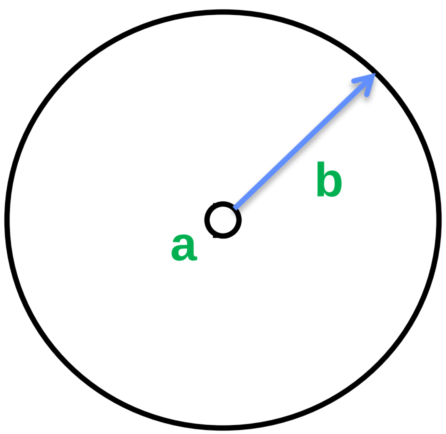

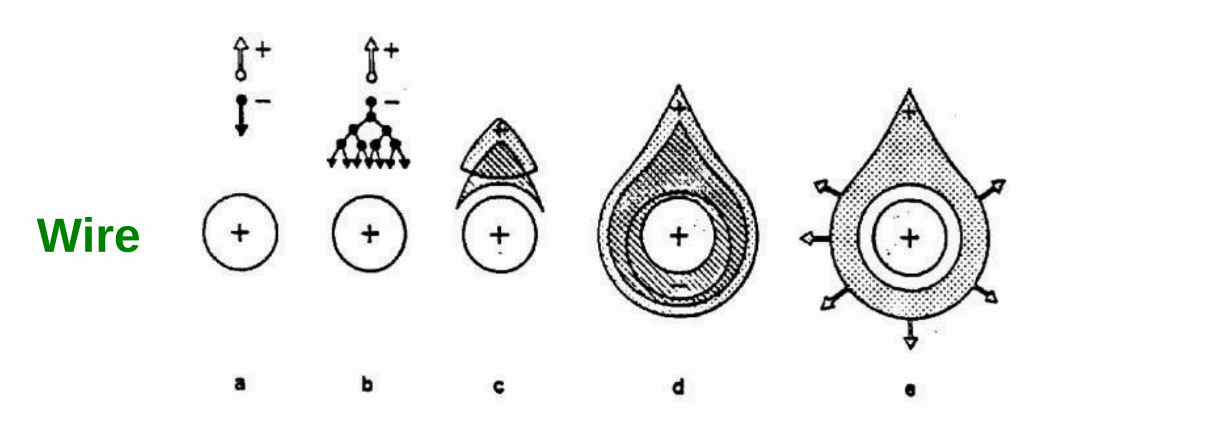

Wire Chamber Signals

The electrons are produced very close to the wire, so for now we assume that N_{tot} ions are moving from the wire surface to the tube wall

$$E(r) = \frac{\lambda}{2\pi\varepsilon_0}\frac{1}{r} = \frac{U}{\ln\frac{b}{a}\, r}, \qquad V(r) = \frac{U}{\ln\frac{b}{a}}\ln\frac{r}{a},$$

Ions move with a velocity proportional to the electric field.

$$v = \mu E$$

$$\frac{dr(t)}{dt} = \mu\frac{U}{r(t)\ln(b/a)} \quad \rightarrow \quad r(t) = a\sqrt{1+\frac{t}{t_0}} \qquad t_0 = \frac{a^2\ln(b/a)}{2\mu U}$$

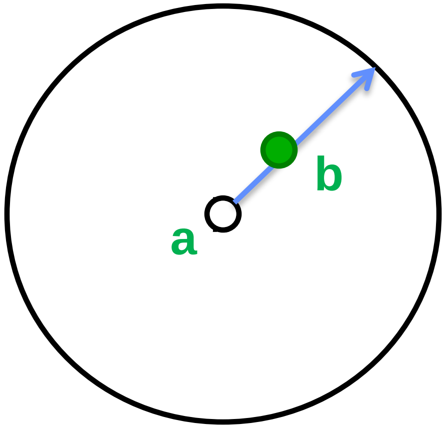

Weighting Field of the wire: Remove charge and set wire to V_w while grounding the tube wall.

$$E_1(r) = \frac{V_w}{r\ln(b/a)}$$

The induced current is therefore

$$I_1^{ind}(t) = -\frac{N_{tot}e_0}{V_w}E_1[r(t)]\,\dot{r}(t) = -\frac{N_{tot}e_0}{2\ln(b/a)}\frac{1}{t+t_0}.$$

Wire Chamber Signals

$$I_1^{ind}(t) = -\frac{N_{tot}e_0}{V_w}E_1[r(t)]\,\dot{r}(t) = -\frac{N_{tot}e_0}{2\ln(b/a)}\frac{1}{t+t_0}.$$

$$Q_1^{ind}(t) = \int_0^t I_1^{ind}(t')dt' = -\frac{N_{tot}e_0}{2\ln(b/a)}\ln\left(1+\frac{t}{t_0}\right)$$

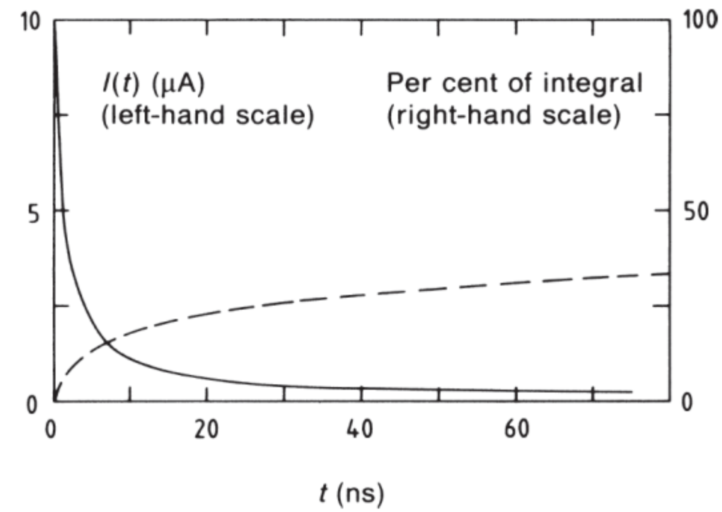

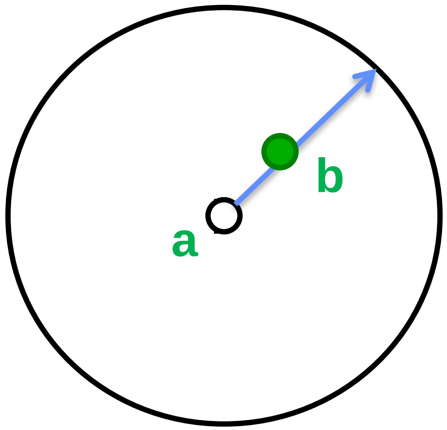

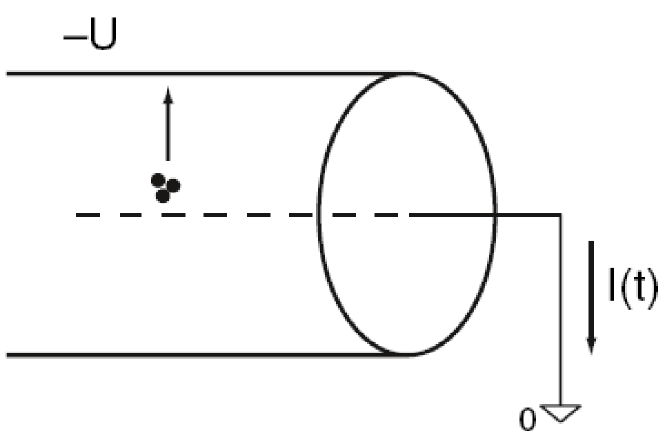

Wire Chamber: Electron Avalanches on the Wire

Proportional region: $A \approx 10^3$-10^4 — **LHC**

Semi proportional region: $A \approx 10^4$-10^5
(space charge effect)

Saturation region: $A > 10^6$
Independent the number of primary electrons.

1970ies

Streamer region: $A > 10^7$
Avalanche along the particle track.

Limited Geiger region:
Avalanche propagated by UV photons.

Geiger region: $A \approx 10^9$
Avalanche along the entire wire.

1950ies

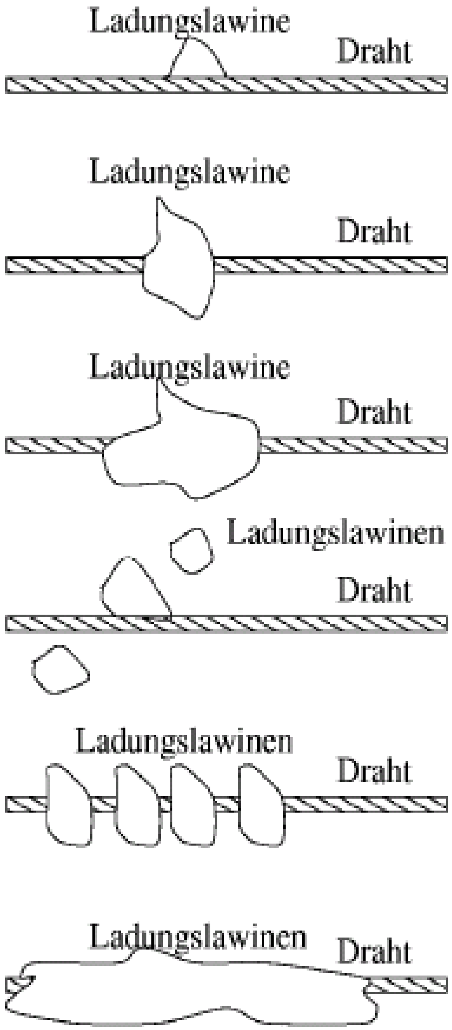

Wire Chamber: Signals from Electron Avalanches

The electron avalanche happens very close to the wire. First multiplication only around R =2x wire radius. Electrons are moving to the wire surface very quickly (<<1ns). Ions are difting towards the tube wall (typically several 100μs.)

The signal is characterized by a very fast 'spike' from the electrons and a long Ion tail.

The total charge induced by the electrons, i.e. the charge of the current spike due to the short electron movement amounts to 1-2% of the total induced charge.

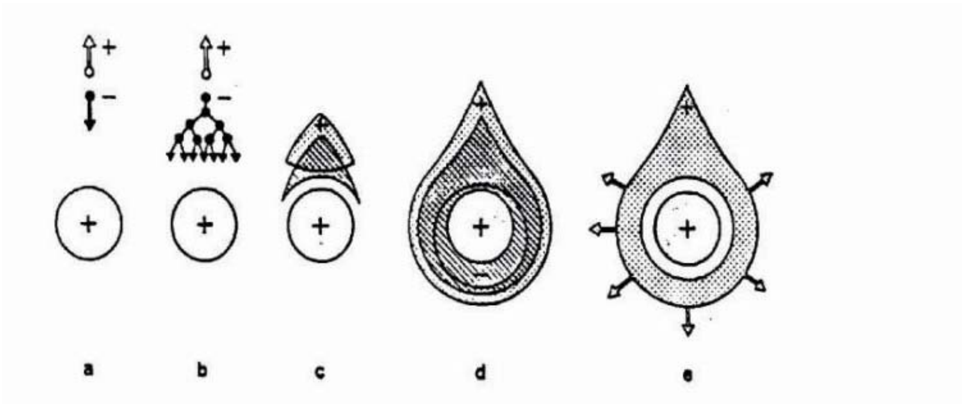

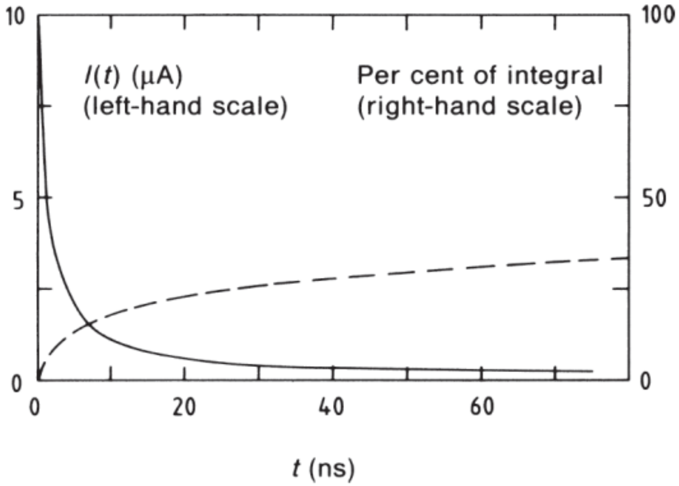

Detectors with Electron Multiplication

Rossi 1930: Coincidence circuit for n tubes

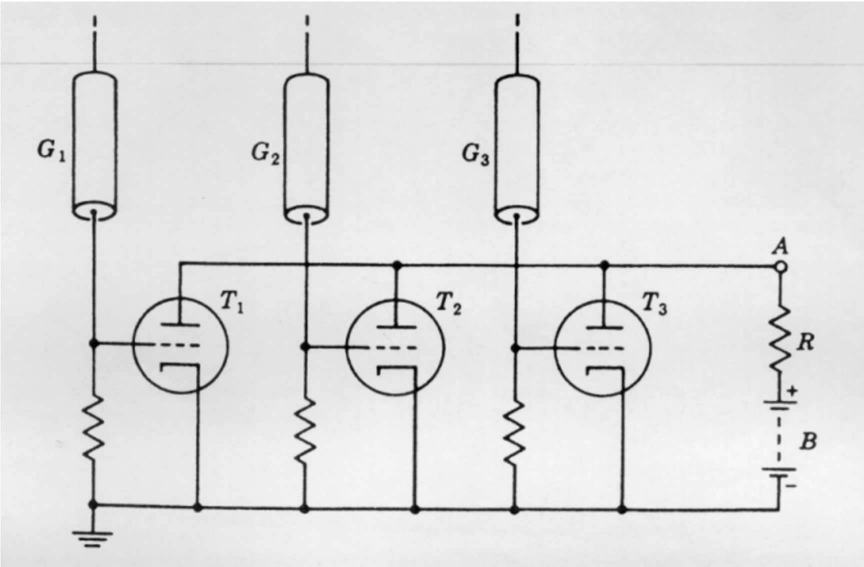

Cosmic ray telescope 1934

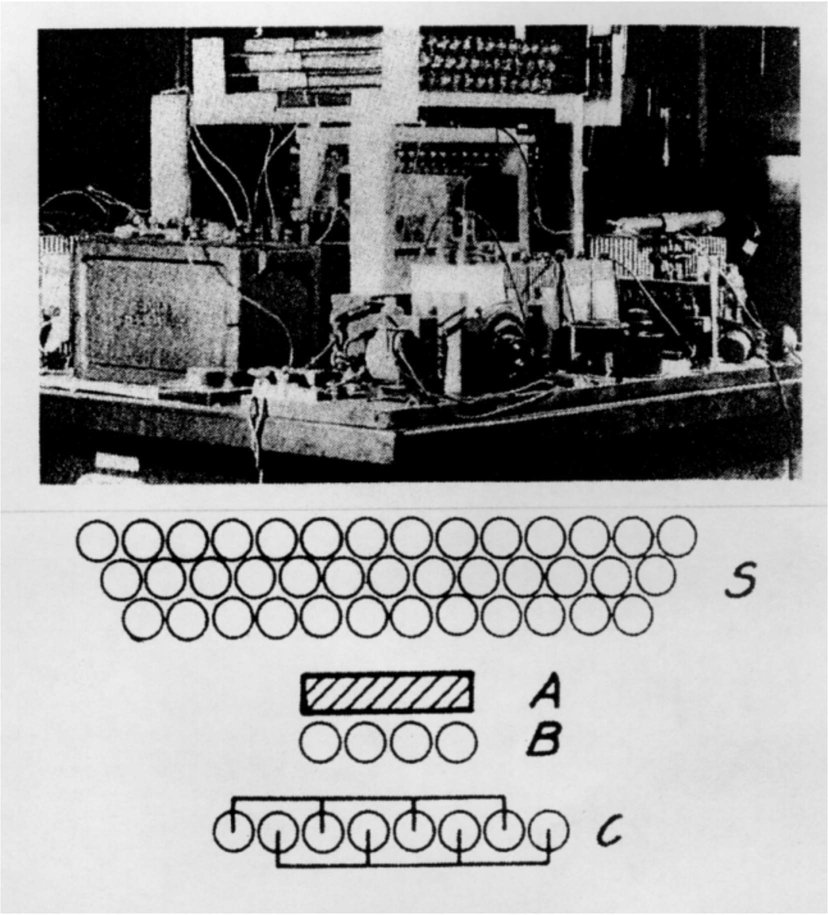

Geiger mode, large deadtime

Position resolution is determined by the size of the tubes.

Signal was directly fed into an electronic tube.

The Geiger Counter reloaded: Drift Tube

Primary electrons are drifting to the wire.

Electron avalanche at the wire.

The measured drift time is converted to a radius by a (calibrated) radius-time correlation.

Many of these circles define the particle track.

ATLAS MDT R(tube) =15mm

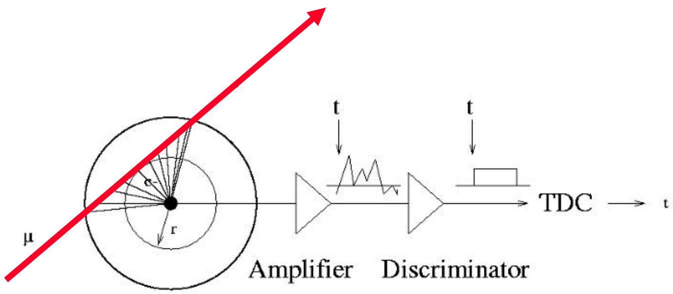

Calibrated Radius-Time correlation

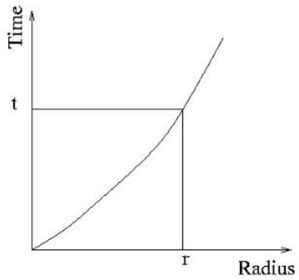

ATLAS Muon Chambers

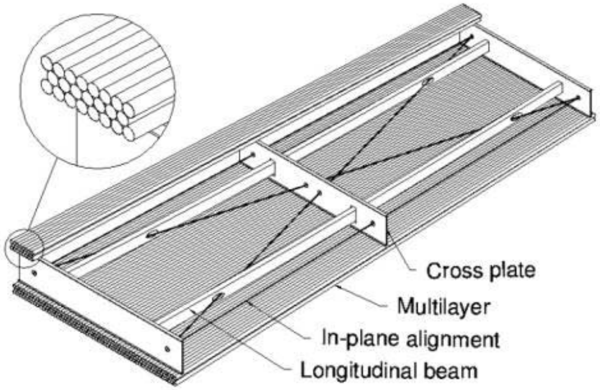

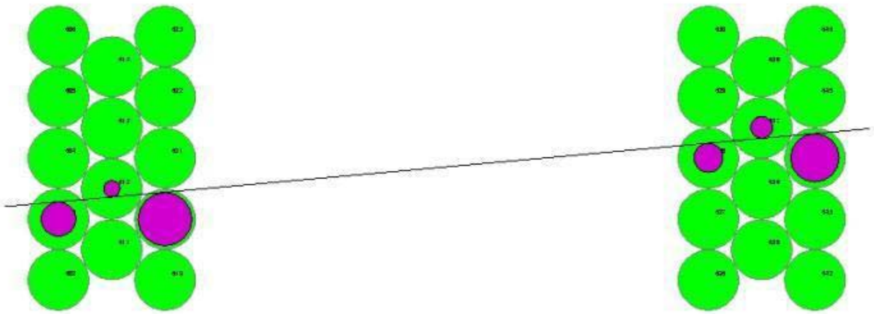

ATLAS MDTs, 80μm per tube

1938: How to make a good Geiger Counter

1. Starting with a copper-in-glass counter with a tungsten wire, clean the copper thoroughly with about 6 normal nitric acid. (A water aspirator is indispensable for admitting and removing solutions.) Such a concentration of acid will leave the copper very bright.

2. After rinsing well, introduce a solution of 0.1 normal nitric acid. This will remove any copper compounds formed by the stronger acid.

3. Rinse thoroughly (at least 10 times) with distilled water and dry.

4. With dry air inside, heat the whole counter in a large flame until the copper turns a uniform brownish-black color.

5. Seal the counter off temporarily and then heat for several hours at about 400°C. Upon cooling, the copper cylinder will be coated with the bright red oxide, Cu_2O.

6. Evacuate and admit dry NO_2 gas to a pressure of 1 atmosphere. (This gas can be made by the action of 16 normal nitric acid on copper. It may be dried by passing through $CaCl_2$ and P_2O_5.)

7. Heat the counter with the NO_2 until the Cu_2O turns a dark velvety color. Pump out the NO_2.

8. Admit argon (commercial, 99 per cent pure is satisfactory), which has been bubbled through xylene, to a pressure of 6 to 10 cm of mercury pressure. The counter should be tried at this point. For a 1-inch counter the threshold should be 600 to 800 volts for 8 cm of mercury pressure. If the counter does not work properly, the gas should be pumped out and more argon, which has been bubbled through the xylene, admitted.

9. When the counter is found to work satisfactorily, it may be sealed off.

Neher, 1938, Procedures in Experimental Physics

Although all the above steps may not be necessary in all cases, yet this procedure has been found to give very satisfactory counters having reaction times of 10^{-5} second or better. The characteristics of the counters also seem to be permanent. The photoelectric properties as well as the electrical resistance of the surface are probably radically changed by this treatment.

In today's large scale applications of particle detectors it is extremely important to understand the 'detector physics' of the device.

Readout electronics is much more sophisticated and integrated.

Similar to Astronomy where the 'old' large telescopes are still there, but the new 'readout' like CCDs etc. improve the instrument by orders of magnitude.

The Geiger counter reloaded: Drift Tube

Atlas Muon Spectrometer, 44m long, from r=5 to11m.

1200 Chambers

6 layers of 3cm tubes per chamber.

Length of the chambers 1-6m !

Position resolution: 80μm/tube, <50μm/chamber (3 bar)

Maximum drift time $\approx$700ns

Gas Ar/CO_2 93/7

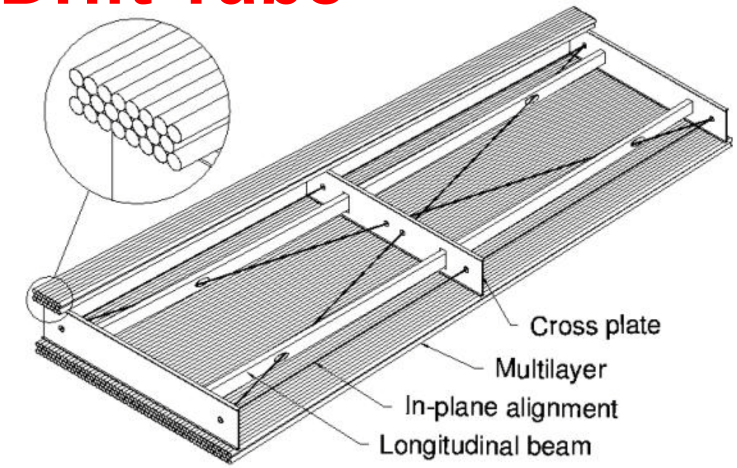

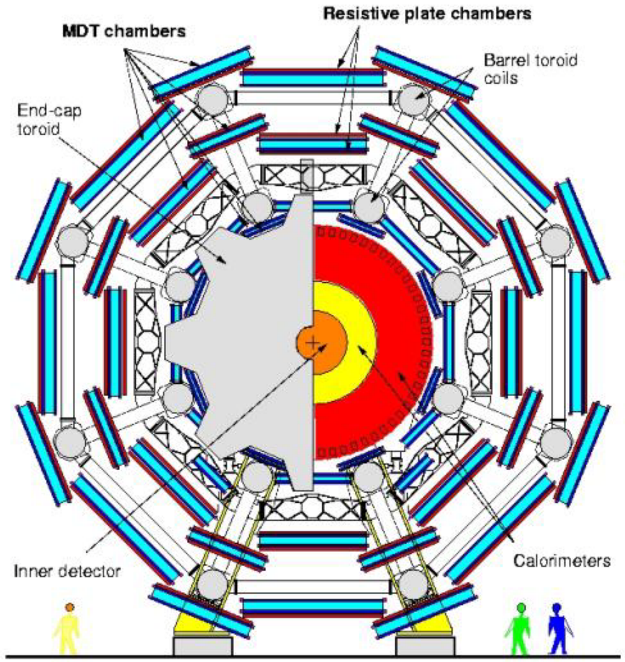

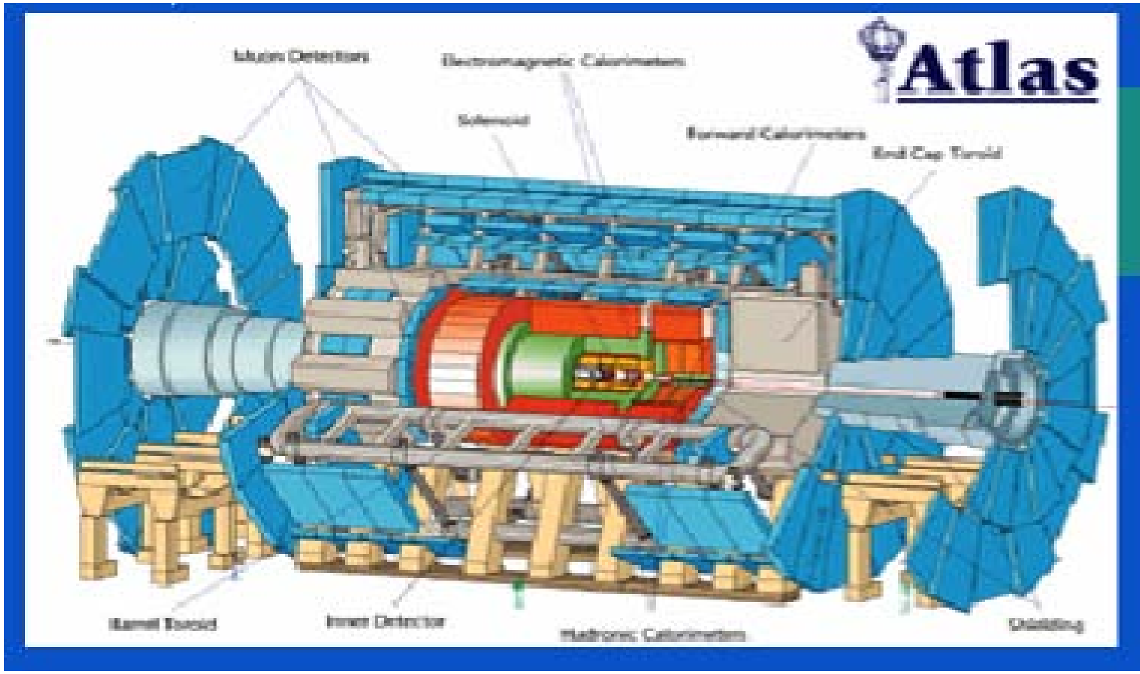

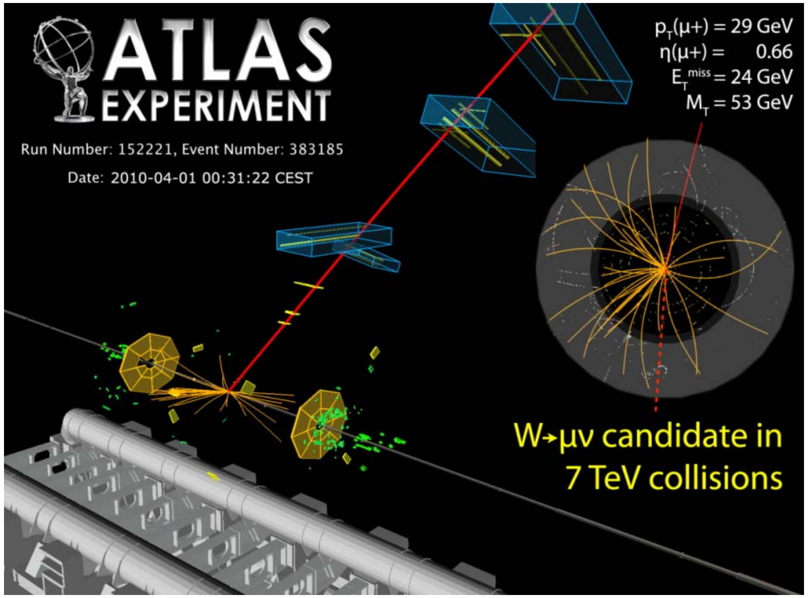
ATLAS EXPERIMENT
Run Number: 152221, Event Number: 383185
Date: 2010-04-01 00:31:22 CEST
$p_T(\mu+)$ = 29 GeV
$\eta(\mu+)$ = 0.66
E_T^{miss} = 24 GeV
M_T = 53 GeV
W→μν candidate in 7 TeV collisions

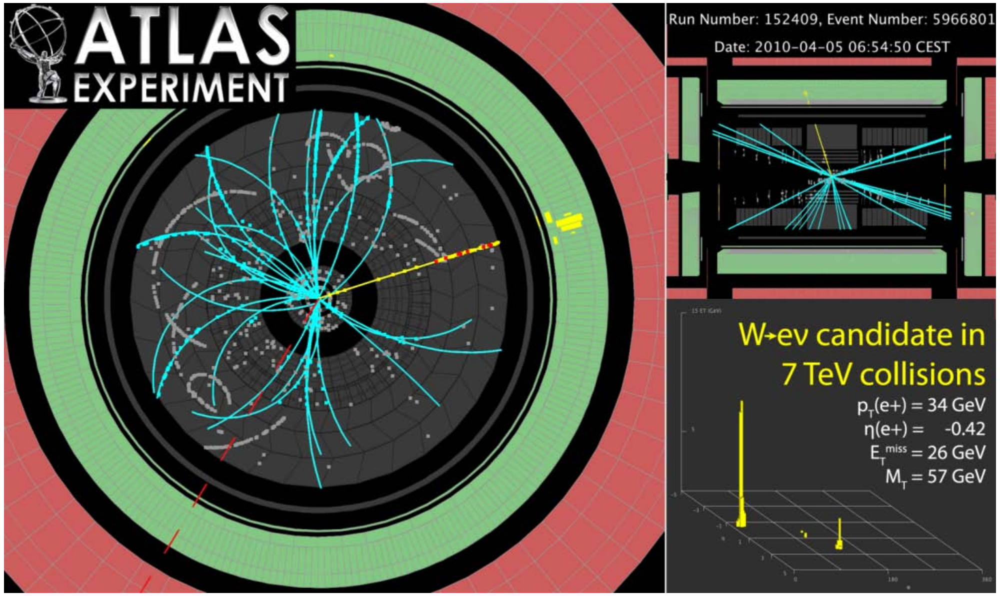
ATLAS EXPERIMENT
Run Number: 152409, Event Number: 5966801
Date: 2010-04-05 06:54:50 CEST
W→eν candidate in 7 TeV collisions
$p_T(e+)$ = 34 GeV
$\eta(e+)$ = -0.42
E_T^{miss} = 26 GeV
M_T = 57 GeV

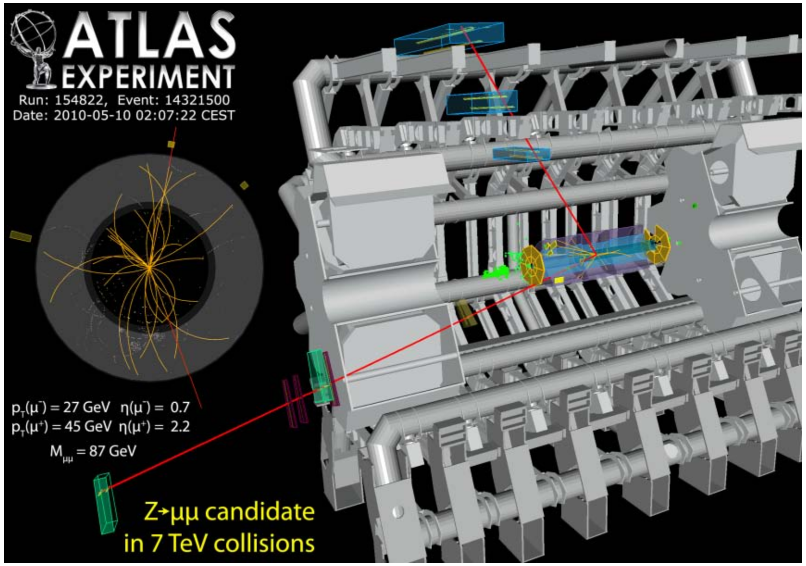
ATLAS EXPERIMENT
Run: 154822, Event: 14321500
Date: 2010-05-10 02:07:22 CEST
$p_T(\mu^-)$ = 27 GeV $\eta(\mu^-)$ = 0.7
$p_T(\mu^+)$ = 45 GeV $\eta(\mu^+)$ = 2.2
$M_{\mu\mu}$ = 87 GeV
Z→μμ candidate in 7 TeV collisions

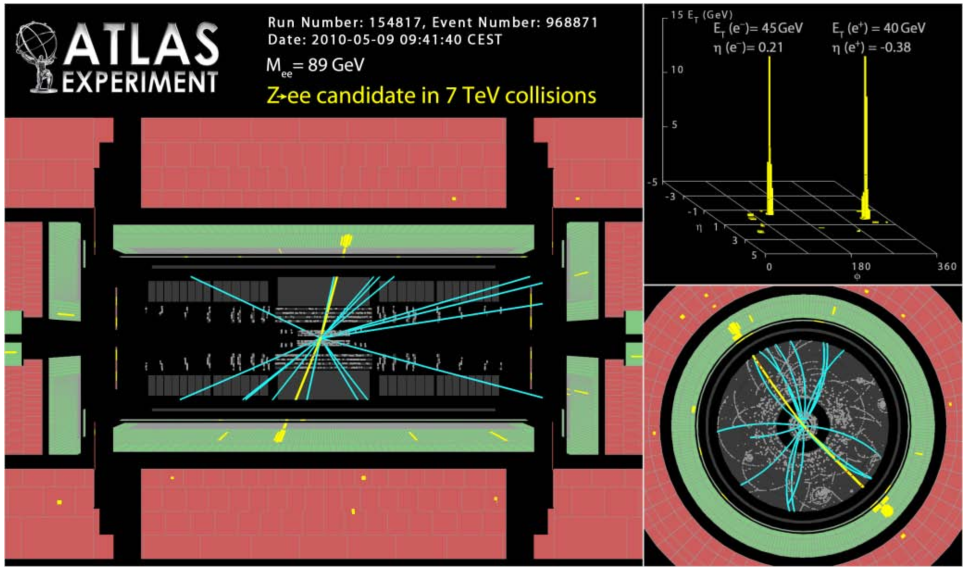
ATLAS EXPERIMENT
Run Number: 154817, Event Number: 968871
Date: 2010-05-09 09:41:40 CEST
M_{ee} = 89 GeV
Z→ee candidate in 7 TeV collisions
$E_T(e^-)$ = 45 GeV
$\eta(e^-)$ = 0.21
$E_T(e^+)$ = 40 GeV
$\eta(e^+)$ = -0.38

Solid State Detectors

Gas Detectors

In gaseous detectors, a charged particle is liberating electrons from the atoms, which are freely bouncing between the gas atoms.

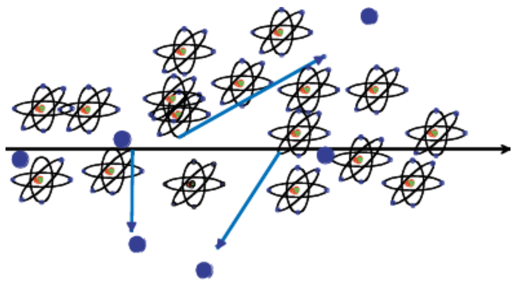

An applied electric field makes the electrons and ions move, which induces signals on the metal readout electrodes.

For individual gas atoms, the electron energy levels are discrete.

Solid State Detectors

In solids (crystals), the electron energy levels are in 'bands'.

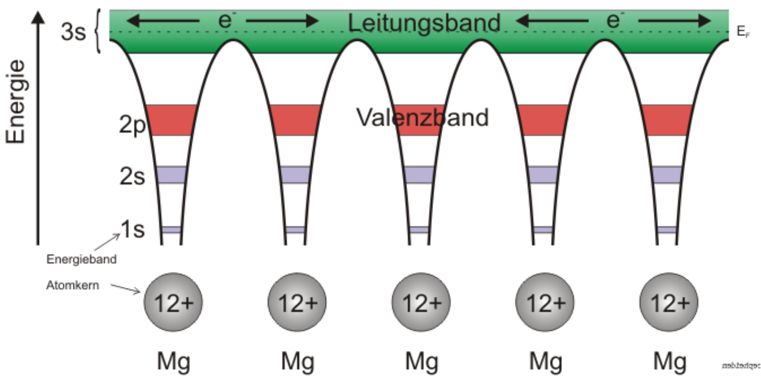

Inner shell electrons, in the lower energy bands, are closely bound to the individual atoms and always stay with 'their' atoms.

In a crystal there are however energy bands that are still bound states of the crystal, but they belong to the entire crystal. Electrons in these bands and the holes in the lower band can freely move around the crystal, if an electric field is applied.

Solid State Detectors

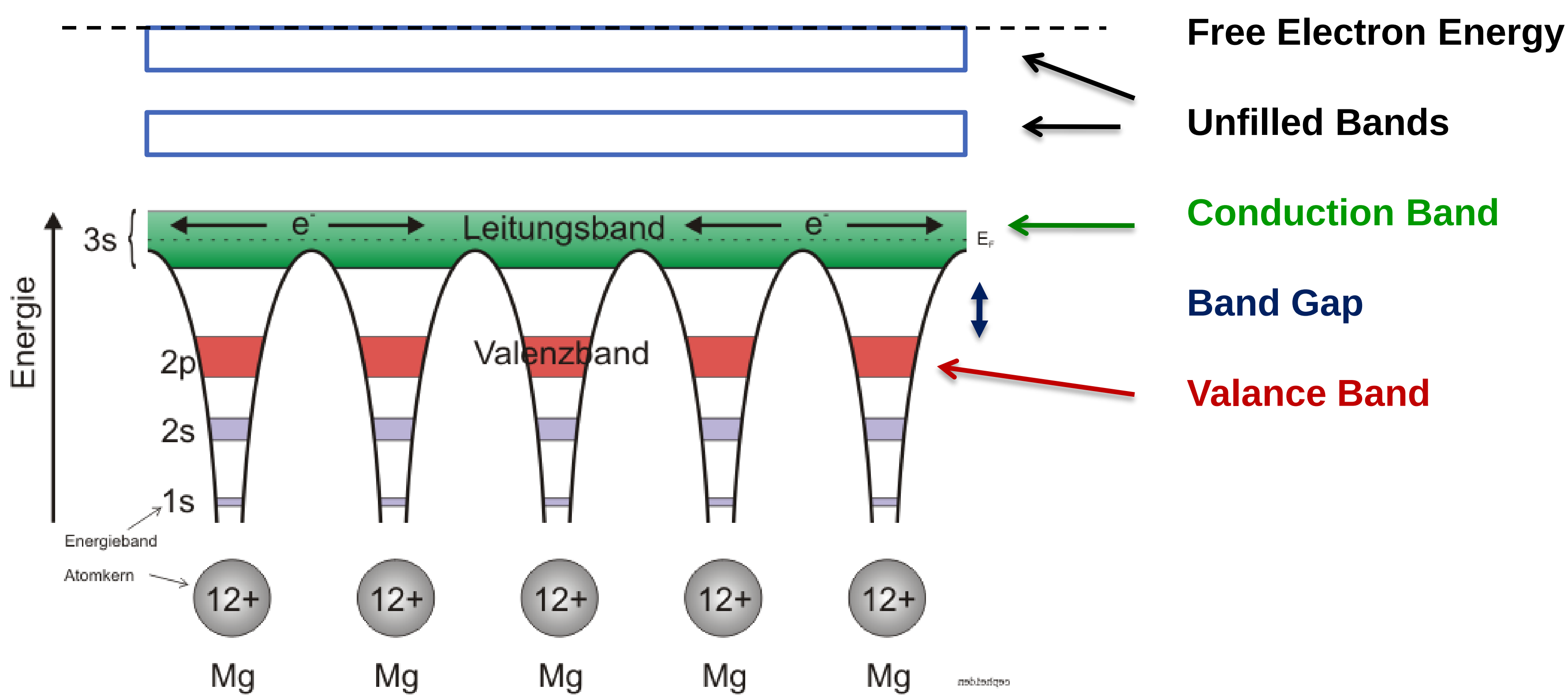

Conductor, Insulator, Semiconductor

In case the conduction band is filled the crystal is a conductor.

In case the conduction band is empty and 'far away' from the valence band, the crystal is an insulator.

In case the conduction band is empty but the distance to the valence band is small, the crystal is a semiconductor.

Solid State Detectors

Band Gap, e-h pair Energy

The energy gap between the last filled band – the valence band – and the conduction band is called band gap E_g.

The band gap of Diamond/Silicon/Germanium is 5.5, 1.12, 0.66 eV.

The average energy to produce an electron/hole pair for Diamond/Silicon/Germanium is 13, 3.6, 2.9eV.

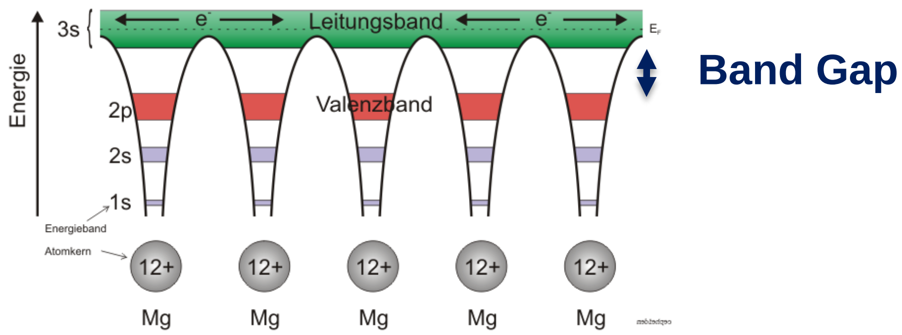

Temperature, Charged Particle Detection

In case an electron in the valence band gains energy by some process, it can be excited into the conduction band and a hole in the valence band is left behind.

Such a process can be the passage of a charged particle, but also thermal excitation → probability is proportional Exp($-E_g$/kT).

The number of electrons in the conduction band is therefore increasing with temperature i.e. the conductivity of a semiconductor increases with temperature.

Solid State Detectors

Electron, Hole Movement:

It is possible to treat electrons in the conduction band and holes in the valence band similar to free particles, but with an effective mass different from elementary electrons not embedded in the lattice.

This mass is furthermore dependent on other parameters such as the direction of movement with respect to the crystal axis. All this follows from the QM treatment of the crystal (solid state physics).

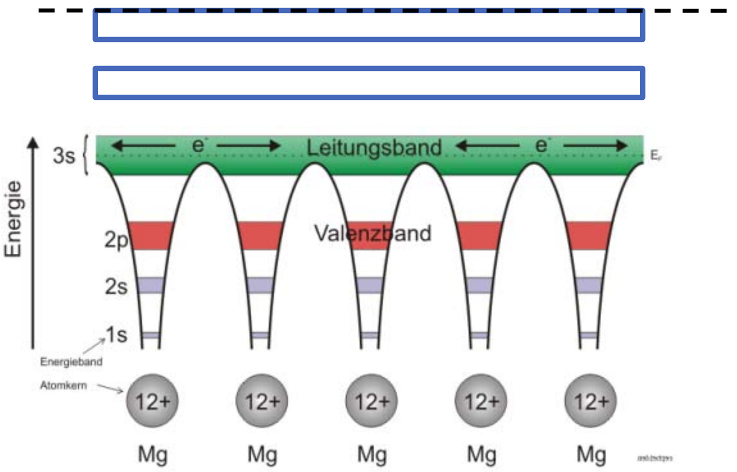

Cooling:

If we want to use a semiconductor as a detector for charged particles, the number of charge carriers in the conduction band due to thermal excitation must be smaller than the number of charge carriers in the conduction band produced by the passage of a charged particle.

Diamond (E_g=5.5eV) can be used for particle detection at room temperature,
Silicon (E_g=1.12 eV) and Germanium (E_g=0.66eV) must be cooled, or the free charge carriers must be eliminated by other tricks → doping → see later.

Solid State Detectors

Primary 'ionization':
The average energy to produce an electron/hole pair is:
Diamond (13eV), Silicon (3.6eV), Germanium (2.9eV)

Comparing to gas detectors, the density of a solid is about a factor 1000 larger than that of a gas and the energy to produce and electron/hole pair e.g. for Si is a factor 7 smaller than the energy to produce an electron-ion pair in Argon.

Solid State vs. Gas Detector:
The number of primary charges in a Si detector is therefore about 10^4 times larger than the one in gas → while gas detectors need internal charge amplification, solid state detectors don't need internal amplification.

While in gaseous detectors, the velocity of electrons and ions differs by a factor 1000, the velocity of electrons and holes in many semiconductor detectors is quite similar → very short signals.

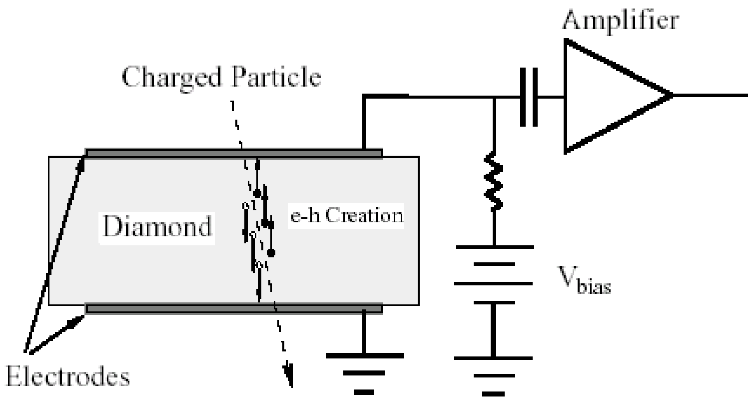

Diamond → A solid state ionization chamber

Diamond Detector

Typical thickness – a few 100μm.

<1000 charge carriers/cm³ at room temperature due to large band gap.

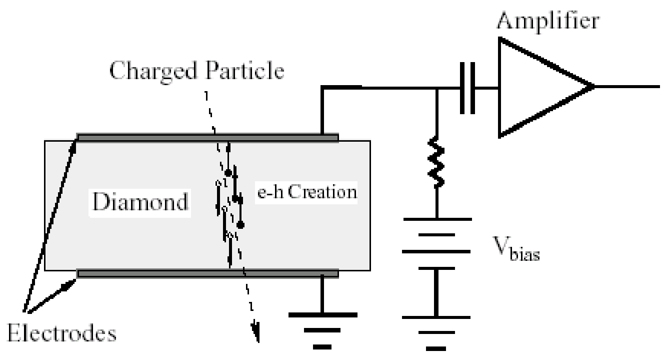

Velocity:

μ_e=1800 cm²/Vs, μ_h=1600 cm²/Vs

Velocity = μE, 10kV/cm → v=180 μm/ns → Very fast signals of only a few ns length !

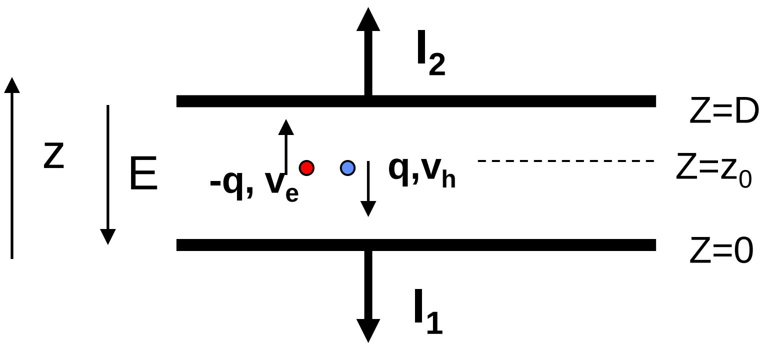

Diamond Detector

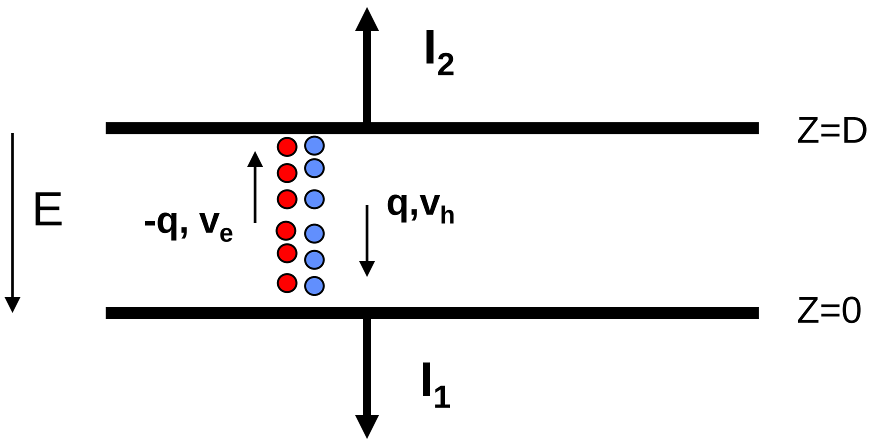

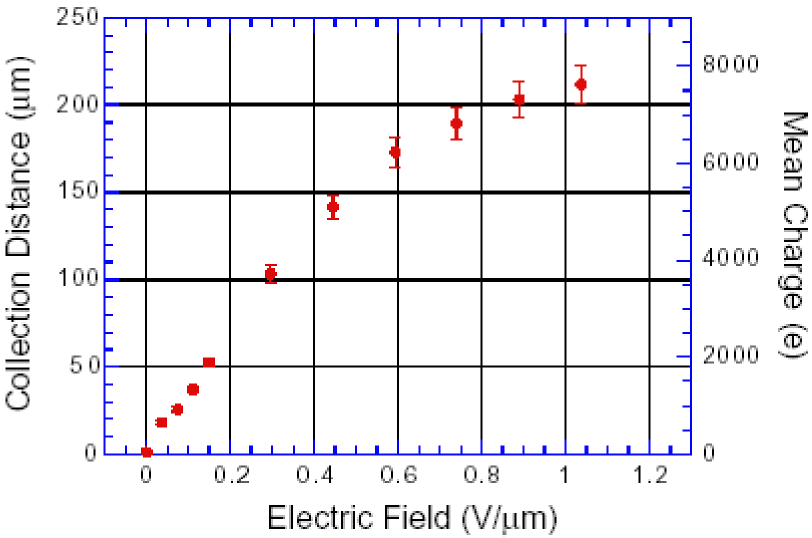

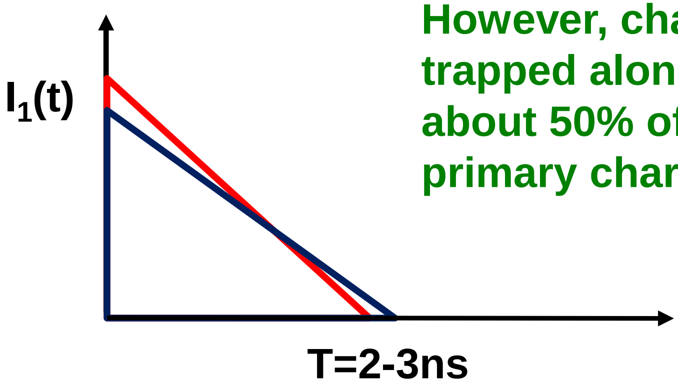

However, charges are trapped along the track, only about 50% of *produced* primary charge is *induced* →

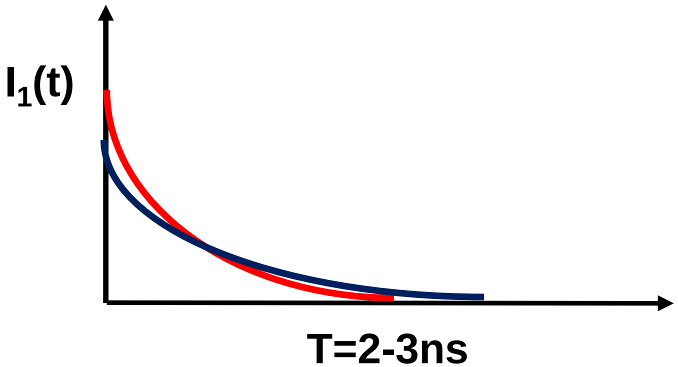

Silicon Detector

Velocity:
μ_e=1450 cm^2/Vs, μ_h=505 cm^2/Vs, 3.63eV per e-h pair.
~33000 e/h pairs in 300µm of silicon.

However: Free charge carriers in Si:
T=300 K: e,h = 1.45 x 10^{10} / cm^3 but only 33000 e/h pairs in 300µm produced by a high energy particle.

Why can we use Si as a solid state detector ???

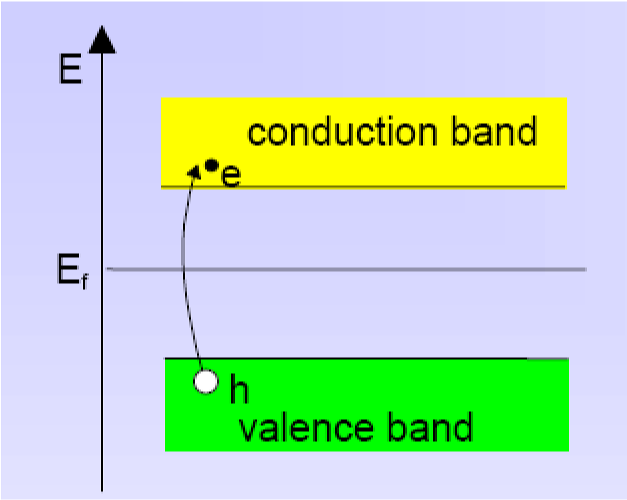

Doping of Silicon

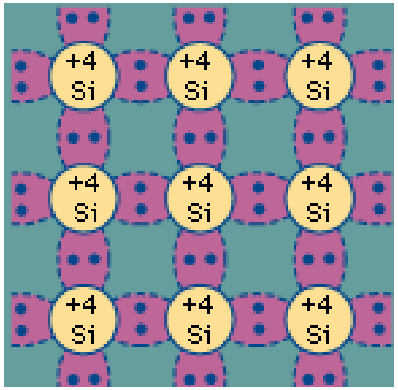

doping

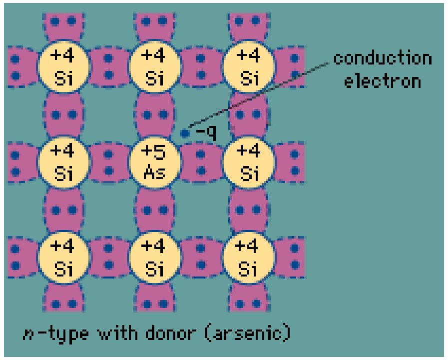

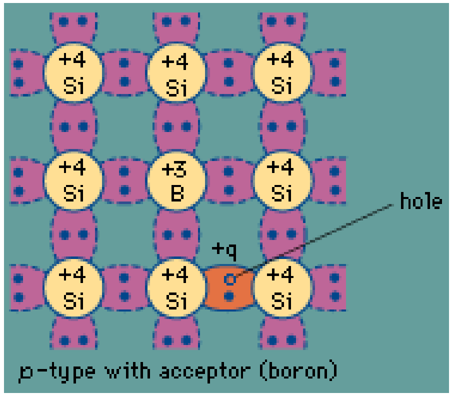

In a silicon crystal at a given temperature the number of electrons in the conduction band is equal to the number of holes in the valence band.

Doping Silicon with Arsen (+5) it becomes and n-type conductor (more electrons than holes).

Doping Silicon with Boron (+3) it becomes a p-type conductor (more holes than electrons).

Bringing p and n in contact makes a diode.

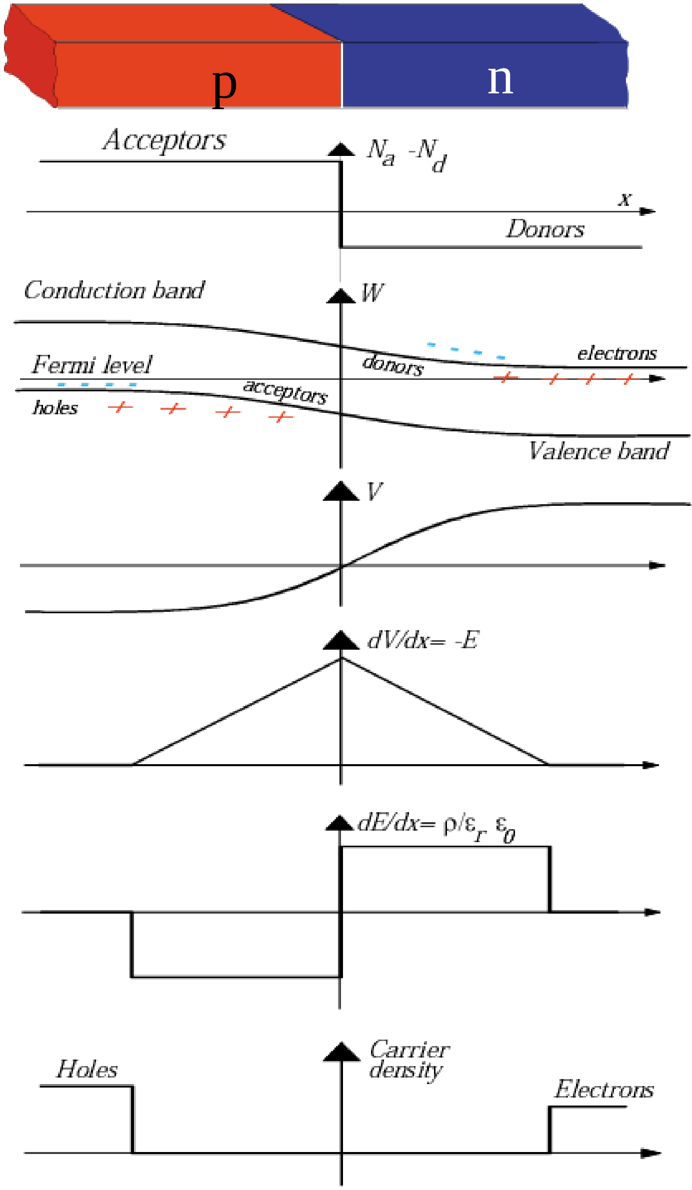

Si-Diode used as a Particle Detector !

At the p-n junction the charges are depleted and a zone free of charge carriers is established.

By applying a voltage, the depletion zone can be extended to the entire diode → highly insulating layer.

An ionizing particle produces free charge carriers in the diode, which drift in the electric field and induce an electrical signal on the metal electrodes.

As silicon is the most commonly used material in the electronics industry, it has one big advantage with respect to other materials, namely highly developed technology.

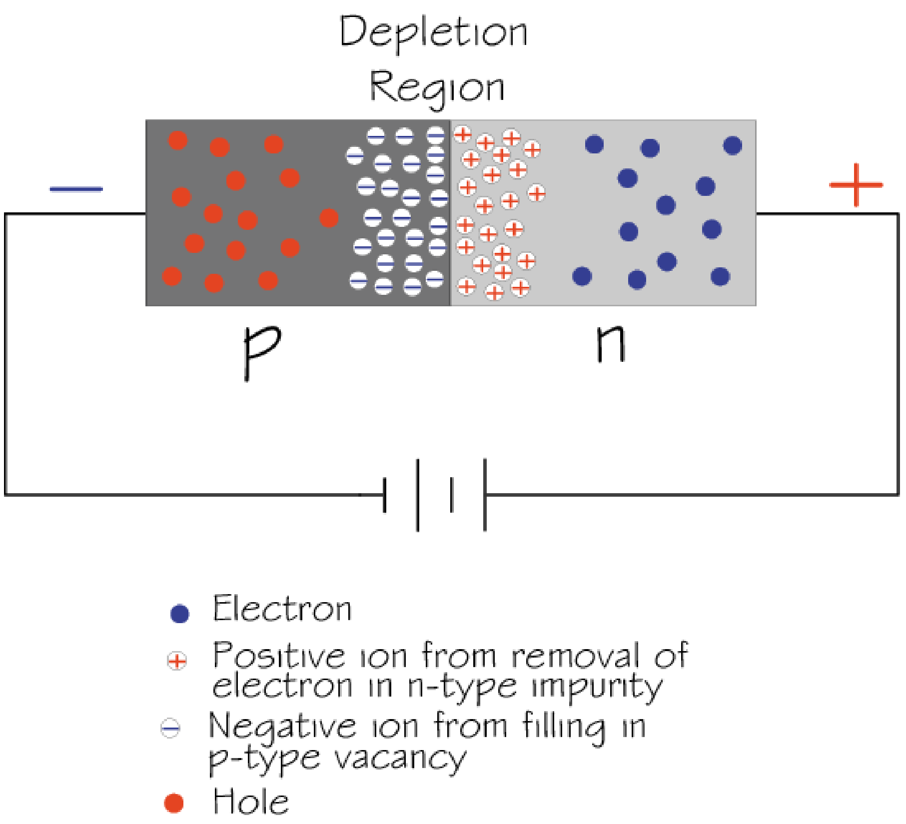

Under-Depleted Silicon Detector

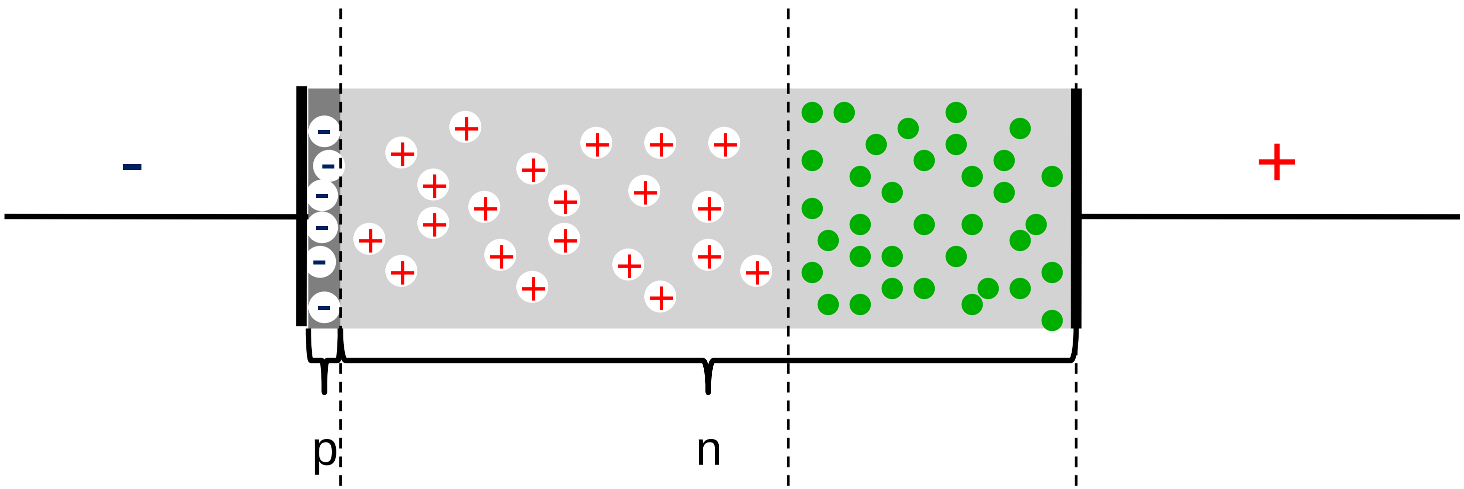

Zone without free charge carriers positively charged. Sensitive Detector Volume.

Zone with free electrons. Conductive. Insensitive to particles.

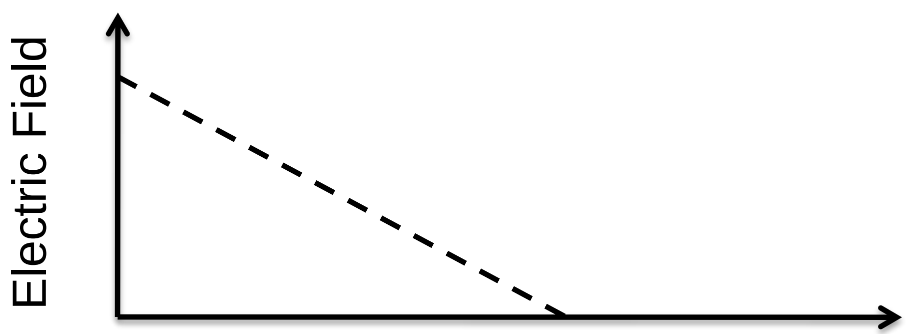

Fully-Depleted Silicon Detector

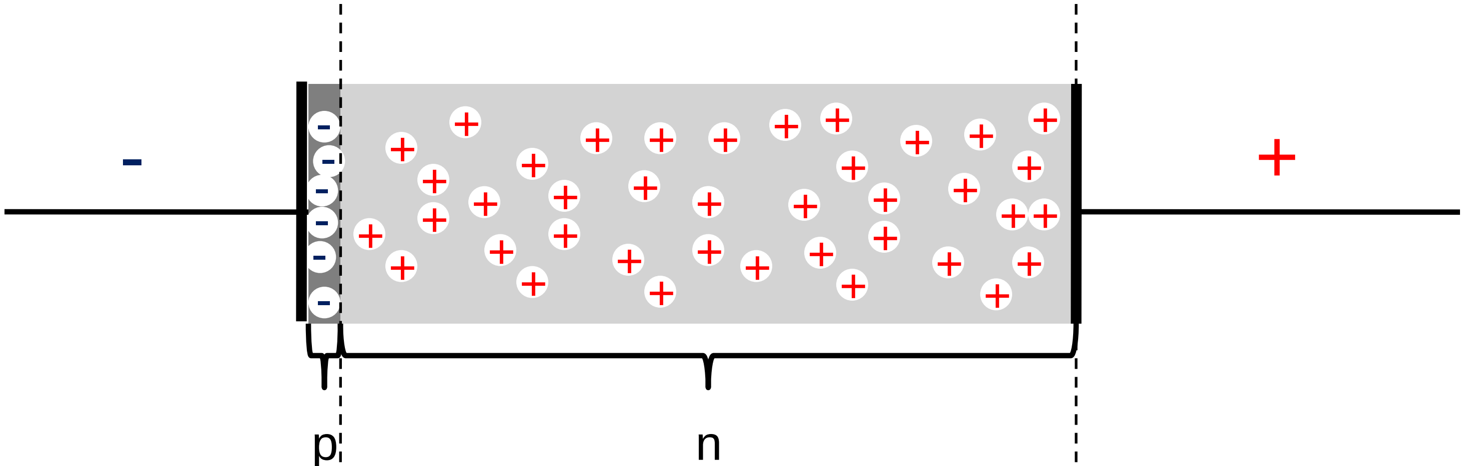

Zone without free charge carriers positively charged.
Sensitive Detector Volume.

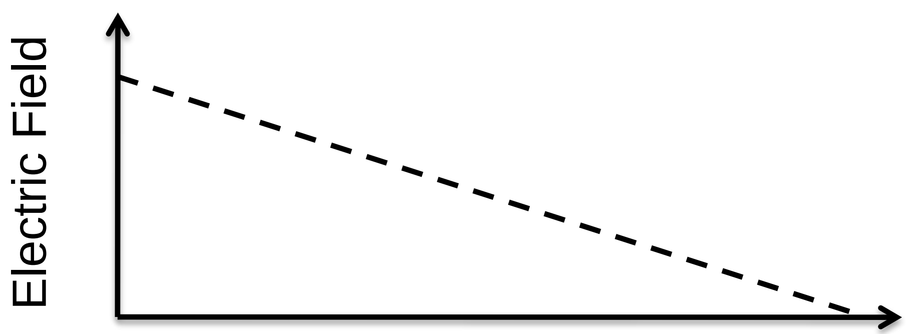

Over-Depleted Silicon Detector

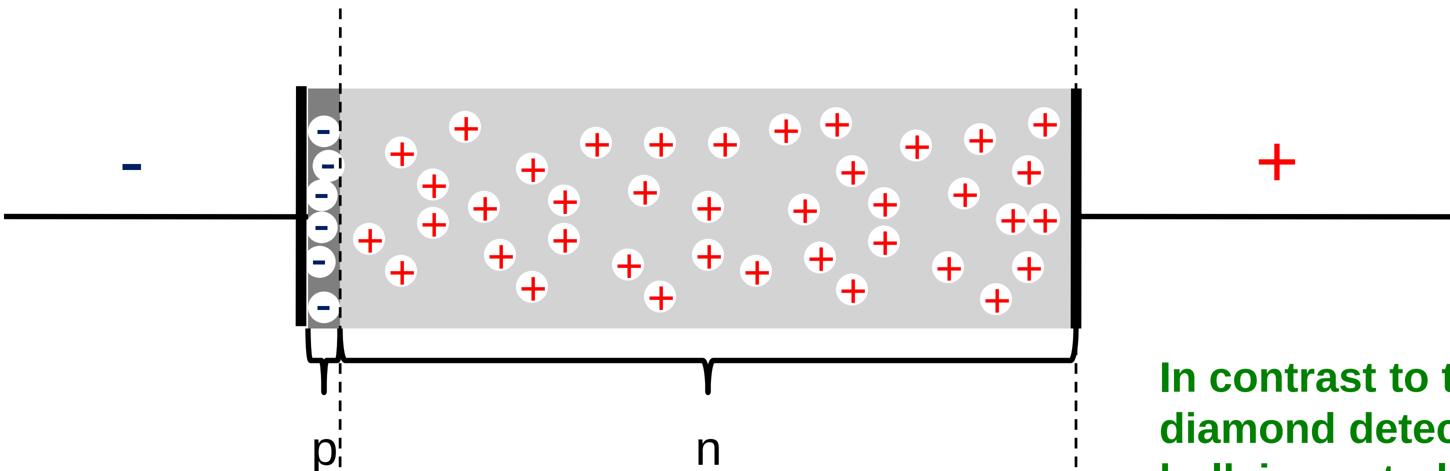

Zone without free charge carriers positively charged. Sensitive Detector Volume.

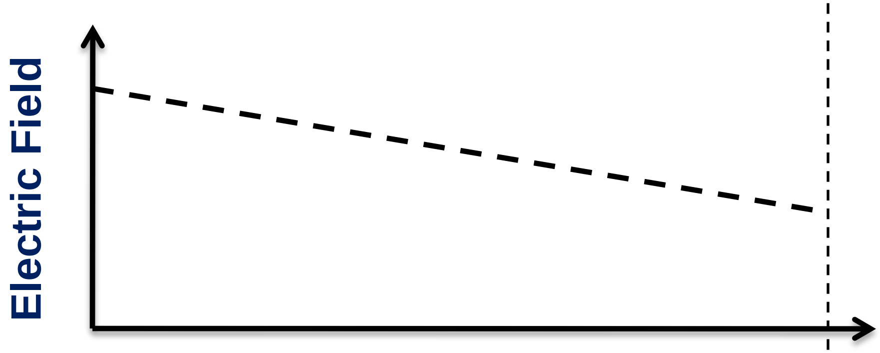

In contrast to the (un-doped) diamond detector where the bulk is neutral and the electric field is therefore constant, the sensitive volume of a doped silicon detector is charged (space charge region) and the field is therefore changing along the detector.

→ Velocity of electrons and holes is not constant along the detector.

Silicon Detector

Fully depleted zone

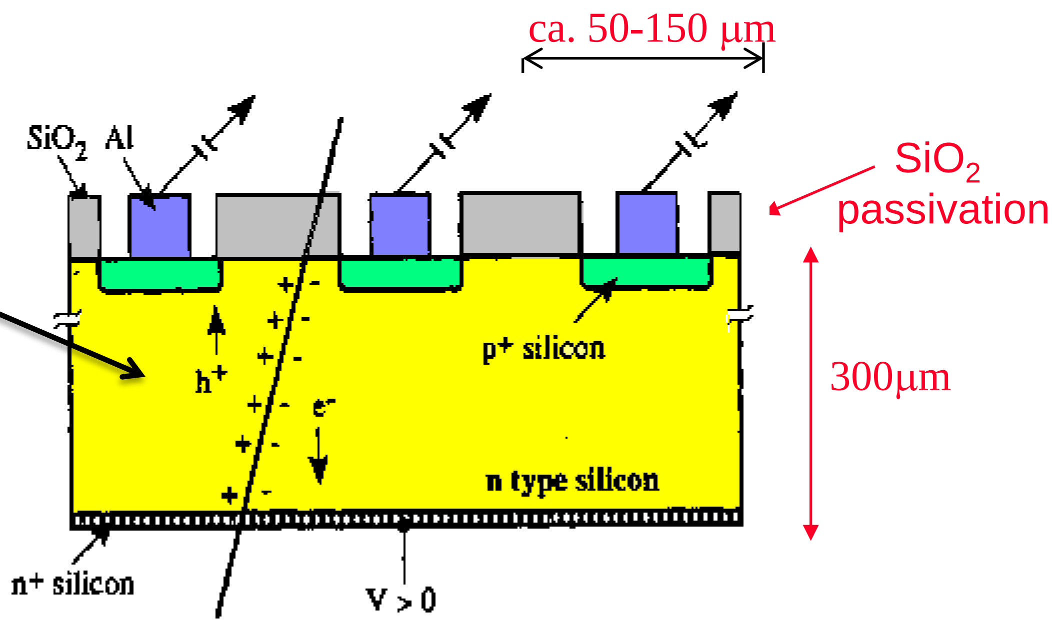

N (e-h) = 11 000/100μm

Silicon Detector Signals

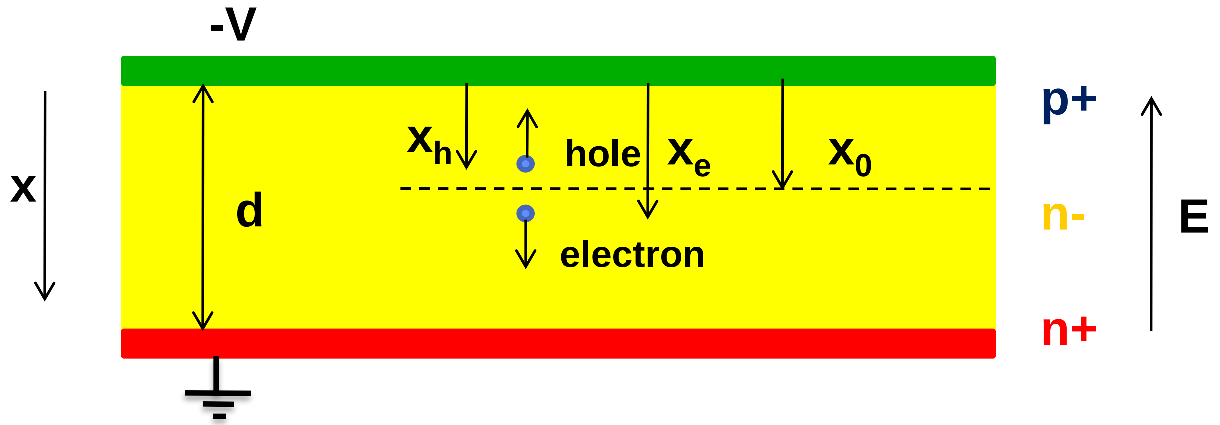

What is the signal induced on the p+ 'electrode' for a single e/h pair created at x_0=d/2 for a 300um Si detector ?

$$E(x) = -\left[2\frac{d-x}{d^2}V_{dep} + \frac{V-V_{dep}}{d}\right] \qquad v_e(x) = \mu_e E(x) \qquad v_h(x) = \mu_h E(x)$$

$$\frac{dx_e(t)}{dt} = \mu_e E(x(t)) \qquad x_e(t) = d\frac{V+V_{dep}}{2V_{dep}} + \left[x_0 - d\frac{V+V_{dep}}{2V_{dep}}\right] e^{-2\mu_e V_{dep} t/d^2}$$

$$\boxed{\frac{dx_e(t)}{dt} = \mu_e \left[\frac{2V_{dep}}{d^2}x_0 - \frac{V+V_{dep}}{d}e^{-2\mu_e V_{dep} t/d^2}\right]}$$

$$\frac{dx_h(t)}{dt} = -\mu_h E(x(t)) \qquad x_h(t) = d\frac{V+V_{dep}}{2V_{dep}} + \left[x_0 - d\frac{V+V_{dep}}{2V_{dep}}\right] e^{2\mu_h V_{dep} t/d^2}$$

$$\boxed{\frac{dx_h(t)}{dt} = \mu_h \left[\frac{2V_{dep}}{d^2}x_0 - \frac{V+V_{dep}}{d}e^{2\mu_h V_{dep} t/d^2}\right]}$$

Silicon Detector Signals

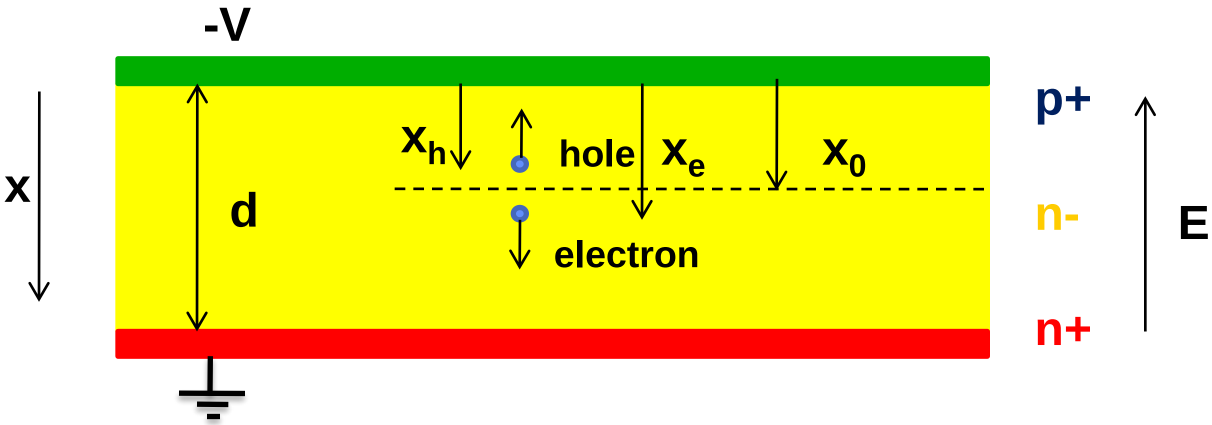

$$x_e(t_e) = d \qquad t_e = \frac{d^2}{2\mu_e V_{dep}} \ln\left[\frac{V + V_{dep}}{V - V_{dep}}\left(1 - \frac{x_0}{d}\frac{2V_{dep}}{V + V_{dep}}\right)\right]$$

$$x_h(t_h) = 0 \qquad t_h = -\frac{d^2}{2\mu_e V_{dep}} \ln\left(1 - \frac{x_0}{d}\frac{2V_{dep}}{V + V_{dep}}\right)$$

$$E_w(x) = \frac{V_w}{d} \qquad i(t) = -\frac{q}{V_w} E_w(x(t)) \frac{dx(t)}{dt}$$

$$i(t) = i_e(t) + i_h(t) = \frac{e_0}{d}\frac{dx_e(t)}{dt} - \frac{e_0}{d}\frac{dx_h(t)}{dt}$$

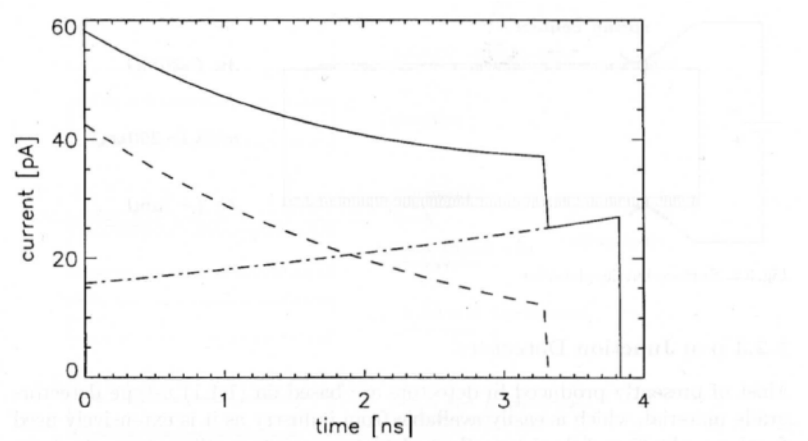

Fig. 5.4. Signal current formation induced by the separation of an electron–hole pair in the electric field of the space-charge region of the detector. The electron–hole pair is created in the center plane of a slightly (20%) overdepleted diode (see Example 5.2). Plotted are the electron-induced (*dashed line*), hole-induced (*dash-dot line*) and total (*continuous line*) currents

Silicon Detector Signals

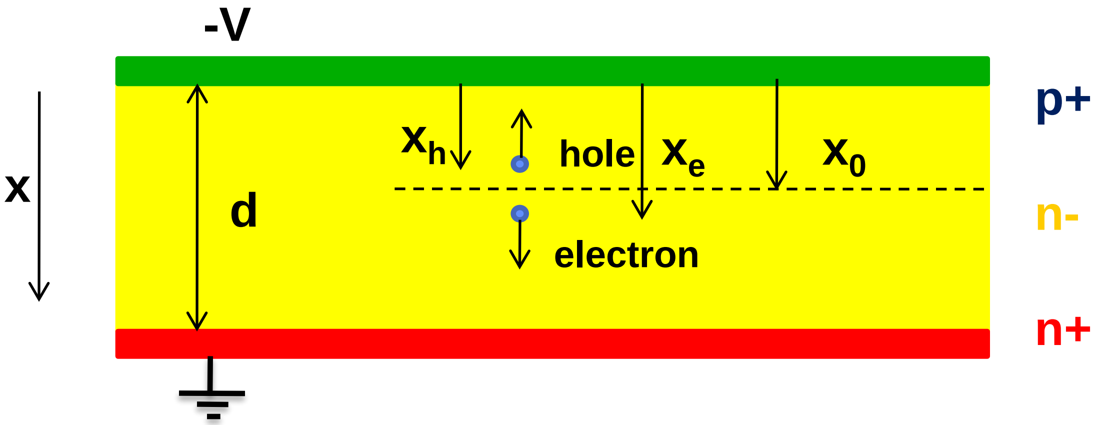

What is the signal induced on the p+ 'electrode' for a single e/h pair created at x_0=d/2 for a 300um Si detector ?

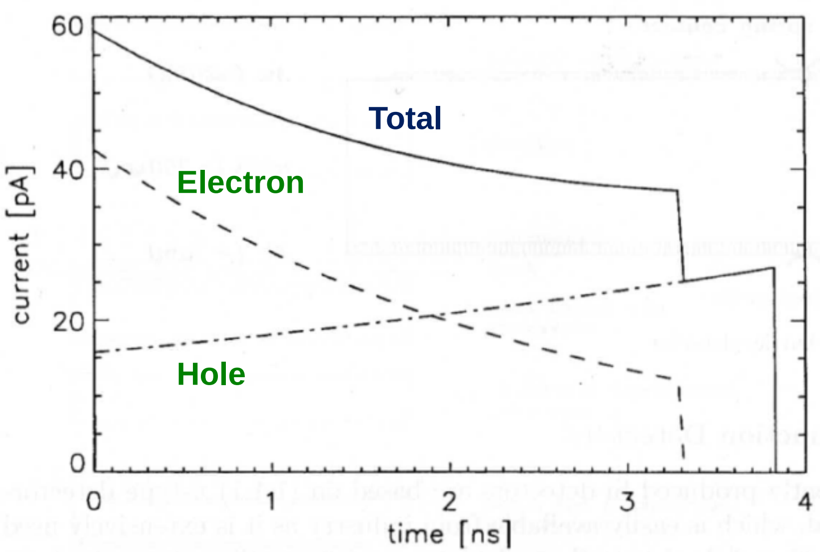

Fig. 5.4. Signal current formation induced by the separation of an electron–hole pair in the electric field of the space-charge region of the detector. The electron–hole pair is created in the center plane of a slightly (20%) overdepleted diode (see Example 5.2). Plotted are the electron-induced (*dashed line*), hole-induced (*dash-dot line*) and total (*continuous line*) currents

To calculate the signal from a track one has to sum up all the e/h pair signal for different positions x_0.

Si Signals are fast T<10-15ns. In case the amplifier peaking time is >20-30ns, the induced current signal shape doesn't matter at all.

The entire signal is integrated and the output of the electronics has always the same shape (delta response) with a pulse height proportional to the total deposited charge.

Extensions of the Ramo Shockley Theorem

The Ramo Shockley Theorem applies to electrodes that are surrounded by insulating materials.

What about particle detectors with resistive materials ?

RPCs, undepleted silicon detectors, resistive layers for charge spread in micropattern detectors, Resistive layers for HV application in RPCs, resistive layers for electronics input protection …

→ W. Riegler, Extended theorems for signal induction in particle detectors, Nucl. Instr. and Meth. A 535 (2004) 287.

Extensions of the Ramo Shockley Theorem

Resistive Plate Chambers

R. Santonico, R. Cardarelli

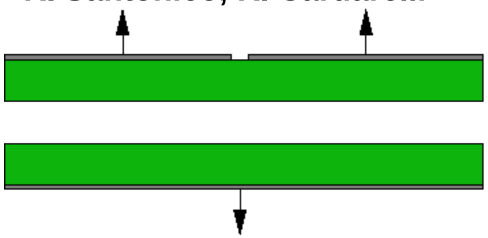

2mm Bakelite, ρ ≈ 10^{10} Ωcm

P. Fonte, V. Peskov et al.

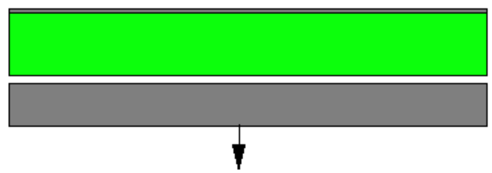

3mm glass, ρ ≈ 2×10^{12} Ωcm

M.C.S. Williams et al.

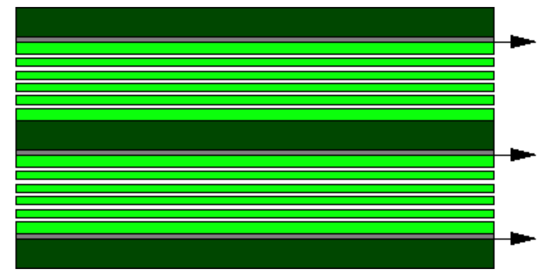

0.4mm glass, ρ ≈ 10^{13} Ωcm

Silicon Detectors

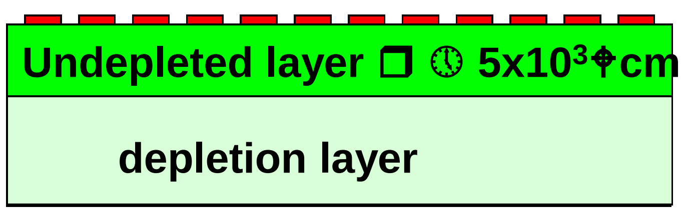

Irradiated silicon typically has larger volume resistance.

Quasistatic Approximation of Maxwell's Equations

In an electrodynamic scenario where Faraday's law can be neglected,
I.e. the time variation of magnetic fields induces electric fields that are small compared to the fields resulting from the presence of charges, Maxwell's equations 'collapse' into the following equation:

$$\vec{\nabla}\left[\varepsilon(\vec{x})\vec{\nabla}\right]\frac{d}{dt}\phi(\vec{x},t)+\vec{\nabla}\left[\sigma(\vec{x})\vec{\nabla}\right]\phi(\vec{x},t)=-\frac{d}{dt}\rho_{ext}(\vec{x},t) \quad \text{and} \quad \vec{E}(\vec{x},t)=-\vec{\nabla}\phi(\vec{x},t)$$

This is a first order differential equation with respect to time, so we expect that in absence of external time varying charges electric fields decay exponentially.

Performing Laplace Transform gives the equation.

$$\vec{\nabla}\left[\varepsilon_{eff}(\vec{x},s)\vec{\nabla}\right]\phi(\vec{x},s)=-\rho_{ext}(\vec{x},s) \quad \text{with} \quad \varepsilon_{eff}(\vec{x},s)=\varepsilon(\vec{x})+\frac{1}{s}\sigma(\vec{x})$$

This equation has the same form as the Poisson equation for electrostatic problems !

Quasistatic Approximation of Maxwell's Equations

This means that in case we know the electrostatic solution for a given ε we find the electrodynamic solution by replacing ε with ε +σ/s and performing the inverse Laplace transform.

Point charge in infinite space with conductivity σ.

$$\phi(r) = \frac{Q}{4\pi\varepsilon_r\varepsilon_0}\frac{1}{r} \quad \rightarrow \quad \phi(r,s) = \frac{Q/s}{4\pi(\varepsilon_r\varepsilon_0 + \sigma/s)}\frac{1}{r}$$

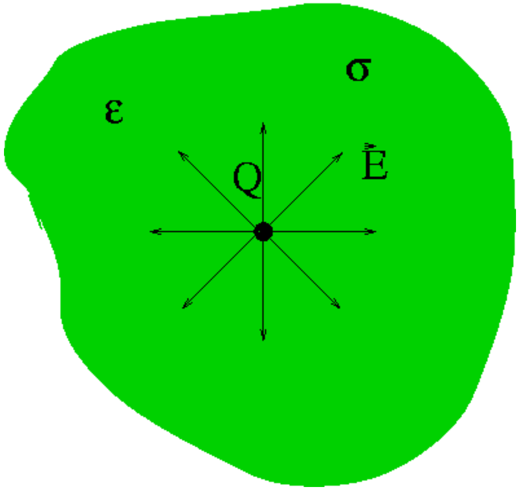

$$\phi(r,t) = \mathcal{L}^{-1}\left[\phi(r,s)\right] = \frac{Q}{4\pi\varepsilon_r\varepsilon_0}\frac{e^{-t/\tau}}{r} \quad \text{with} \quad \tau = \frac{\varepsilon_r\varepsilon_0}{\sigma}$$

The fields decays exponentially with a time constant τ.

Formulation of the Problem

At t=0, a pair of charges +q,-q is produced at some position in between the electrodes.

From there they move along trajectories $x_0(t)$ and $x_1(t)$.

What are the voltages induced on electrodes that are embedded in a medium with position and frequency dependent permittivity and conductivity, and that are connected with arbitrary discrete elements ?

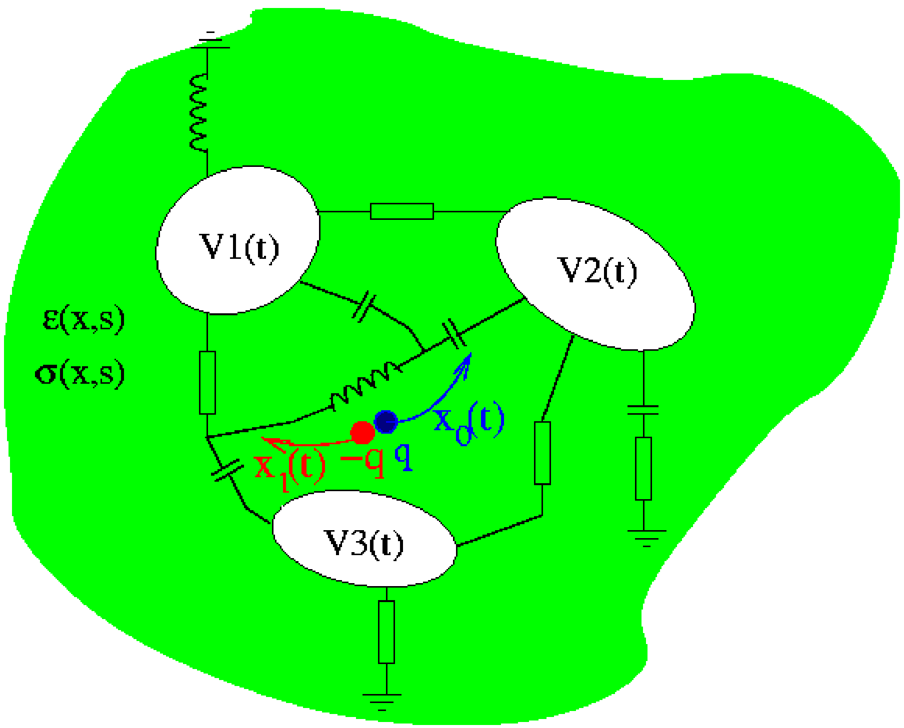

W. Riegler: NIMA 491 (2002) 258-271

Quasistatic approximation

$$\vec{\nabla}\left[\varepsilon_{eff}(\vec{x},s)\vec{\nabla}\right]\phi(\vec{x},s) = -\rho_{ext}(\vec{x},s)$$

$$\varepsilon_{eff}(\vec{x},s) = \varepsilon(\vec{x},s) + \frac{1}{s}\sigma(\vec{x},s)$$

Extended version of Green's 2nd theorem

$$\int_A \left[\psi(\vec{x})f(\vec{x})\vec{\nabla}\phi(\vec{x}) - \phi(\vec{x})f(\vec{x})\vec{\nabla}\psi(\vec{x})\right]d\vec{A}$$

$$= \int_V \left[\psi(\vec{x})\vec{\nabla}[f(\vec{x})\vec{\nabla}]\phi(\vec{x}) - \phi(\vec{x})\vec{\nabla}[f(\vec{x})\vec{\nabla}]\psi(\vec{x})\right]d^3x$$

Theorem (1,4)

Remove the charges and the discrete elements and calculate the weighting fields of all electrodes by putting a voltage $V_0\delta(t)$ on the electrode in question and grounding all others.

In the Laplace domain this corresponds to a constant voltage V_0 on the electrode.

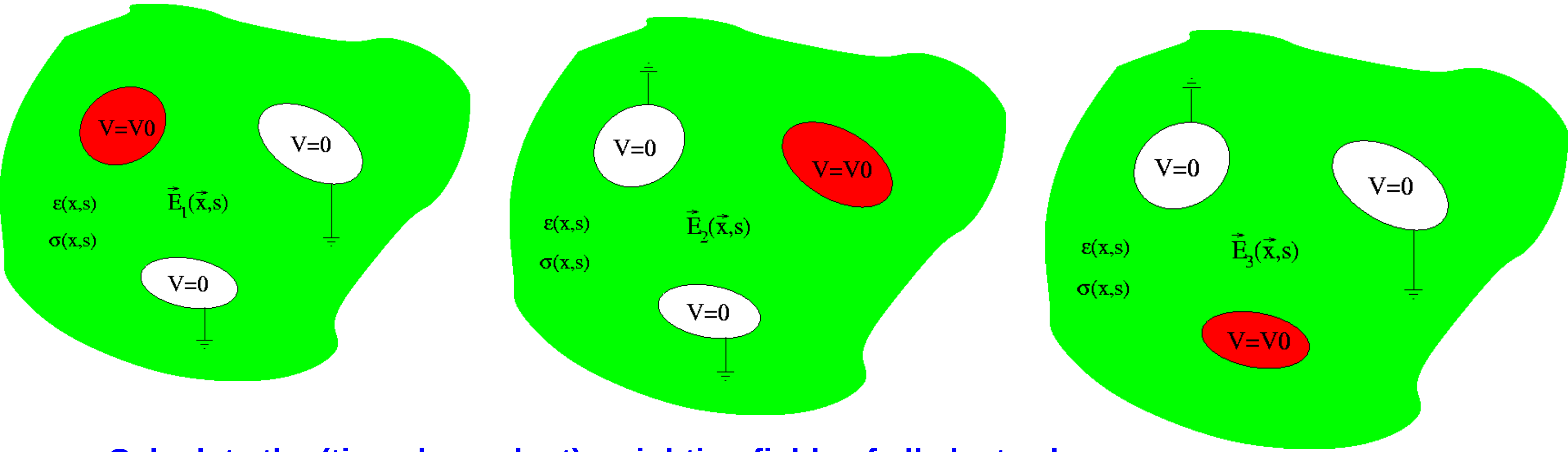

Calculate the (time dependent) weighting fields of all electrodes

$$\vec{\nabla}\left[\varepsilon_{eff}(\vec{x},s)\vec{\nabla}\right]\phi(\vec{x},s)=0 \qquad \phi_n(\vec{x},s)\big|_{\vec{x}=\vec{A}_m}=V_0\delta_{nm}$$

$$\vec{E}_n(\vec{x},s)=-\vec{\nabla}\phi_n(\vec{x},s) \qquad \vec{E}_n(\vec{x},t)=\mathcal{L}^{-1}\left[\vec{E}_n(\vec{x},s)\right]$$

Theorem (2,4)

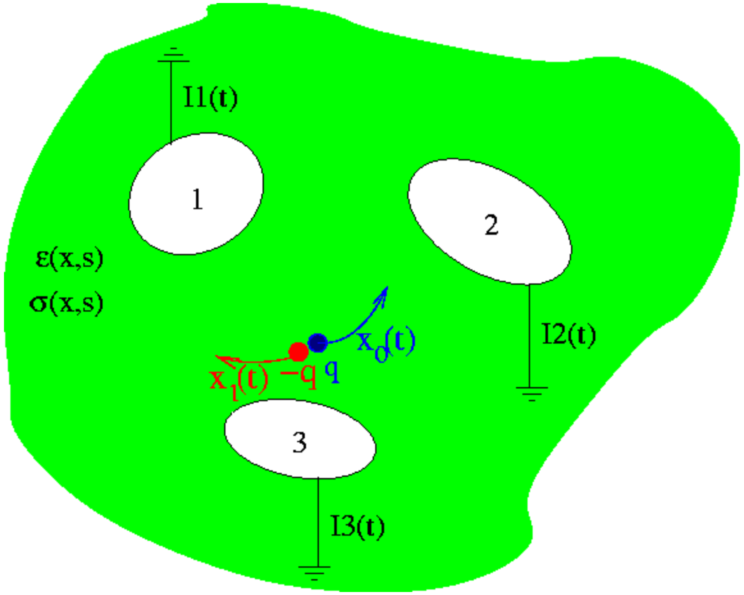

Using the time dependent weighting fields, calculate induced currents for the case where the electrodes are grounded according to

$$I_n(t) = \frac{q}{V_0}\int_0^t \vec{E}_n\left[\vec{x}_0(t'), t-t'\right]\dot{\vec{x}}_0(t')dt' - \frac{q}{V_0}\int_0^t \vec{E}_n\left[\vec{x}_1(t'), t-t'\right]\dot{\vec{x}}_1(t')dt'$$

Theorem (3,4)

Calculate the admittance matrix and equivalent impedance elements from the weighting fields.

$$y_{nm}(s) = \int_{A_n} \varepsilon_{eff}(\vec{x},s)\vec{E}_m(\vec{x},s)d\vec{A} \qquad y_{nm}(s) = y_{mn}(s)$$

$$Z_{nm}(s) = -\frac{1}{y_{nm}(s)} \qquad Z_{nn}(s) = \frac{1}{\sum_{m=1}^{N} y_{nm}(s)}$$

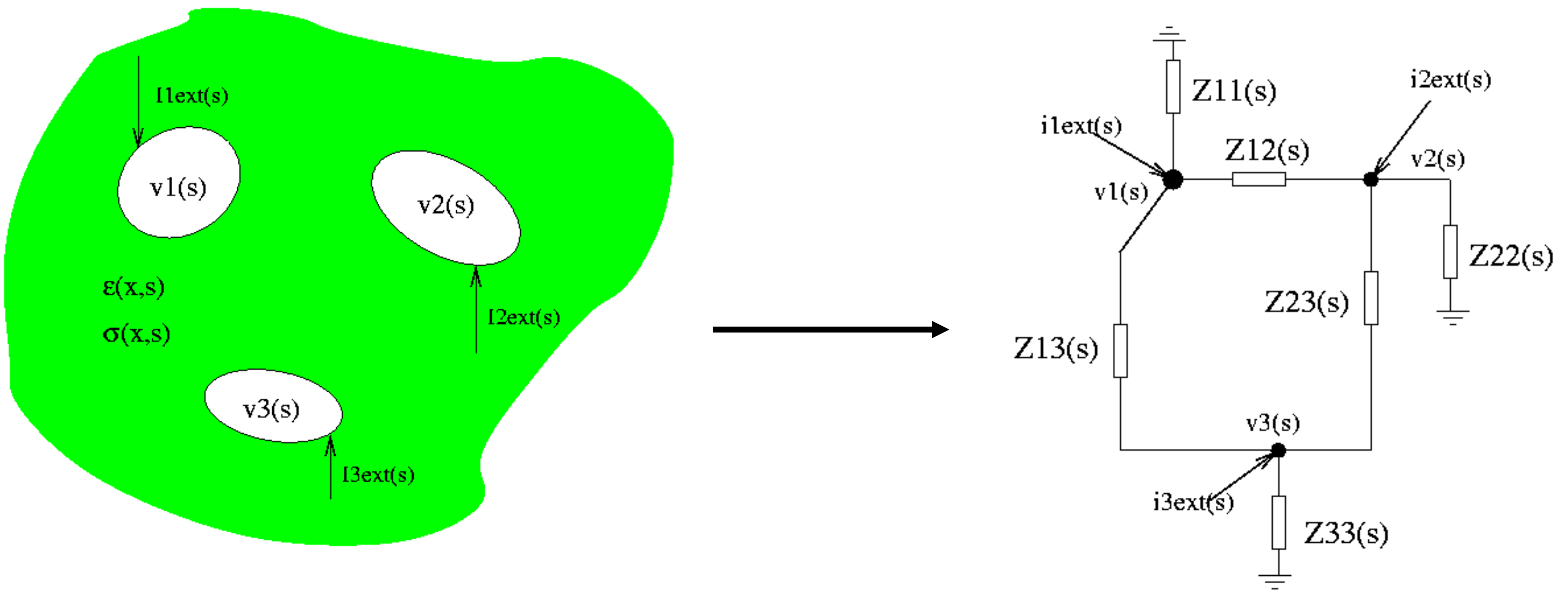

Theorem (4,4)

Add the impedance elements to the original circuit and put the calculated currents On the nodes 1,2,3. This gives the induced voltages.

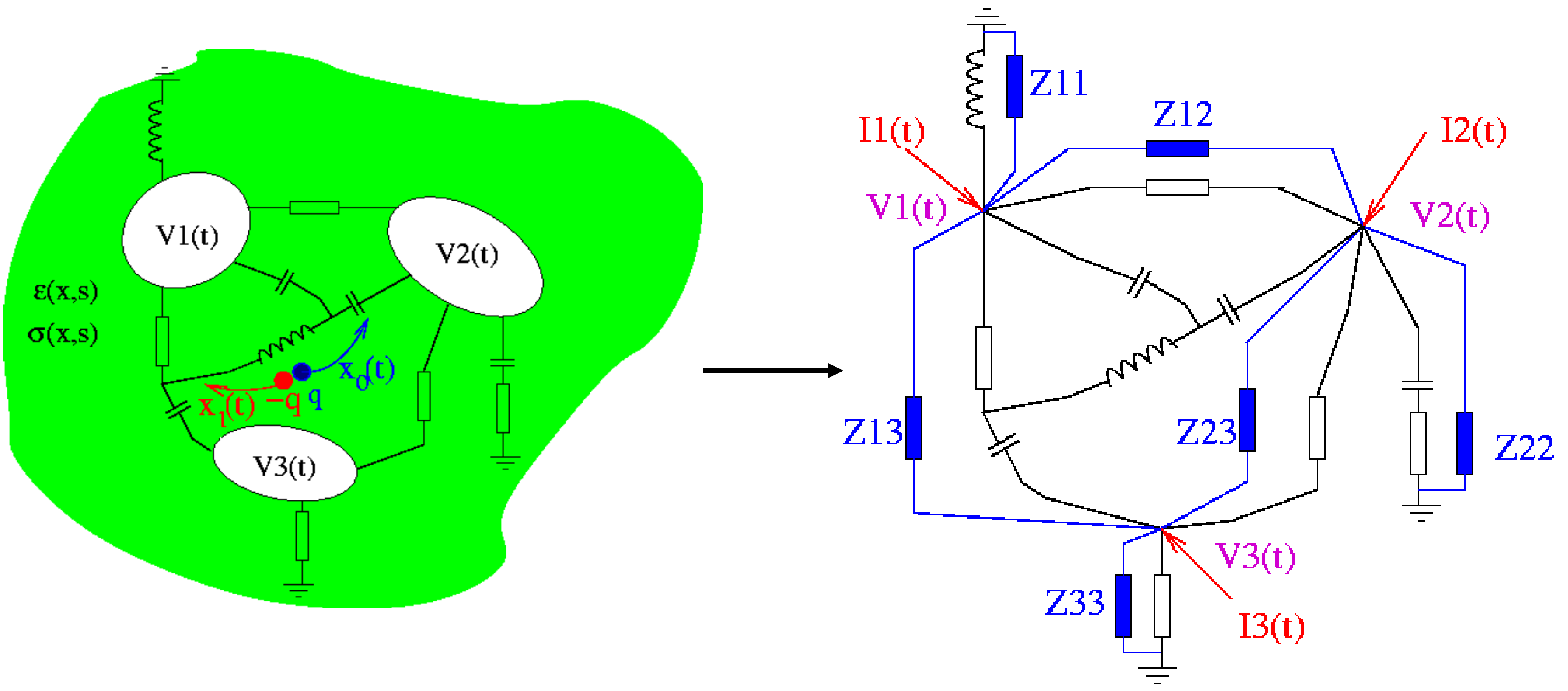

Examples

RPC

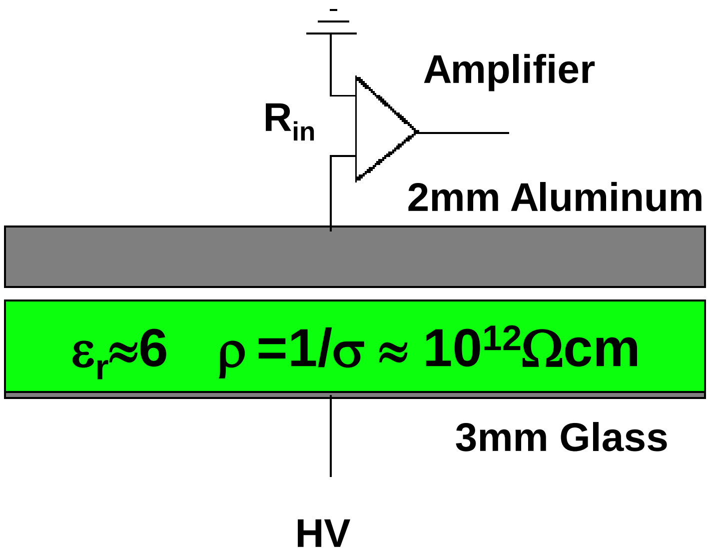

300μm Gas Gap

$\tau \approx \varepsilon_0 / \sigma \approx$ 100msec

Silicon Detector

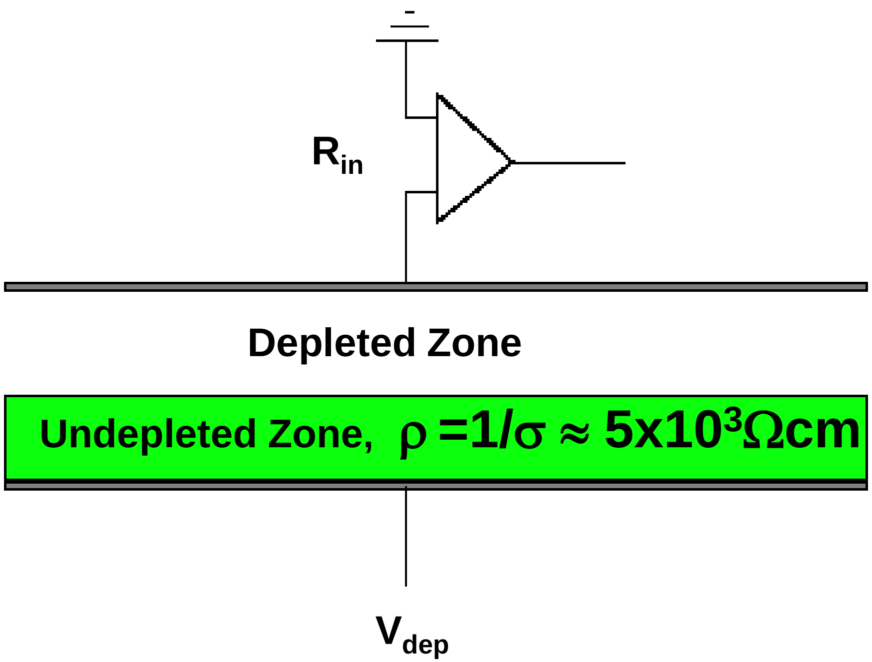

$\tau \approx \varepsilon_0 / \sigma \approx$ 1ns

heavily irradiated silicon has larger resistivity

that can give time constants of a few hundreds of ns,

Example, Weighting Fields (1,4)

Weighting Field of Electrode 1

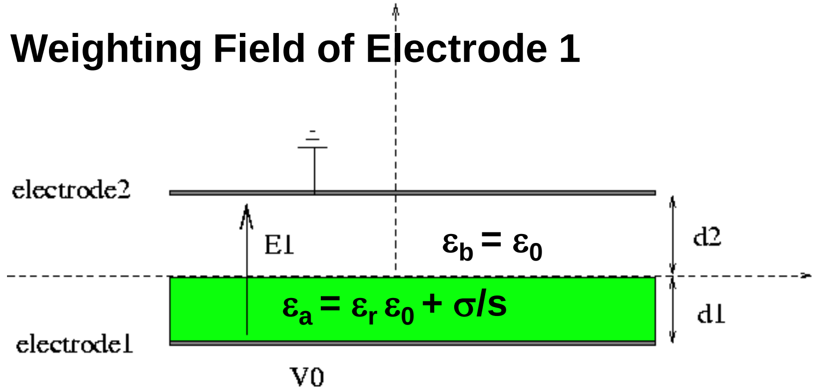

$$E_{1z}(s) = \frac{\varepsilon_a V_0}{\varepsilon_a d_2 + \varepsilon_b d_1} = \frac{V_0 \varepsilon_r}{(d_1 + d_2 \varepsilon_r)} \frac{s + \frac{1}{\tau_1}}{s + \frac{1}{\tau_2}} \qquad z > 0$$

$$= \frac{\varepsilon_b V_0}{\varepsilon_a d_2 + \varepsilon_b d_1} = \frac{V_0}{(d_1 + d_2 \varepsilon_r)} \frac{s}{s + \frac{1}{\tau_2}} \qquad z < 0$$

$$\tau_1 = \frac{\varepsilon_r \varepsilon_0}{\sigma} \qquad \tau_2 = \frac{\varepsilon_0}{\sigma} \left(\frac{d_1 + d_2 \varepsilon_r}{d_2} \right)$$

Weighting Field of Electrode 2

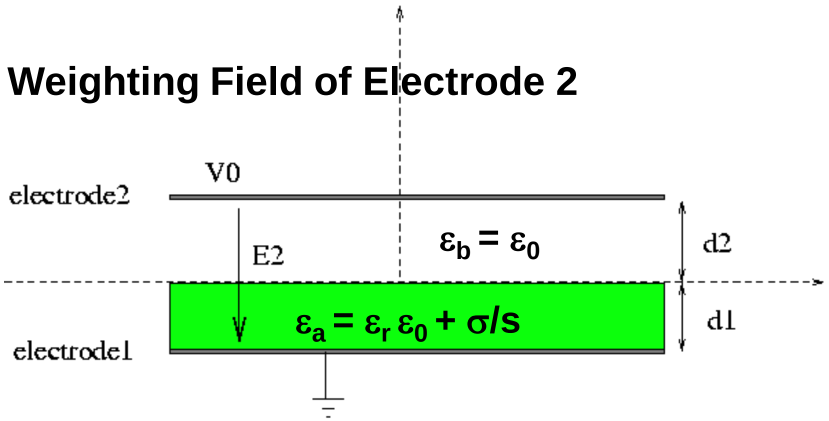

$$E_{2z}(s) = -E_{1z}(s)$$

Example, Induced Currents (2,4)

At t=0 a pair of charges q, -q is created at z=d$_2$.
One charge is moving with velocity v to z=0
Until it hits the resistive layer at T=d$_2$/v.

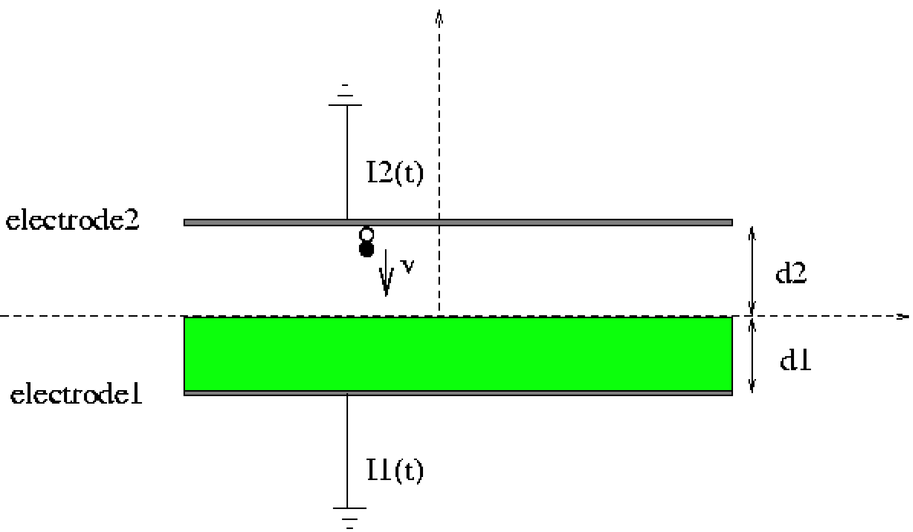

$$x_0(t) = d_2 - vt \qquad t < T$$
$$= 0 \qquad t > T$$

$$\dot{x}_0(t) = -v \qquad t < T$$
$$= 0 \qquad t > T$$

$$E_{1z}(\vec{x},t) = \frac{\varepsilon_r V_0}{d_1+\varepsilon_r d_2}\left[\delta(t) + \frac{\tau_2-\tau_1}{\tau_1\tau_2}\, e^{-\frac{t}{\tau_2}}\right] \qquad z > 0$$

$$I_1(t) = qv\frac{\varepsilon_r}{d_1+\varepsilon_r d_2}\left[1 + \frac{d_1}{d_2\varepsilon_r}(1 - e^{-\frac{t}{\tau_2}})\right] \qquad t < T$$
$$= qv\frac{1}{d_1+\varepsilon_r d_2}\frac{d_1}{d_2}\left(e^{\frac{T}{\tau_2}} - 1\right) e^{-\frac{t}{\tau_2}} \qquad t > T$$

Example, Induced Currents (2,4)

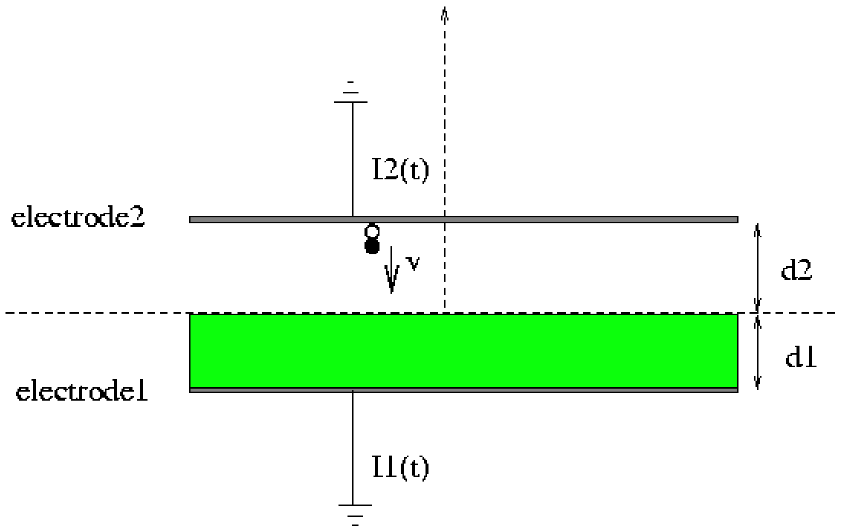

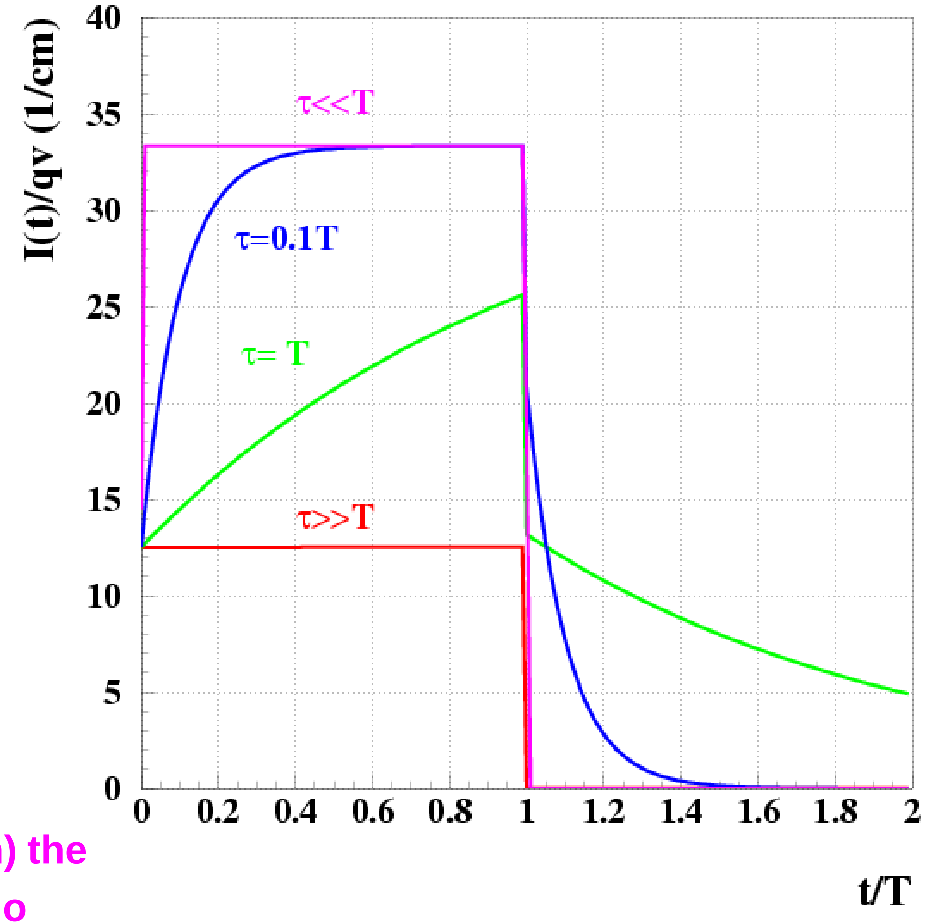

In case of high resistivity (τ>>T, RPCs, irradiated silicon) the layer is an insulator.

In case of very low resistivity (τ <<T, silicon) the layer acts like a metal plate and the scenario is equal to a parallel plate geometry with plate separation d_2.

Example, Admittance Matrix (3,4)

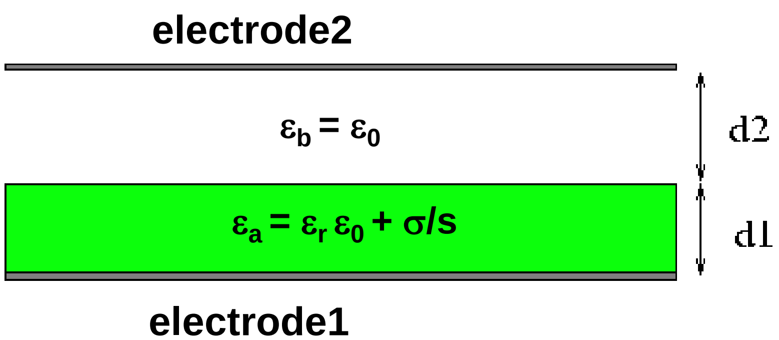

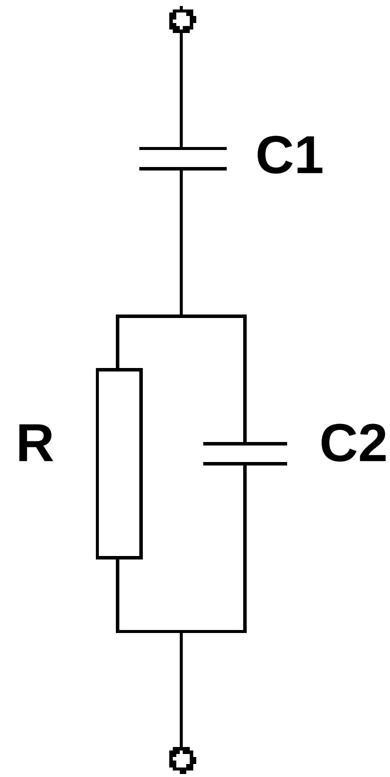

$$y_{nm}(s) = \frac{A\varepsilon_0 s(\sigma + \varepsilon_0 s)}{\sigma d_2 + (d1_1 + d_2)\varepsilon_0 s}\begin{pmatrix} 1 & -1 \\ -1 & 1 \end{pmatrix}$$

$$Z_{11}(s) = \infty$$
$$Z_{22}(s) = \infty$$
$$Z_{12}(s) = \frac{1}{sC_1} + \frac{R/sC_2}{R + 1/sC_2}$$

$$C_1 = \varepsilon_0\frac{A}{d_2} \qquad C_2 = \varepsilon_r\varepsilon_0\frac{A}{d_1} \qquad R = \frac{1}{\sigma}\frac{d_1}{A}$$

Example, Voltage (4,4)

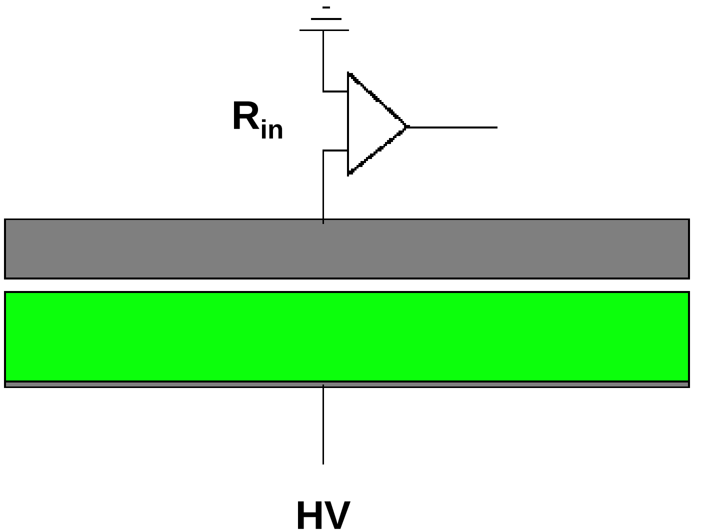

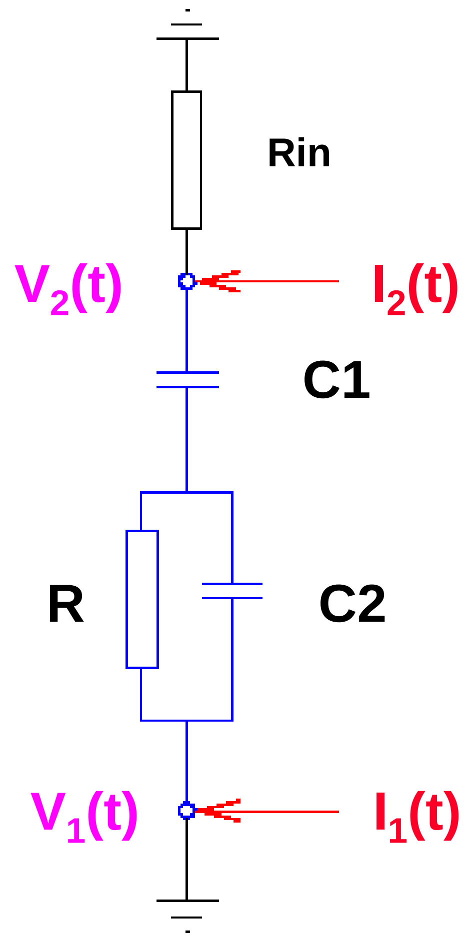

Strip Example

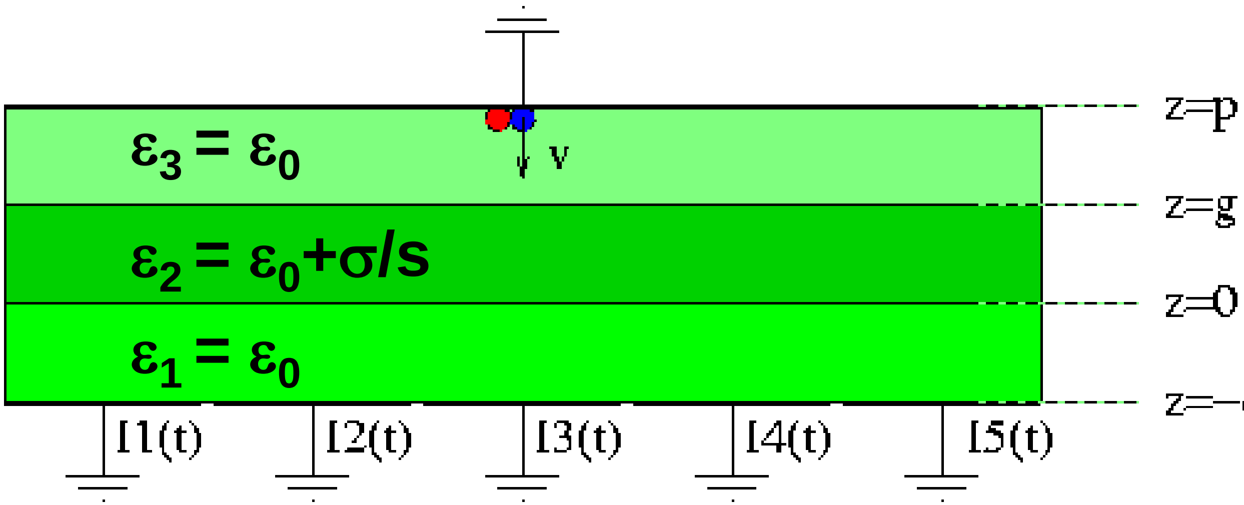

What is the effect of a conductive layer between the readout strips and the place where a charge is moving ?

Strip Example

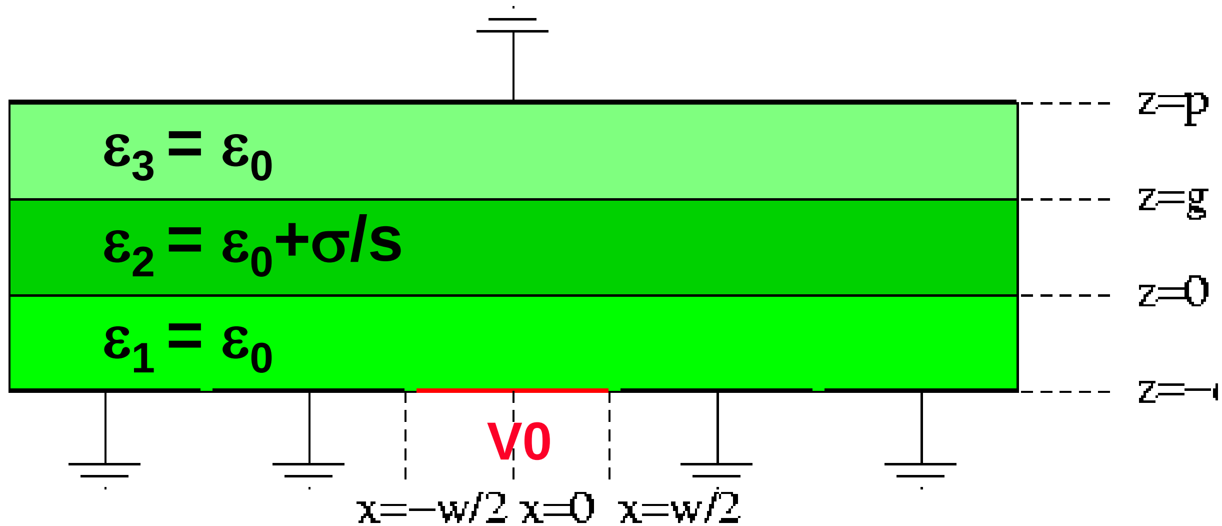

Electrostatic Weighting field (derived from B. Schnizer et. al, CERN-OPEN-2001-074):

$$E_z(x,z) = \frac{4V_0}{\pi}\int_0^\infty d\kappa \cos(\kappa x)\sin\left(\kappa\frac{w}{2}\right)\frac{2\varepsilon_1\varepsilon_2\cosh[\kappa(p-z)]}{(\varepsilon_1+\varepsilon_2)(\varepsilon_2+\varepsilon_3)\sinh[\kappa(p+q)]-(\varepsilon_1-\varepsilon_2)(\varepsilon_2+\varepsilon_3)\sinh[\kappa(q-p)]-(\varepsilon_1+\varepsilon_2)(\varepsilon_2-\varepsilon_3)\sinh[\kappa(2g+q-p)]+(\varepsilon_1-\varepsilon_2)(\varepsilon_2-\varepsilon_3)\sinh[\kappa(p+q-2g)]}$$

Replace $\varepsilon_1 \rightarrow \varepsilon_0$, $\varepsilon_2 \rightarrow \varepsilon_0+\sigma/s$, $\varepsilon_3 \rightarrow \varepsilon_0$ and perform inverse Laplace Transform $\rightarrow E_z(x,z,t)$. Evaluation with MATHEMATICA:

Strip Example

T<<τ
T=τ
T=10τ
T=50τ
T=500τ

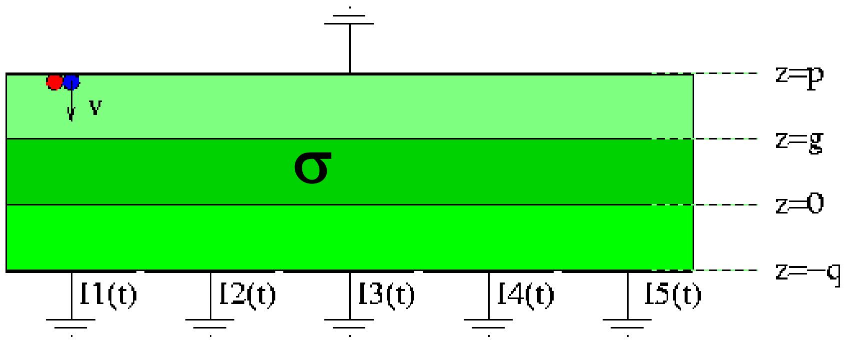

$\tau = \varepsilon_0 / \sigma$

$I_1(t)$ $I_3(t)$ $I_5(t)$

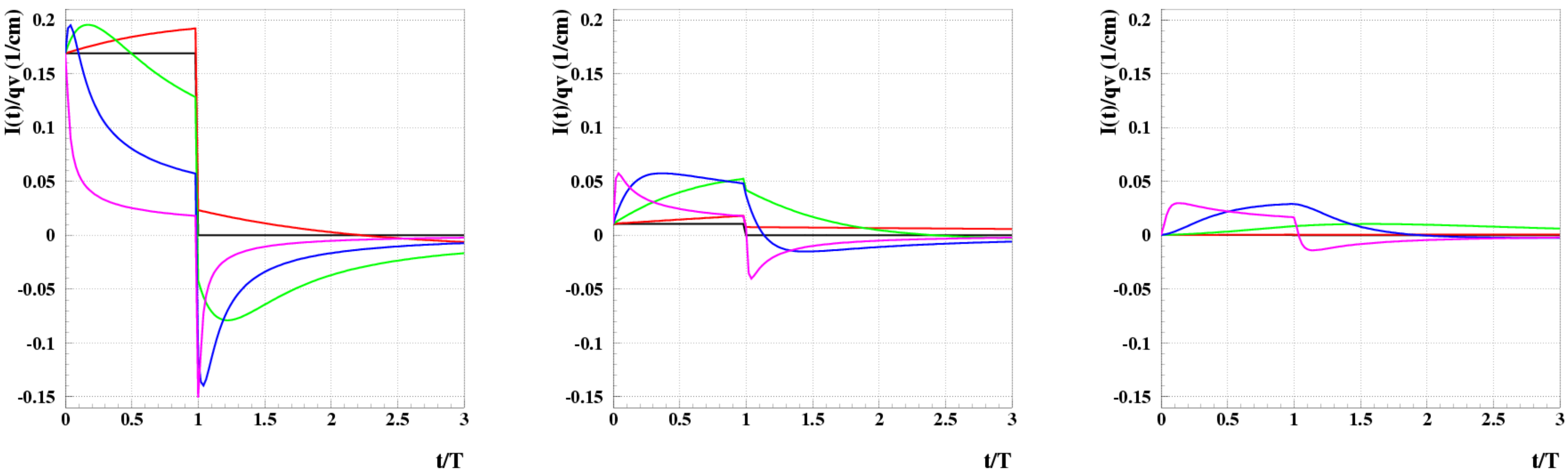

The conductive layer 'spreads' the signals across the strips.

Position Resolution/Time resolution

Wire chambers can reach tracking precisions down to 50 micrometers at rates up to <=1MHz/cm^2.

What about time resolution of wire chambers ?

It takes the electrons some time to move from thir point of creation to the wire. The fluctuation in this primary charge deposit together with diffusion limits the time resolution of wire chambers to about 5ns (3ns for the LHCb trigger chambers).

By using a parallel plate geometry with high field, where the avalanche is starting immediately after the charge deposit, the timing fluctuation of the arriving electrons can be eliminated and time resolutions down to 50ps can be achieved !

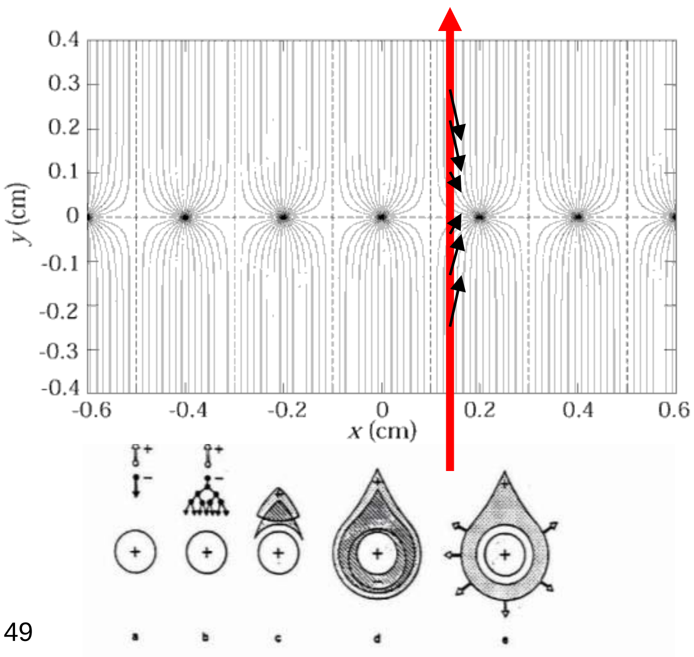

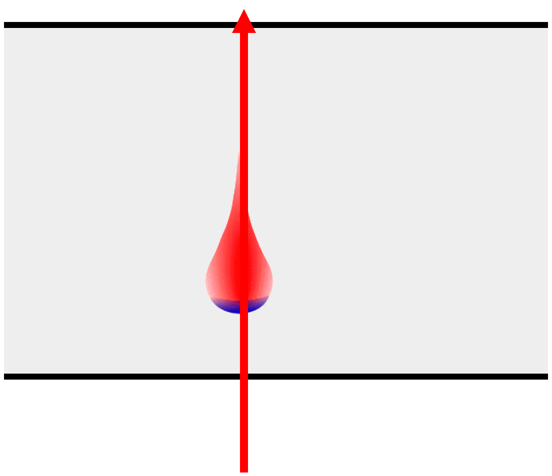

Resistive Plate Chambers (RPCs)

Keuffel 'Spark' Counter:

High voltage between two metal plates. Charged particle leaves a trail of electrons and ions in the gap and causes a discharge (Spark).

→Excellent Time Resolution(<100ps).

Discharged electrodes must be recharged → Dead time of several ms.

Parallel Plate Avalanche Chambers (PPAC):

At more moderate electric fields the primary charges produce avalanches without forming a conducting channel between the electrodes. No Spark → induced signal on the electrodes. Higher rate capability.

However, the smallest imperfections on the metal surface cause sparks and breakdown.
→ Very small (few cm^2) and unstable devices.

In a wire chamber, the high electric field (100-300kV/cm) that produces the avalanche exists only close to the wire. The fields on the cathode planes area rather small 1-5kV/cm.

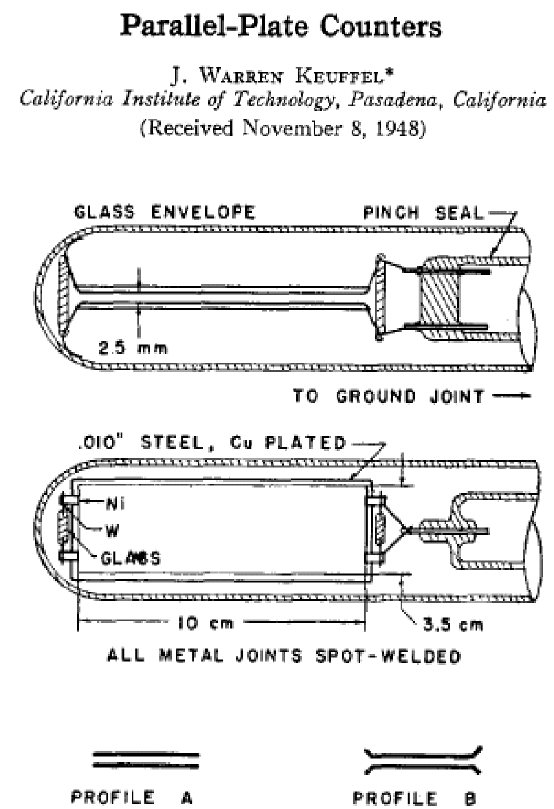

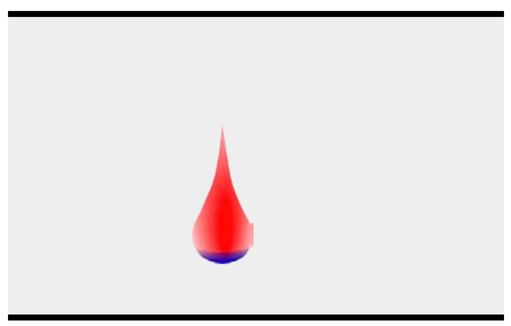

Resistive Plate Chambers (RPCs)

→Place resistive plates in front of the metal electrodes.

No spark can develop because the resistivity together with the capacitance (tau ~ $\varepsilon\rho$) will only allow a very localized 'discharge'. The rest of the entire surface stays completely unaffected.

→ Large area detectors are possible !

Resistive plates from Bakelite ($\rho = 10^{10}$-10^{12} Ωcm) or window glass ($\rho = 10^{12}$-10^{13} Ωcm).

Gas gap: 0.25-2mm.
Electric Fields 50-100kV/cm.
Time resolutions: 50ps (100kV/cm), 1ns(50kV/cm)

Application: Trigger Detectors, Time of Flight (TOF)

Resistivity limits the rate capability: Time to remove avalanche charge from the surface of the resistive plate is (tau ~ $\varepsilon\rho$) = ms to s.

Rate limit of kHz/cm^2 for 10^{10} Ωcm.

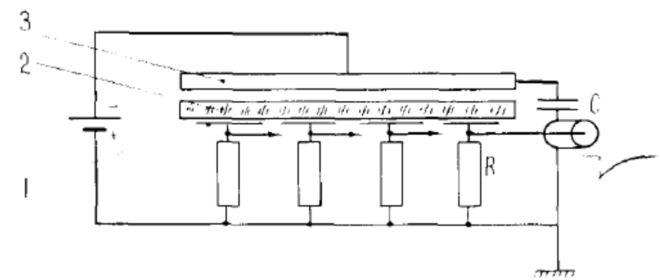

Fig. 1. The principal experimental lay-out. 1. Conductive layer; 2. electrode of semiconductive glass; 3. copper electrode.

V. Pestov 1971, 1mm gas gap, glass electrode, 1ns resolution, "Pestov counter"

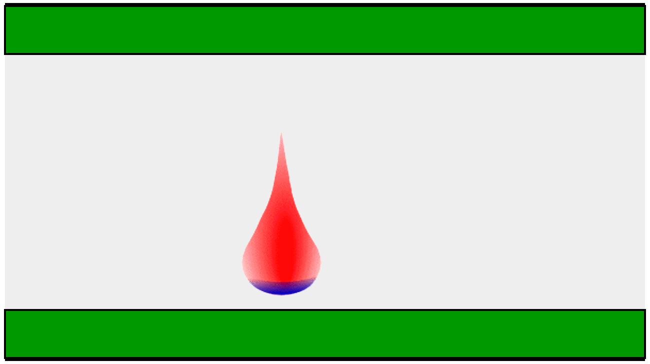

Bakelite instead of Glass,
R. Santonico, R. Cardarelli 1980

Resistive Plate Chambers (RPCs)

By decreasing the size of the gas gap to 0.1mm (to improve the time resolution) and operating the detector at 12 bar pressure (to still have good efficiency), a time resolution of 27 ps was achieved with this detector and it found it's first application for Time of Flight measurement at the Vepp-2m accelerator in Novosibirsk (Pestov 1977).

High Pressure is of course tricky for large area detectors → multigap RPC with many small gaps for good time resolution and migh efficiency.

M.C.S. Williams et al. 1996

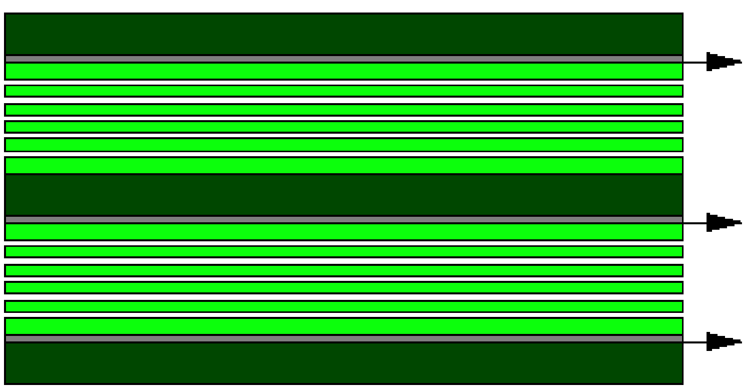

0.4mm glass, $\rho \approx 10^{13}\,\Omega$cm

Intermediate plates are floating and they charge up such that the charges in all the gas gaps are equalized.

<50ps time resolution
>99% detection efficiency for MIPS

ALICE TOF RPCs

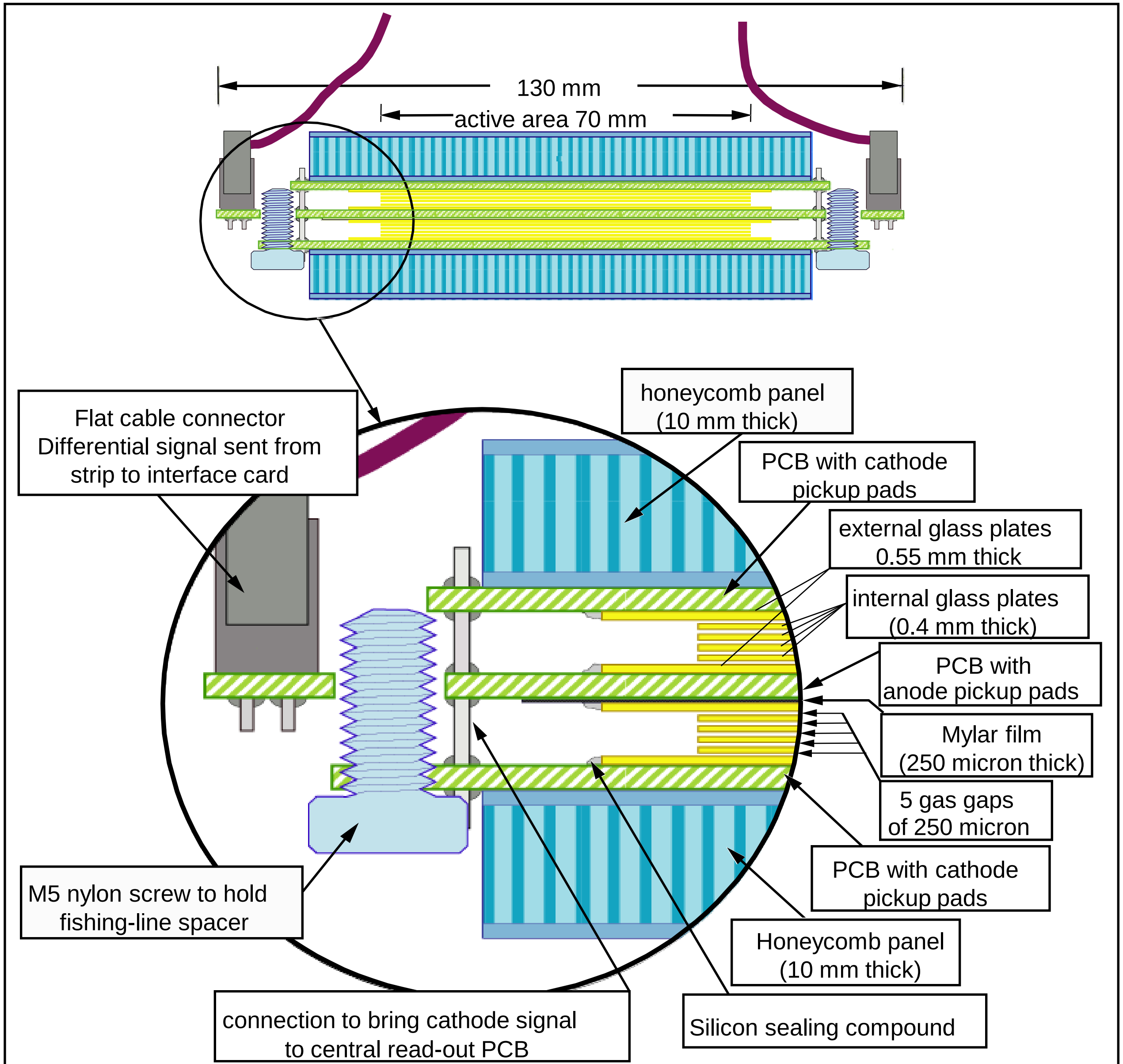

Several gaps to increase efficiency. Stack of glass plates.

Small gap for good time resolution: 0.25mm.

Fishing lines as high precision spacers !

Large TOF systems with 50ps time resolution made from window glass and fishing lines !

Before RPCs → Scintillators with very special photomultipliers – very expensive. Very large systems are unaffordable.

Conclusion

Signals in particle detectors can nicely be calculated by using the weighting field formalism (Ramo Shockley theorem).

Theorems for the case where the detector materials have finite conductivity exist.

Layers of low resistivity in front of segmented readout pads cause spreading of the charges to adjacent pads.

Resistive Plate Chambers with excellent time resolution of <50ps have revolutionized the TOF and Trigger systems. Large area detectors can be built in a very cost effective way.